EFFECT OF ADRENOMEDULLIN OVER-EXPRESSION IN THE CARDIOVASCULAR SYSTEM DURING DEVELOPMENT AND DISEASE

Sarah Elizabeth Wetzel-Strong

A dissertation submitted to the faculty at the University of North Carolina at Chapel Hill in partial fulfillment of the requirements for the degree of Doctor of Philosophy in the Department of Cell Biology and Physiology (Cell and Molecular Physiology).

Chapel Hill
2015

Approved by:

Kathleen Caron

Arjun Deb

P. Kay Lund

Robert Sealock

Joan Taylor

ABSTRACT

Sarah Elizabeth Wetzel-Strong: Effect of adrenomedullin over-expression in the cardiovascular system during development and disease
(Under the direction of Kathleen Caron)

Since the discovery of adrenomedullin (*Adm* – gene; AM – protein) in 1993, many roles for this widely expressed peptide have been described in the cardiovascular system. Numerous studies have determined that circulating levels of AM in human blood are elevated during many disease conditions, leading to questions about the feasibility of using this peptide as a biomarker of disease severity, as well as inquiries into the function of elevated AM in these contexts. In order to evaluate the effect of elevated AM during disease, gene-targeting techniques were used to generate mice that constitutively over-express *Adm*, abbreviated as $Adm^{hi/hi}$. The initial phenotypical analysis of this line revealed that $Adm^{hi/hi}$ mice have enlarged hearts due to hyperplasia during development. Through genetic approaches, we determined that *Adm* over-expression primarily in the epicardium promotes this cardiac hyperplasia.

Analysis of *Adm* expression levels between male and female $Adm^{hi/hi}$ animals led to the unexpected finding that female $Adm^{hi/hi}$ mice express *Adm* at levels 60-times greater than wildtype controls in the heart; whereas $Adm^{hi/hi}$ males over-express *Adm* by 3-fold in the heart. Previous studies have demonstrated that *Adm* expression can be induced by estrogen; however, the potential for estrogen-induced negative regulation of *Adm* had not been explored. We found that many estrogen-induced microRNAs target the 3′UTR of *Adm*, including the novel microRNA, miR-879, to balance *Adm* expression in the female heart.

Finally, many groups have demonstrated that AM provides protection to the heart during cardiovascular disease. Nonetheless, whether the physiological elevation of AM during human disease affects disease progression remains unknown. We asked whether constitutive over-expression of AM in the context of chronic hypertension provided any benefit by crossing the renin transgenic mouse model of hypertension to the *Adm*$^{hi/hi}$ line. From this study, we found that *Adm* over-expression did not alter the degree of hypertrophy or fibrosis in the heart. However, the results from this study are inconclusive, as the renin transgenic mice with wildtype levels of *Adm* did not exhibit the cardiac fibrosis previously reported, indicating that the mixed genetic background of our experimental animals alters cardiovascular pathology independent of *Adm* status.

ACKNOWLEDGEMENTS

First and foremost, I would like to thank all current and former members of the Caron lab for their insightful feedback and discussions. With regards to the data presented in Chapter III, I would like to specifically thank Scott T. Espenschied, Helen Willcockson, and Kimberly Fritz-Six of the Caron lab for technical support and assistance. Additionally, I would like to acknowledge Kirk McNaughton of the Histology Research Core facility (UNC-Chapel Hill) and Dr. Mauricio Rojas of the Rodent Advanced Surgical Models Core (UNC – Chapel Hill) for technical assistance and helpful discussions. Furthermore, I would like to thank Dr. Monte Willis (UNC-Chapel Hill) for generously providing the lab with HL-1 cells and Dr. Joan Taylor (UNC-Chapel Hill) for providing us with cardiac troponin antibody. With respect to the scientific data presented in Chapter IV, I would like to thank Claire Trincot for her technical assistance, as well as members of the Rodent Advanced Surgical Models Core (UNC-Chapel Hill) for technical assistance and helpful discussion. Finally, with regards to the data presented in Chapter V, I would like to thank members of the Rodent Advanced Surgical Models Core (UNC-Chapel Hill) for assisting with acquisition of conscious echocardiograph data. Additionally, I would like to thank the Animal Histopathology Core (UNC-Chapel Hill) for paraffin embedding tissues and members of the Histology Research Core facility (UNC-Chapel Hill) for sectioning and staining assistance.

TABLE OF CONTENTS

LIST OF TABLES

LIST OF FIGURES

LIST OF ABBREVIATIONS

AAR = area at risk

AAV = adeno-associated virus

ACE = angiotensin-converting enzyme

Adm = adrenomedullin (gene)

AM = adrenomedullin (protein)

AngII = angiotensin II

AV = atrioventricular

bGH = bovine growth hormone

Calcrl = calcitonin receptor-like receptor (gene)

CFH = complement factor H

CGRP = calcitonin gene-related peptide

CLR = calcitonin receptor-like receptor (protein)

EMT = epithelial to mesenchymal transition

EPDC = epicardial-derived cell

eNOS = endothelial nitric oxide synthase

ERα = estrogen receptor alpha

ERβ = estrogen receptor beta

ERE = estrogen response element

FGF = fibroblast growth factor

GPCR = G-protein coupled receptor

GPER = G protein-coupled estrogen receptor 1

HIF-1α = hypoxia inducible factor 1α

HRT = hormone replacement therapy

HSP72 = heat shock protein-72

HW:BW = heart weight to body weight

IGF = insulin-like growth factor

LAD = left anterior descending

LV:BW = left ventricle to body weight

Meef = Mouse eukaryotic translation elongation factor 1 alpha 1

MR-proAM = mid-regional pro-adrenomedullin

OVX = ovariectomized

PAM = peptidylglycine alpha-amidating monooxygenase

PAMP = proadrenomedullin N-terminal 20 peptide

PEO = proepicardial organ

RAAS = renin-angiotensin aldosterone system

RAMP = receptor activity-modifying protein

RenTgMK = renin transgene

ROS = reactive oxygen species

RTK = receptor tyrosine kinase

RXRα = retinoic acid X receptor alpha

SDS = sodium dodecyl sulfate

SNP = single nucleotide polymorphism

SVR = systemic vascular resistance

TTC = triphenyl tetrazolium chloride

UTR = untranslated region

VSMC = vascular smooth muscle cell

CHAPTER I: ROLE OF ADRENOMEDULLIN IN THE CARDIOVASCULAR SYSTEM

Overview of adrenomedullin

Adrenomedullin (*Adm* = gene; AM = protein) is a highly conserved, 52-amino acid peptide originally isolated from pheochromocytoma, a tumor derived from the medulla cells of the adrenal gland, in 1993 (108). Additional studies have revealed that AM is ubiquitously expressed in normal tissues beginning during embryonic development and continuing into the adult. In mice, expression of *Adm* within embryonic tissues begins at e8.0 in the heart (152, 153). By e10, expression of *Adm* has increased in the heart and other tissues within the embryo have begun to express *Adm* (152, 153). The early and widespread expression of AM during development indicates an important role for this peptide during embryonic development. This assertion is supported by the fact that several groups have demonstrated an essential role for AM in proper embryonic development and shown that AM is absolutely critical for survival (24, 59, 203, 204). These studies have revealed that the ablation of AM in mice results in cardiovascular abnormalities (24, 204), in addition to abnormalities in the development of the lymphatic system (24, 59), ultimately leading to embryo demise between e13.5 and e14.5. Specifically, the hearts of $Adm^{-/-}$ embryos are smaller compared to wildtype littermates, characterized by a thin compact zone and enhanced trabeculation (24). Furthermore, studies by Fritz-Six et al determined that the loss of other AM signaling system components results in a reduction of jugular lymph sac size due to decreased lymphatic proliferation (59). Together, these findings indicate that AM signaling is required for modulating proliferation in subsets of cells, which is further supported by recent work published by Wetzel-Strong et al demonstrating that over-expression of *Adm* promotes cardiac hyperplasia (245).

Several approaches have been utilized to elucidate the function of AM, including the infusion of AM peptide into animal models and human patients (77, 78, 98, 107, 157-159, 165, 166, 170, 173, 223, 228), the study of *Adm* heterozygous (*Adm*$^{+/-}$) animals during disease (20, 171, 203), and most recently, the study of *Adm* over-expressing mice (245). These studies have revealed that AM has a multitude of functions depending on the scenario, including, but not limited to: antioxidant (19), anti-inflammatory (37), anti-microbial (4), vasodilatory (108, 132), anti-fibrotic (168), anti-hypertrophic (140, 231), inotroptic (87), and angiogenic (60, 106) properties. Given the many diverse functions of AM, it is not surprising that several factors, including estrogen (240), angiotensin II (AngII) (175, 215), glucocorticoids (80), cytokines (215), and hypoxia inducible factor-1α (HIF-1α) (39), can induce *Adm* expression via association with upstream response elements. The control of *Adm* expression by many different factors facilitates fine-tuned control of *Adm* in specific cell populations, and thus permits localized action of AM in response to specific stimuli. Finally, as expected, the diverse functions of *Adm* can have broad implications during human disease. Depending on the disease condition, these effects may be beneficial or detrimental to an individuals overall health, as discussed in greater detail in later sections.

Adrenomedullin structure and signaling

The gene encoding adrenomedullin, located on chromosome 11 in humans and chromosome 7 in mice, produces a 185-amino acid precursor peptide, referred to as preproadrenomedullin (53). Post-translational processing of preproadrenomedullin results in the production of proadrenomedullin N-terminal 20 peptide (PAMP) in addition to the immature glycine-extended AM (109). Biological activity of AM is dependent on the presence of several key features, including amidation of the C-terminus (109), which is catalyzed by peptidylglycine alpha-amidating monooxygenase (PAM) and a disulfide bridge between cysteine residues located at positions 16 and 21 (108). These key features are conserved between several

members of the calcitonin peptide superfamily, including calcitonin gene-related peptide (CGRP), amylin (108), and AM, indicating the relationship between these peptides **(Figure 1**).

Although several features critical to the activity of AM have been characterized, to date, a limited amount of information is available regarding the three-dimensional structure of AM. Recently, Pérez-Castells et al have reported the structure of AM when associated with SDS-micelles (181). In this situation, AM comprises an α-helix spanning amino acids 22 to 34, while the flanking regions remain disorganized. The authors note that AM did not organize in the presence of cholesterol or ergosterol, indicating that the α-helix of AM may allow for the preferential association with cell membranes of bacteria, to ultimately promote the destruction of the bacterial cell, while leaving the host cells unaffected (181). This finding is interesting since it suggests a function of AM independent of receptor binding. However, since binding of AM to its receptor is believed to account for the majority of the actions of AM, it remains to be determined whether the structure of AM bound to the receptor complex differs drastically from the micelle-bound structure.

After the discovery of AM, many groups sought to identify the receptor through which AM mediated its effects. Initially, several receptors, including the G-protein coupled receptor (GPCR) AM-R (95), now known as GPR182, as well as the GPCR RDC-1 (96), now identified as ACKR3 were identified as AM receptors. Although these initial studies showed an increase in cAMP when COS-7 cells were transfected with either putative receptor and treated with AM, these results could not be repeated by other groups for the AM-R (99), leading to its re-orphanization. The discovery of receptor activity-modifying proteins, abbreviated as RAMPs, in 1998 (145) brought about significant changes in the understanding of GPCR signaling. Studies of the RAMPs have revealed that these single-pass transmembrane proteins serve a number of functions in the cell (16, 145). The initial characterization of the RAMPs by McLatchie and colleagues showed that association of RAMPs with the GPCR calcitonin receptor-like receptor

(*Calcrl* = gene, CLR = protein) increased trafficking of CLR to the cellular membrane (145). This study also revealed that RAMPs can modulate GPCR ligand affinity (145). In this particular case, McLatchie et al found that the association of CLR with RAMP1 produced a receptor that favored calcitonin gene-related peptide (CGRP), while the association of RAMP2 or RAMP3 with CLR resulted in a receptor favoring AM (145). Finally, Bomberger et al demonstrated that RAMP3 is capable of recycling CLR to the plasma membrane after endocytosis (16), indicating that the RAMP associated with a receptor can modulate the length of time a cell will respond to a particular ligand (**Figure 2**).

The identification of the RAMPs was paradigm-shifting for the field of GPCR biology and prompted a series of investigations into the role RAMPs play *in vivo*. Thus, several groups proceeded to generate knockout animals for each of the RAMPs (41, 230). Tsujikawa et al (230) found that the complete loss of RAMP1, achieved by gene-targeted deletion of exon 2 of the mouse RAMP1 gene, produced viable mice with an overtly normal phenotype; although the adult *Ramp1*$^{-/-}$ animals were hypertensive compared to control animals. These findings reflect the results of earlier studies utilizing α-CGRP knockout mice (63, 137), indicating that CGRP signaling, primarily via the CLR/RAMP1 interface, while not required for proper embryonic development, may play an important role in blood pressure regulation. However, in contrast to these findings, an independent mouse model of *Ramp1* loss published recently by Li et al (127) found that although the loss of RAMP1 is compatible with life, changes in blood pressure were not observed. This difference could perhaps be attributed to differences in the genetic background of the *Ramp1* knockout mice. Studies of RAMP2 knockout mice revealed that this RAMP is essential for survival (41, 59). These studies revealed that *Ramp2*$^{-/-}$ embryos have small lymphatic vessels due to decreased proliferation, ultimately contributing to severe hydrops fetalis and fetal demise around e14.5 (59). In addition to severe defects in lymphatic development, *Ramp2*$^{-/-}$ mice have abnormal hearts characterized by an overall small size and thin compact zone compared to wildtype controls (59). The phenotype observed in the *Ramp2*$^{-/-}$

mice closely mirrors the phenotype observed not only in the *Adm*$^{-/-}$ animals (24), but also in *Calcrl*$^{-/-}$ mice (42), indicating that CLR/RAMP2 is the primary receptor for mediating the effects of AM during embryonic development. Finally, the loss of RAMP3 in mice does not disrupt embryonic development (41), further supporting the conclusion that the effects of AM during development are mediated primarily via the CLR/RAMP2 complex. Interestingly, the loss of RAMP3 does inhibit weight gain in aged mice (41), and exacerbates cardiovascular disease in the context of chronic hypertension (8), indicating a role for RAMP3 in modulating AM signaling in normal physiology and pathological conditions in adult animals. Together, the published studies examining the roles of RAMPs *in vivo* have demonstrated the differential role for each RAMP during embryonic and adult stages. However, additional studies are needed to determine what GPCRs are associating with the RAMPs to elicit the observed effects and to determine the role of each RAMP during disease.

Roles of adrenomedullin in cardiovascular disease

Hypertension is a disease in which the blood pressure is chronically elevated. This persistent elevation in blood pressure promotes several pathological changes, including cardiomyocyte hypertrophy, damage to the vasculature, and renal damage. Several studies have indicated that AM is a powerful vasodilator (108, 132), and therefore, may mitigate cardiovascular and renal damage in the context of hypertension by working to lower blood pressure. To determine if AM is protective in hypertension, numerous groups have used animal models to address the role of AM during hypertensive cardiovascular disease. Overall, these studies have demonstrated a protective role for AM; however, the direct effects of AM are varied depending on the study design.

One approach that has been taken to study the role of AM in the context of hypertension is the utilization of *Adm*$^{+/-}$ mice (20, 171, 203). In one such study, Shimosawa and colleagues induced hypertension by infusion of AngII combined with salt-loading in *Adm*$^{+/-}$ mice (203). With

this model, a 50% reduction of AM resulted in exacerbated perivascular fibrosis in the heart, however blood pressure was unaffected (203), indicating that AM exerts protective effects independent of its vasodilatory effects. Niu et al assessed the effect of decreased AM on cardiovascular health by challenging *Adm*$^{+/-}$ mice with either AngII infusions or transverse aortic constriction (171). The reduction of AM in both of these models promoted an exacerbation of cardiovascular disease pathology, characterized by increased cardiomyocyte hypertrophy and increased interstitial fibrosis in the heart (171). Additionally, Niu et al found that renal damage was augmented in *Adm*$^{+/-}$ mice following AngII infusion (171). Finally, Caron et al utilized the renin transgene (RenTgMK) mouse model of chronic hypertension to assess the impact of reduced AM in both male and female mice (20). Similar to observations made by Shimosawa et al (203), Caron et al found that a 50% reduction in AM failed to alter blood pressure (20). Interestingly, Caron et al found that males were more adversely affected by a reduction in AM, while females were largely unaffected (20). In particular, Caron et al found that cardiomyocyte hypertrophy and renal damage were enhanced in *RenTgMK*+:*Adm*$^{+/-}$ males compared to *RenTgMK*+:*Adm*$^{+/+}$ males (20), reflecting some of the findings by Niu et al (171). Overall, these studies utilizing *Adm* heterozygous mice have revealed that AM has protective properties in the heart and kidneys independent of alterations to blood pressure in the context of hypertension.

Since the studies described above revealed a worsening of cardiovascular outcome with a 50% reduction of AM, researchers were then interested in determining whether over-expression of AM in the context of hypertension afforded additional protection to, thereby, further solidify the function of AM as a cardioprotective peptide (170, 237, 243). Using Dahl salt-sensitive rats, Nishikimi et al demonstrated that infusion of human AM resulted in a small decrease in blood pressure after induction of hypertension through a high salt diet compared to vehicle-treated rats (170). This study also revealed that AM infusion improved cardiac output and reduced systemic vascular resistance, which presumably contributes to the improved survival of rats that received AM (170). Wei et al used adeno-associated virus (AAV) to deliver

either the gene for GFP or human AM to spontaneously hypertensive rats (243). Compared to animals receiving the AAV expressing GFP, animals that received the AAV expressing AM had a significant reduction of blood pressure, decreased cardiomyocyte hypertrophy, reduced interstitial fibrosis in the heart, and diminished renal damage (243), further supporting the broad protective properties of AM in the cardiovascular and renal systems. Finally, Wang et al also used AAV to over-express human AM in rats (237). In contrast to the study performed by Wei et al (243), this study used the Goldblatt model of hypertension (70), in which a clip is placed on one of the renal arteries, ultimately leading to an increase in renin secretion by the clipped kidney and hypertension resulting from over-activation of the renin-angiotensin aldosterone system (RAAS) (160). Although the model of hypertension in this study differed from the model employed by Wei et al, the effects of AM over-expression by AAV on cardiovascular and renal pathology were comparable between the two studies (237). Together, these studies indicate that over-expression of AM is beneficial in the context of hypertension, potentially due in part to blood pressure reductions.

Ischemia-reperfusion injury, commonly referred to as a heart attack in human patients, occurs when one of the coronary arteries, which supply blood to the ventricular tissue, becomes occluded due to plaque formation (247). This occlusion of the vessel deprives the underlying cardiac muscle of important nutrients and oxygen, ultimately resulting in death of the underlying cardiomyocytes (247). In order to maintain structural integrity of the heart, the infarcted, area of the heart is initially replenished by myofibroblasts (232). These fibroblasts deposit extracellular matrix, including collagen, which drastically reduces the compliance of the ventricular wall, leading to impaired cardiac function. Although some lower-order vertebrates, including zebrafish, have the capability to regenerate cardiac muscle (238, 251), higher-level vertebrates, including rodents and humans, have limited cardiac regenerative abilities. As a result of low cardiac regeneration, the fibrotic scar formed during the initial stages of wound healing persists for the life of the animal, resulting in reduced cardiac output and increased risk for adverse

cardiac events in the future. Although we currently do not have the knowledge to promote the replacement of scar tissue with functional cardiomyocytes in mammals, there is great interest in identifying molecules that can reduce the size of the infarct, which in turn, reduces the degree of scar tissue deposition and preserves a greater amount of cardiac function. Due to the protective role of AM in the context of hypertension, researchers were interested in determining if and how AM may be protective in the context of ischemia-reperfusion.

In animal models, researchers mimic a heart attack by ligating the left anterior descending (LAD) coronary artery to promote ischemic injury to the tissue fed by the ligated vessel. The suture is then released, usually 30 minutes after initiation of ischemia, to reperfuse the tissue with blood and oxygen, thereby simulating the re-opening of a vessel after dissolving a clot. Using this approach, several groups have assessed the effect of AM status on injury after ischemia-reperfusion (77, 78, 165, 173, 223). Overall, these studies have revealed a protective effect of AM in this model of cardiac injury. Of the studies that assessed the impact of AM on infarct size, it was unanimously found that either infusion of AM or over-expression of AM by AAV significantly reduced infarct size (77, 78, 165, 173). Accompanying this reduction in infarct area, these studies also found a reduction in cardiomyocyte apoptosis (173) and improved recovery of left ventricular function (165). Although Torigoe et al did not assess the effect of AM administration on infarct size, they did report improved recovery of left ventricular function (223), indicating that infarct size in this model is likely reduced. Together, these studies indicate one way in which elevated levels of AM following myocardial infarction serve to mitigate injury is through a reduction in the area of tissue injured, thus leading to better prognosis.

In addition to identifying the effect of AM on cardiac pathology after ischemia-reperfusion, several groups sought to identify the signaling pathways by which AM mediates its protective effects. Several of these studies identified the PI3K/Akt pathway as an important mediator of the protective effects of AM (77, 173, 223). Moreover, two of these studies identified downstream targets of Akt signaling that may be responsible for mediating the protective effects

of AM, including endothelial nitric oxide synthase (eNOS) (77) and heat shock protein-72 (HSP72). Interestingly, Nishida et al found that administration of AM immediately after ischemia activated the PI3K/Akt pathway and offered cardioprotection (165); however, they reported that this protection was less robust than the protection offered by AM administered prior to the ischemia period, which was found to offer protection via PKA-dependent activation of mitochondrial K_{Ca} channels (165). These findings differ slightly from other studies that have reported Akt activation with AM administration prior to ischemia (77, 223), however these differences might be attributed to the use of different animal models or due to the fact that some of these studies performed the ischemia-reperfusion in live animals, while other studies performed the ischemia-reperfusion on Langendorff perfused hearts. Overall, these studies demonstrate that AM mitigates cardiac damage resulting from ischemia-reperfusion injury although the exact mechanism remains a source of debate.

To date, a limited number of studies have been performed to study the effect of AM infusion of cardiovascular disease pathology in human patients (98, 107, 157-159, 166, 228). Overall, these studies have found that infusion of AM improves several cardiovascular and renal parameters, indicating a potential therapeutic use for AM in the clinic. Hypertension is detrimental to overall cardiovascular health as persistent elevations in blood pressure necessitate increased force generation by the left ventricle to pump blood to the systemic vasculature. This promotes cardiomyocyte hypertrophy to increase to force-generating capabilities of the ventricle, allowing for compensation. Eventually, if the pressure remains elevated, the cells of the left ventricle fail under the increased workload, resulting in cell death and thinning of the ventricular wall and heart failure. Therefore, the reductions in blood pressure (98, 107, 159, 166, 228) and systemic vascular resistance (SVR) (158, 159, 166) observed in patients with several forms of cardiovascular disease following infusion of AM could offer protection by reducing the load on the heart. Cardiac output is a measure of the volume of blood pumped by the heart during a specified interval of time and reflects overall cardiac function.

With AM infusion, increases in cardiac output were noted in patients with several forms of cardiovascular disease, including heart failure (159, 166), essential (228) and pulmonary hypertension (158), and myocardial infarction (157), ultimately leading to improved delivery of oxygenated blood to the rest of the body for improved patient prognosis. Several studies also noted that AM infusion reduced plasma levels of aldosterone (107, 158, 159, 166). Since aldosterone acts on the kidney to promote retention of sodium, blood pressure is elevated due to increased fluid retention. Therefore, a reduction in circulating aldosterone with AM infusion may be beneficial to patients by reducing blood pressure through the secretion of sodium in the urine. In fact, one study by Nagaya et al (159) found that AM infusion did indeed increase urine production and excretion of sodium supporting the mechanism described above. Finally, in patients presenting with acute myocardial infarction, Kataoka et al (98) found that administration of AM for 12 hours reduced the size of the infarct, contributing to an increase in wall motion within the infarcted area and overall improved cardiac function and patient outcome. Although the effect of AM infusion in human patients varied between studies, it is clear that AM can offer therapeutic benefits to patients with cardiovascular disease.

Adrenomedullin as a biomarker of human disease

Several clinical studies have noted increases in plasma levels of AM above basal levels during many human conditions, including: cancer, cardiovascular, renal, pulmonary, and autoimmune diseases (97). Given the protective role of AM during cardiovascular disease, clinicians have been interested in determining whether circulating levels of AM could be used as a novel biomarker of cardiovascular disease severity. However, since the mature form of AM is difficult to assess in the plasma due to its instability (146) and affinity for other peptides (184), clinical research teams instead assess circulating levels of mid-regional pro-adrenomedullin (MR-proAM). Mid-regional pro-adrenomedullin is a stable, 48-amino acid byproduct formed by the cleavage of preproadrenomedullin to produce mature AM (101, 212). Since MR-proAM is

produced and circulates in the plasma at equal ratios to AM, this stable fragment provides a more reliable read-out of plasma AM levels.

To date, several studies have examined the feasibility of using circulating MR-proAM as a biomarker of cardiovascular disease severity (48, 101, 111, 142, 195, 209, 229). In both the context of acute myocardial infarction as well as in patients with heart failure following a myocardial infarction, circulating plasma levels of MR-proAM were highly associated with adverse events (48, 101, 111). These studies also found that MR-proAM alone was a stronger biomarker than traditional biomarkers such as BNP (48, 111) and when combined with traditional biomarkers, allowed for better stratification of patient risk (101, 142). In addition to showing that elevated MR-proAM levels are correlated with increased risk of death in patients with coronary artery disease (195), Sabatine et al found that patients with the highest circulating levels of MR-proAM benefitted from treatment with trandolapril (195), an angiotensin-converting enzyme (ACE) inhibitor used to treat hypertension, unlike patients with lower MR-proAM levels. These data reveal that circulating levels of MR-proAM may be useful for identifying patients that may benefit from therapeutic interventions, in addition to identifying patients that require more intensive monitoring and care.

Other studies have revealed that the usefulness of AM as a biomarker for adverse outcomes is not limited to cardiovascular disease. One such study examined plasma MR-proAM levels in patients admitted to the hospital for dyspnea (142). This study found that elevated MR-proAM was correlated with adverse events not only in patients suffering from acute heart failure, but all other patients suffering from dyspnea for any other cause (142). Additionally, Maisel et al found that elevated levels of MR-proAM at the time of discharge from the hospital in these patients were correlated with poor patient survival in the following three months (142), suggesting that high levels of AM at discharge are indicative of underlying problems. A separate study performed by Chen et al found that circulating levels of MR-proAM are elevated in patients with sepsis, and that patients with the most severe sepsis had the greatest amount of

circulating AM (31). Moreover, within each tier of septic severity, patients who died while in the hospital consistently had higher levels of AM compared to survivors within the same tier (31), highlighting the prognostic value of AM. Finally, work by Seissler et al suggests that MR-proAM may be a useful biomarker for metabolic syndrome (202). In this study, plasma levels of MR-proAM were elevated in patients with metabolic syndrome and type II diabetes (202), although it remains to be seen whether this elevation of MR-proAM is indicative of future complications. Together, the current literature demonstrates that MR-proAM may prove to be an extremely useful biomarker for disease severity in many human conditions.

Polymorphisms of adrenomedullin in human disease

In recent years, there has been increased interest in identifying small genomic changes that pre-dispose individuals to disease later in life. Single-nucleotide polymorphisms (SNPs) are locations within the genome of a species in which a single nucleotide differs between individuals. Depending on the location of these SNPs, this alteration of the genetic sequence may change the expression of surrounding genes, thereby potentially altering an individual's susceptibility to disease. Given the involvement of AM in many human disease conditions, researchers over the past decade have been interested in determining whether SNPs located near or within *Adm* alter disease susceptibility.

Some of the earliest studies examining the relationship between AM polymorphisms and disease susceptibility were focused on determining whether AM polymorphisms predisposed individuals to essential hypertension (90, 112, 199). The first study by Ishimitsu et al focused on a microsatellite region of cysteine-arginine (CA) repeats downstream of the *Adm* gene (90). This study found that in a Japanese population, four haplotypes were present, which included individuals with 11-, 13-, 14-, or 19-CA repeats in the microsatellite region (90). Ishimitsu et al found that individuals with 19-CA repeats were more likely to have essential hypertension, however, this alteration in the microsatellite region did not seem to alter expression levels of AM

(90), leading the authors to postulate that this change might alter expression of other genes. Kobayashi et al also examined the relationship of AM polymorphisms with essential hypertension in a Japanese cohort (112). Although Kobayashi et al did not find a correlation between AM polymorphisms and risk for essential hypertension, they did find that the A-G-19 haplotype for SNP rs4399321, SNP rs7944706, and the microsatellite region of *Adm* was correlated with proteinuria in patients with essential hypertension (112). Finally, Sano et al examined the relationship between polymorphism in *Calcrl*, the GPCR that mediates AM signaling, and essential hypertension (199). This study found that the T allele for SNP rs696574, located in exon 6 of *Calcrl*, was enriched in women with essential hypertension (199). Although it is not clear from this study what impact this polymorphism has on *Calcrl* expression, this study nonetheless adds further support to the conclusion that polymorphism within AM signaling system genes may predispose certain individuals to essential hypertension.

In addition to the studies testing for associations with essential hypertension (90, 112, 199), a few studies have been conducted to examine the relationship between AM polymorphisms and blood pressure (29, 129). Li et al found that individuals carrying a G allele at position -1984 in the *Adm* promoter, corresponding to SNP rs3814700, had lower pulse pressures compared to other individuals (129). This finding may be due to the fact that there was a trend for elevated plasma levels of AM in individuals with two copies of the G allele compared to other groups, which may be attributed to the creation of a binding site for the glucocorticoid receptor in the *Adm* promoter by this polymorphism (129). A more recent study performed by Chen et al revealed that individuals homozygous for the G allele at SNP rs4399321 were more likely to have elevated blood pressure compared to individuals with at least one copy of the A allele (29). Interestingly, Chen et al found this SNP was even more highly correlated with elevated blood pressure in individuals who did not consume alcohol (29), although the underlying mechanism behind this finding remains unclear. In summary, these

studies demonstrate that polymorphisms in *Adm* may be correlated with changes in blood pressure, although these SNPs may differ between different populations of individuals.

Polymorphisms near and within the *Adm* gene have been correlated with diseases other than hypertension, including type II diabetes (91, 174), inflammation (32), and cancer (143). A study performed by Ong and colleagues found that individuals with the minor A allele at SNP rs11042725 were more likely to develop dysglycemia within six years, indicating development of type II diabetes (174). Previous studies using a luciferase assay found that this allele resulted in the increased production of AM (69), indicating that elevated plasma levels of AM may be contributing directly to the development of dysglycemia and subsequent type II diabetes. A separate study performed by Ishimitsu et al found that 19 CA-repeats within the microsatellite region of *Adm* were correlated with the development of renal failure in individuals with pre-existing type II diabetes, although this polymorphism did not seem to alter levels of AM (91). Together, these studies indicate that polymorphisms of *Adm* may be predictive of type II diabetes and resulting renal failure. Inflammation is a common occurrence during many disease conditions, and thus, differences in AM levels due to genetic polymorphism may alter the degree of inflammation due to the anti-inflammatory properties of AM (37). In support of these findings, Cheung et al found that individuals with increasing levels of plasma AM had a significant decrease in circulating IL-6 (32), a marker of inflammation. Interestingly, this study also revealed that individuals with the minor T allele for SNP rs4910118, located in the 3′ un-translated region (UTR) of *Adm,* had a significant reduction in plasma AM (32). Given the importance of AM in many disease conditions, this SNP may be a useful marker for identifying patient risk in many disease states. Finally, several studies have demonstrated that elevated levels of AM during cancer are often detrimental (163). Consistent with these findings, Martínez-Herrero and Martínez found the minor T allele of SNP rs4910118 was less prevalent in individuals with breast or lung cancer compared to healthy individuals (143). Since the T allele of this SNP is correlated with reduced circulating levels of plasma AM (32), it appears that reduced AM may

be protective against cancer. Overall, polymorphisms of the *Adm* gene, diagrammed in Figure 3, may be useful markers for identifying individuals at risk for numerous diseases.

Summary

In summary, *Adm* is widely expressed throughout the body from the earliest developmental stages through adult life. This widespread expression underscores the importance of this peptide not only in modulating proper embryonic development, but also for maintaining normal physiology and eliciting responses to disease. As a result of the wide-ranging effects of AM, it is not surprising that many factors have been shown to regulate *Adm* expression, allowing for fine-tuned control in different scenarios. Several studies have demonstrated that plasma levels of AM are elevated during many human disease conditions, including cardiovascular disease. This elevation of AM during cardiovascular disease most likely serves as a protective mechanism considering that previous studies using animal models have revealed that AM is beneficial in many forms of cardiovascular disease. These findings have generated interest in examining the usefulness of plasma AM as a biomarker during human cardiovascular disease events and have sparked queries investigating whether SNPs within *Adm* alter cardiovascular disease risk. Finally, since AM signals via a pharmacologically-tractable GPCR-RAMP interface, the AM signaling system pathway may provide a unique opportunity to provide therapies for a wide range of human conditions.

Figures

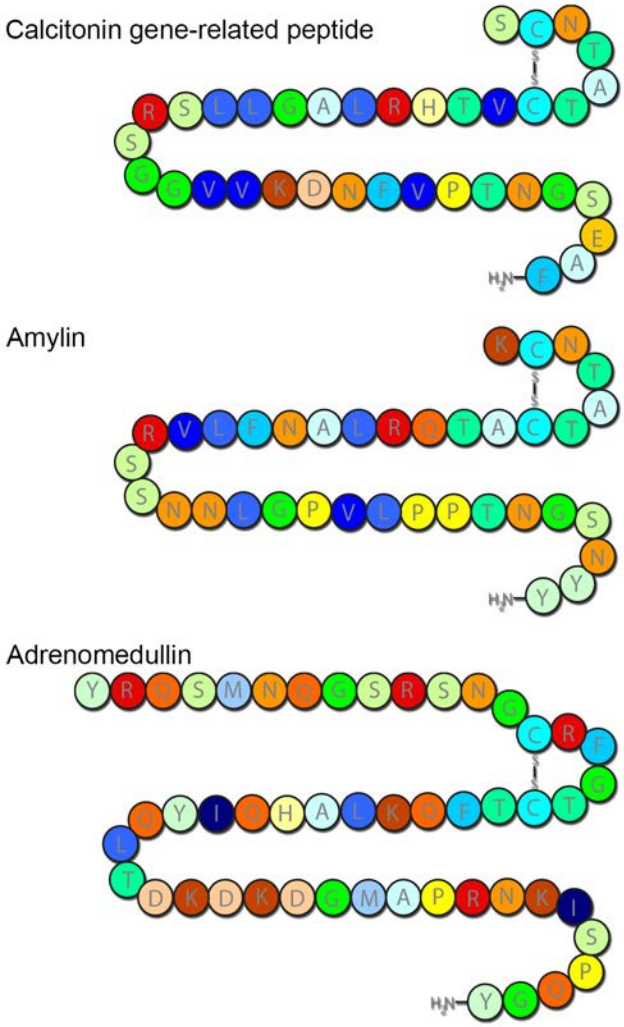

FIGURE 1.1. Peptide sequences for members of the calcitonin gene-related peptide family.
Amino acid sequences for the members of the calcitonin gene-related peptide (CGRP) family are depicted. Each member shares a conserved disulfide bond between cysteine residues, forming a ring-like structure. Additionally, biological activity of each peptide is dependent on amidation of the C-terminus. Letters depict individual amino acids.

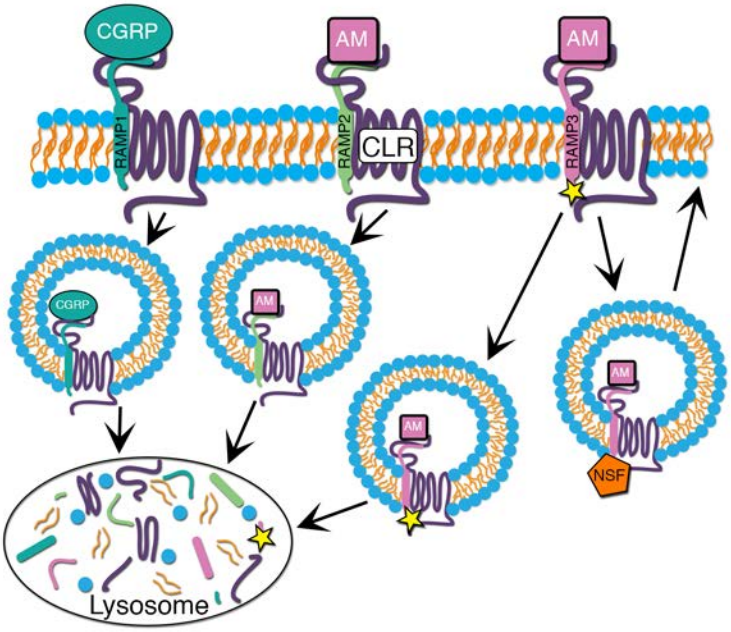

FIGURE 1.2. Receptor activity-modifying protein function in AM signaling.
Interaction of the GPCR calcitonin receptor-like receptor (CLR) with either receptor activity-modifying protein (RAMP) -2 or -3 results in a receptor for adrenomedullin (AM). However, the association of CLR with RAMP1 produces a receptor for calcitonin gene-related peptide (CGRP). Unlike the other RAMPs, RAMP3 contains a PDZ domain (depicted as a star in the above diagram), which allows for interaction with N-ethylmaleimide Sensitive Factor (NSF) and recycling of the receptor complex back to the cell surface. Without the interaction with NSF, the RAMP-receptor complex is targeted for degradation in the lysosome.

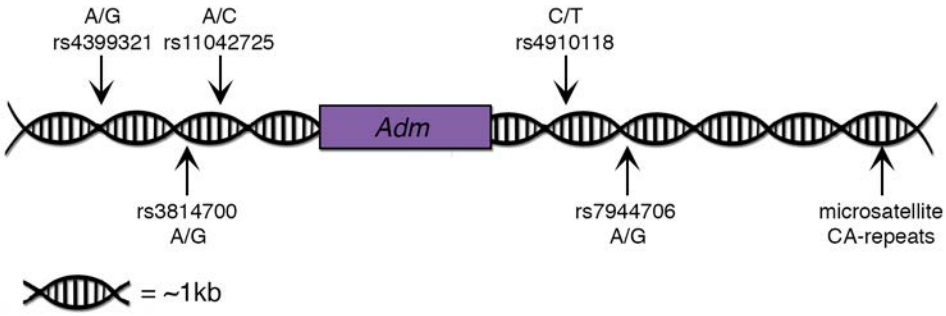

FIGURE 1.3. Single nucleotide polymorphisms located near human *Adm* gene correlated with disease.
Approximate location of single nucleotide polymorphisms (SNPs) near the human *Adm* gene that have been associated with several human diseases. The major and minor alleles are designated above or below each SNP as such: major/minor.

CHAPTER II: THE EPICARDIUM DURING CARDIAC DEVELOPMENT AND DISEASE

Overview

The epicardium plays a critical role in regulating many aspects of cardiac development. Recently, the reactivation of the epicardium during cardiovascular disease has become an area of intense interest due to the regenerative and repair possibilities. This chapter provides an overview of the formation of the epicardium, as well as the function of the epicardium during development and disease.

Origin of the epicardium

During the initial stages of cardiac development, the heart consists of two cell layers: the myocardium and the endocardium. However, by mid-gestation, a third layer of cells enveloping the exterior wall of the heart appears, referred to as the epicardium (**Figure 1**). Prior to the late 1970s, whether the epicardium originated from pre-existing cardiac cells or was derived from an extracardiac source remained unknown. To address this question, Ho and Shimada (83) used scanning electron micrographs to show the migration pattern of epicardial cells over the myocardium. These images revealed that epicardial cells originated from mesothelial cells located in the sinus venosus (83), eventually termed the proepicardial organ (PEO). Since this initial discovery, other groups have corroborated these findings (235), solidifying the PEO as the origin of epicardial cells.

Although the origin of the epicardium was now clear, the signaling pathways that regulate the development of the PEO remained unclear. Work by Watt et al (241) identified the transcription factor GATA4 as a critical regulator of PEO formation. This study revealed that a loss of GATA4 resulted in severe cardiac defects and embryonic demise between e9.5 and e10.

Although GATA4 is expressed in several cell types of the developing heart, including cardiomyocytes and the endocardium, Watt et al found that the loss of GATA4 expression in the PEO seemed to contribute most profoundly to the observed cardiac defects (241). In particular, this study found that the PEO failed to form in embryos lacking GATA4 (241), thereby preventing the formation of the epicardium around the heart and contributing to the observed cardiac defects. Aside from this initial study, very little work has been done to further elucidate the signals required for proper PEO formation. Gaining insight into the underlying mechanisms specifying PEO formation from the primitive mesenchyme may provide valuable information underlying congenital cardiac defects, making this an important area of future study.

In addition to the proper formation of the PEO, proepicardial cells need to migrate from the PEO to the heart and adopt an epithelial morphology to initiate the formation of the epicardium. Therefore, many groups have focused on determining what signaling pathways play a role in regulating these essential processes. Early work performed by Hatcher et al revealed that the transcription factor Tbx5 inhibits migration of cells from the PEO to the heart (79), and thus, aberrant expression could hinder formation of the epicardium. Furthermore, Jenkins et al revealed an important role for retinoic acid X receptor alpha (RXRα) signaling in the outgrowth of proepicardial cells (92). In particular, this study found that formation of the epicardium was delayed in *RXR*$\alpha^{-/-}$ animals, due in part to the decreased migration of proepicardial cells towards the heart (92), potentially caused by increased fibronectin deposition in the PEO of *RXR*$\alpha^{-/-}$ animals. Additionally, signals from the myocardium also play an important role in directing proepicardial cell migration towards the heart. Using chick embryos, Ishii et al (89) determined that bone morphogenic protein (BMP) signals, in particular BMP2, from the atrioventricular junction on the inner curvature of the developing heart promote proepicardial cell migration from the PEO towards the heart. Together, these studies identify several factors important for directing proepicardial cell migration, although further studies are necessary to determine many

of the downstream factors that are responsible for this process.

Finally, proepicardial cells must acquire an epithelial phenotype in order to properly generate the epicardium. To date, few studies have been conducted to elucidate the factors mediating this process. However, one study performed using frog embryos revealed an important role for the transcription factor Tcf21 in this process (219). This study found that the lack of Tcf21 prevented the maturation of proepicardial cells during the migratory process from the PEO towards the heart as indicated by elevated expression of vimentin (219). Additionally, proepicardial cells lacking Tcf21 failed to adhere to the heart properly, indicating improper maturation (219). Together, these data describe an important role for Tcf21-mediated regulation of genes required for the transition from a mesenchymal phenotype to an epithelial phenotype in the PEO. However, further studies to identify the downstream targets of Tcf21, as well as studies investigating the role of other genes in this transition, are warranted.

Roles of the epicardium during cardiac development

Several studies have revealed critical roles for the epicardium in cardiac development. Specifically, epicardial cells play an important role in the regulation of cardiomyocyte proliferation in the compact zone (120, 128, 180) and also undergo epithelial to mesenchymal transition (EMT) to populate the developing heart with fibroblast cells and ensure development of the coronary vessels (7, 38, 136, 147, 208, 220). The following paragraphs will delve into some of the identified regulators of these processes.

Disruption of epicardial formation promotes many cardiac defects, including the appearance of a thin compact zone (180). Numerous studies have determined that the epicardium regulates the expression of several growth factors, which in turn act on cardiomyocytes in the compact zone to promote cell proliferation (120, 128). To date, several members of the fibroblast growth factor (FGF) family have been implicated in compact zone expansion (120, 180). The earliest of these studies, performed by Pennisi et al in 2003 (180) in

chick embryos, identified FGF2 as an important regulator of compact zone cell cycle progression. Interestingly, this study found that FGF2 is produced primarily by the cardiomyocytes; however the epicardium plays an important role in regulating FGF2 levels (180). Although the mechanisms by which the epicardium regulates FGF2 expression in the cardiomyocytes were not elucidated in this study, this finding is interesting nonetheless. Work performed by Lavine et al (120) demonstrated that epicardial-derived FGF9 promotes cardiomyocyte proliferation in the underlying myocardium by acting on the c-splice forms of FGF receptor (FGFR)-1 and -2. Furthermore, Lavine et al demonstrated that FGF16 and FGF20, which are in the same family as FGF9, are also able to induce cardiomyocyte proliferation through the same receptors (120). The results from this study underscore the widespread and redundant involvement of FGF signals in the regulation of compact zone proliferation. Recent work by Li et al has revealed that growth factors other than the FGFs are produced by the epicardium to regulate cardiac development (128). Specifically, this study identified insulin-like growth factor (IGF) 2 as an epicardial-derived mitogen that contributes to cardiomyocyte proliferation during development (128). This study also revealed that the loss of the IGF receptors, specifically IGF1R and INSR, from the cardiomyocytes produced a similar phenotype to mice lacking IGF2 (128), indicating that IGF2 secreted from the epicardium acts directly on the myocardium to regulate compact zone development. Together, these studies, summarized in Figure 2, demonstrate that the epicardium is critical for producing and regulating several mitogenic factors to control cardiac development, particularly the proliferation of the cardiomyocytes in the compact zone.

With the realization that the epicardium produces mitogenic factors, researchers have sought to identify upstream factors that control the production of these factors in the epicardium. Several groups have demonstrated that retinoic acid signaling is critical for proper cardiac development (30, 92, 149). Specifically, these studies have revealed that retinoic acid signaling is essential for proper migration of proepicardial cells and for proper formation of the epicardium

(92). Additionally, retinoic acid signaling in the epicardium is essential for mediating expression of epicardial-derived growth factors and promoting proper proliferation of the cardiomyocytes in the compact zone (30, 149). Along these lines, Guadix et al determined that retinaldehyde dehydrogenase 2 (RALDH2), which is critical for the synthesis of retinoic acid, is directly regulated by the transcription factor, Wt1 (74). Early studies of Wt1 knockout mice revealed that this gene plays a critical role in cardiac development, as the loss of Wt1 during embryonic development resulted in an overall reduction in heart size and thinned ventricular walls, ultimately contributing to embryonic demise between e13.5 and e15.5 (115). Further work performed by Moore et al (154) demonstrated that Wt1 expression is restricted to the proepicardium and epicardium in the thoracic cavity and that the lack of Wt1 inhibited the migration of proepicardial cells towards the heart, resulting in incomplete formation of the epicardium. Together, these studies indicate that regulation of retinoic acid signaling is one mechanism by which Wt1 modulates cardiac development, as shown in Figure 2.

Besides its importance in regulating expansion of the compact zone myocardium, the epicardium is also critical for populating the heart with fibroblasts and is an important contributor to coronary vessel development (182). These processes rely heavily on the assumption of a mesenchymal phenotype by the epicardial cells through EMT. Some of the factors that have been implicated in coronary vessel and cardiac fibroblast formation from the epicardium are highlighted herein.

Given the importance of epicardial EMT in proper cardiac development, several groups have sought to define the factors regulating this process. One study found that the growth factor platelet-derived growth factor-BB (PDGF-BB) promoted epicardial EMT and resulted in the formation of coronary vascular smooth muscle cells (VSMC) (136). This study went on to determine that PDGF-BB promoted these effects through rhoA-RhoK-dependent activation of serum-response factor (136). Another factor important for regulating the process of EMT in epicardial cells is neurofibromin 1 (Nf1) (7). In this study, Baek and Tallquist demonstrated that

Nf1 acts to impede EMT in epicardial cells (7). In particular, Baek and Tallquist found that loss of Nf1 enhanced ERK signaling and resulted in the premature transition of epicardial cells into a mesenchymal lineage (7). Together, these studies provide some insight into the signaling pathways regulating the process of epicardial EMT.

Invasion of epicardial-derived cells (EPDC) following EMT is an important process for the proper formation of the coronary vasculature and cardiac fibroblasts. In addition to its role in EMT, Nf1 has also been linked to the invasion of EPDCs (7). Another factor that has been implicated in modulating EPDC invasion is Nfatc1 (38). This study found that the loss of Nfatc1 from the epicardium reduces the extent of migration of both fibroblasts and VSMCs from the epicardium into the myocardium (38), potentially attributed to reduced expression of cathepsin K, and thus inhibited extracellular matrix degradation. Finally, the transcription factor hypoxia-inducible factor 1-alpha (HIF-1α) has also been identified as an important factor for regulating EPDC invasion (220). Specifically, constitutive over-expression of HIF-1α inhibited migration of EPDCs into the myocardium; however, migration into the sub-epicardial space appeared to be largely unaffected (220). This study indicates that increased Flt-1 expression, and therefore decreased VEGF signaling to the EPDCs, represents one mechanism underlying the impaired invasion of EPDCs by HIF-1α (220). These studies highlight the multifaceted regulation of EPDC migration and underscore the importance of ensuring proper regulation of this process. Additionally, since the epicardium is a hypoxic environment (113), these studies begin to examine how the activation of hypoxia-related genes influences cardiac development.

Some studies have described how the fate of an EPDC determines which signaling pathways are activated to regulate EMT and the subsequent invasion into the myocardium (147, 208). For example, several studies have highlighted the importance of PDGF signaling in the regulation of epicardial EMT and subsequent invasion into the underlying myocardium (7, 136, 147, 208). However, these studies have demonstrated that PDGF signaling through different

PDGF receptor isoforms has different implications on cardiac development. For instance, Mellgren et al determined that PDGF signaling via the beta isoform of the PDGF receptor (PDGFRβ) is essential for migration of coronary VSMCs derived from the epicardium, although EMT does not seem to be altered in this case (147). On the other hand, Smith et al found that PDGF signaling through the alpha isoform of the PDGF receptor (PDGFRα) was required for the formation and migration of cardiac fibroblasts from the epicardium (208). Although it remains to be determined how epicardial cells are assigned a particular fate, these studies identify one mechanism by which migration of these EPDC is regulated.

Lastly, work by several groups has described the importance of coordinated crosstalk between the myocardium and epicardium for the regulation of coronary vascular development. Specifically, Lavine et al noted that, in addition to its role in regulating cardiomyocyte proliferation (120), FGF9 is crucial for regulating coronary vascular development (119). This study found that FGF9 produced by the epicardium acts on the cardiomyocytes to activate sonic hedgehog (Shh) signaling in the epicardium through an unidentified mediator (119). Ultimately, Shh acts on the myocardium to stimulate VEGF production and release (119). Since studies have shown an important role for VEGF in epicardial EMT (161) and coronary vessel development (221), activation of these pathways play an important role in proper development of the vasculature, as shown in Figure 3.

Potential actions of epicardium during disease

After an insult to the heart, several changes occur, including a reversion back towards a fetal gene program (191). Normally, the epicardium is quiescent in the adult (206); however, several studies have demonstrated that after injury, the epicardium is re-activated (124, 130, 252) reflecting the shift towards a more fetal phenotype. This reactivation promotes the invasion of EPDCs into the injured myocardium to promote revascularization and scar formation.

Therefore, the pathways highlighted in the previous section and newly identified pathways may play an important role in the response to injury.

Cardiac interstitial fibroblasts are largely derived from the epicardium and contribute to scar formation after injury. Generally, scar formation is viewed as a detrimental repair process that ultimately contributes to declining heart function after injury. However, work by Duan et al (52) demonstrates that scar formation is essential for preserving heart function immediately after ischemia-reperfusion injury. Specifically, this study reveals that production of cardiac fibroblasts by epicardial EMT is essential for maintaining cardiac function in a Wnt/β-catenin-dependent fashion (52). In addition to the role of Wnt signaling in scar formation, studies by Russell et al (194) have described a role for Notch signaling in activation of the epicardium following injury, leading to epicardial EMT and scar formation. Together, these studies describe some of the pathways regulating scar formation in adult hearts following injury and may provide insight into useful therapeutic targets to obtain an optimal balance between scar formation to preserve heart function immediately following injury and preserving long-term cardiac function.

Several studies have also suggested that the epicardium may be a source of cardiac stem cells. Early studies by Limanan et al (131) determined that a subset of epicardial cells in both human and mouse are positive for stem cells markers, including the marker c-kit. Following myocardial infarction, the number of cardiac stem cells increased, and these cells were found to co-express transcription factors necessary for differentiation into either cardiomyocytes or endothelial cells (131). More recent work by Di Meglio et al (49) indicates that the process of EMT after injury is able to promote the formation of c-kit-positive stem cells, in addition to other cell types. These studies suggest that activation of the epicardium may introduce stem cells in the injured myocardium, potentially providing an opportunity to repair the injured heart. However, in order to successfully repopulate the heart with cardiomyocytes using resident stem cells, several hurdles and remaining questions need to be addressed. For instance, the current studies suggest that the number of resident stem cells in the heart is low, and therefore, the

number of stem cells produced by the heart needs to be greatly enhanced to facilitate repair. Additionally, these stem cells need to be present and activated in the heart after the injury has been stabilized by scar formation, which may prove challenging. Finally, the signals promoting the preferential formation of cardiomyocytes from the stem cells need to be carefully characterized to ensure repopulation of the injured area with viable cardiomyocytes.

Finally, some studies have indicated that epicardial-derived cells are capable of differentiating into cardiomyocytes (18, 254); however, these findings have been subject to debate (33, 182). Although these lineage tracing experiments cannot conclusively determine whether epicardial cells may contribute directly to the formation of cardiomyocytes during development, there has still been interest in determining whether epicardial-derived cardiac progenitor cells in the adult can differentiate into cardiomyocytes following injury to promote cardiac repair. Smart et al (207) found that reactivation of the epicardium by thymosin β4 prior to injury allowed for the formation of new cardiomyocytes from the activated epicardium. However, this result appears to be dependent on the epicardium being reactivated prior to injury, as work by Zhou et al (253) found that activation of the epicardium by thymosin β4 after myocardial infarction did not promote cardiomyocyte differentiation from the activated epicardium. Thus, in the context of human disease, utilizing the activated epicardium to regenerate the damaged myocardium may prove to be futile.

Summary

In conclusion, many studies have demonstrated a critical role for the epicardium during cardiac development. These studies have demonstrated that the epicardium is critical for regulating cardiomyocyte proliferation in the compact zone through the production of growth factors. Additionally, cells from the epicardium undergo EMT and migrate into the heart to populate the heart with interstitial fibroblasts and cover the vessels with smooth muscle. Recent

work has suggested that the epicardium plays an important role in the adult heart following injury. Given that the adult epicardium is normally quiescent and must be re-activated to a fetal-like state following injury, a thorough understanding of the factors that regulate epicardial function during development is essential for manipulating the epicardium for therapeutic use. Finally, whether the epicardium is a source of resident cardiac stem cells needs to be investigated further and potentially exploited for repair following myocardial infarction.

The studies presented in this dissertation explore the role of AM during cardiovascular development and disease. The first portion of this dissertation characterizes the effect of AM over-expression on cardiac development. This study found that epicardial-derived AM drives cardiac hyperplasia during embryogenesis. A second study presented herein investigates sex-dependent differences in cardiac AM expression and explores the importance of estrogen-induced microRNAs in balancing *Adm* expression in female hearts. The final study presented in this dissertation begins examining the impact of AM over-expression in the context of chronic hypertension by crossing the AM over-expression line to the renin transgenic mouse line. This study did not find any differences in disease progression with AM over-expression. However, renin transgenic animals with wildtype levels of AM failed to progress as previously described, thereby making final interpretation of the effect of AM over-expression on chronic hypertension difficult. Overall, these studies further define the role of AM in the cardiovascular system during development and provide insight into some potential mechanisms underlying the cardioprotective potential of AM during disease.

Figures

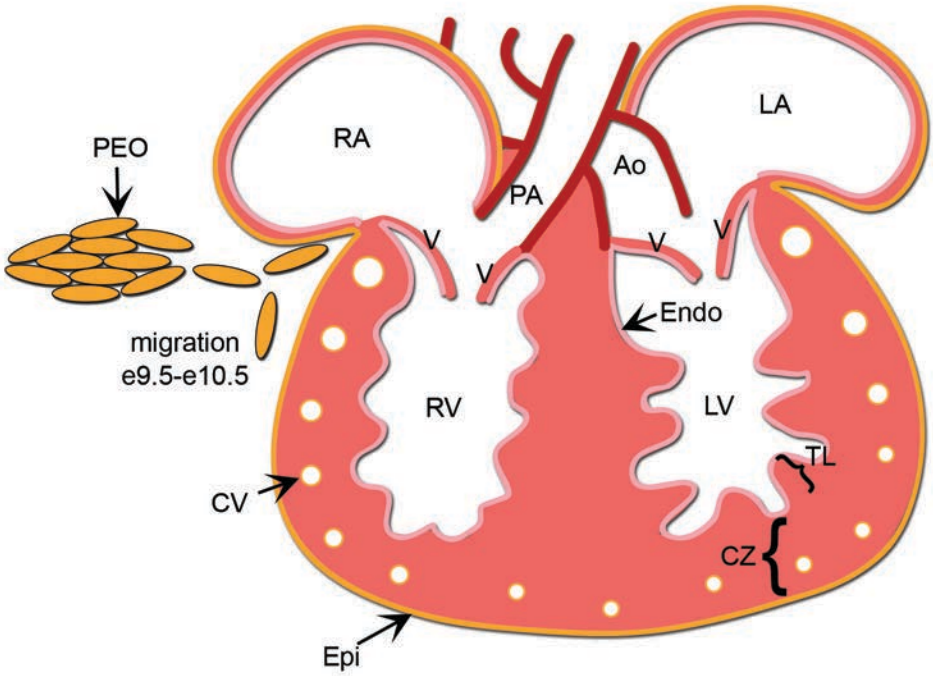

FIGURE 2.1. Schematic of major cardiac structures.
Cells from the proepicardial organ (PEO), located near the atrio-ventriculatr junction, migrate towards the heart beginning around embryonic stage 9.5 (e9.5) in mice. By e10.5, the epicardium completely encapsulates the ventricles. Factors produced by the epicardium regulate cardiomyocyte proliferation in the compact zone. Additionally, the epicardium is crucial for proper coronary vessel development. PEO = proepicardial organ; RA = right atria; LA = left atria; PA = pulmonary artery; Ao = aorta; V = valve; RV = right ventricle; LV = left ventricle; Endo = endocardium; CV = coronary vessel; TL = trabecular layer; CZ = compact zone; Epi = epicardium

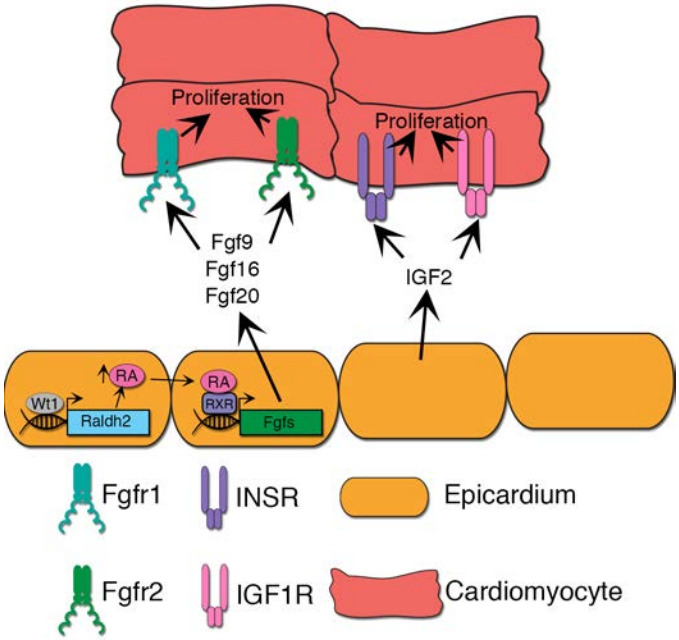

FIGURE 2.2. Epicardial regulation of cardiomyocyte proliferation during development. The epicardium produces and secretes several growth factors, including insulin-like growth factor 2 (IGF2) and several members of the fibroblast growth factor (FGF). For members of the FGF family, the transcription factor Wilm's tumor 1 (Wt1) has been shown to increase retinoic acid (RA) production and signaling by enhancing transcription of retinaldehyde dehydrogenase 2 (Raldh2), which ultimately increases FGF transcription. Once secreted from the epicardium, these growth factors then act on the appropriate receptor on cardiomyocytes in the compact zone to induce proliferation. Fgfr1 = fibroblast growth factor receptor 1; Fgfr2 = fibroblast growth factor receptor 2; INSR = insulin receptor; IGF1R = insulin-like growth factor 1 receptor; WT1 = Wilm's tumor 1; Raldh2 = retinaldehyde dehydrogenase 2; RA = retinoic acid; RXR = retinoid X receptor; Fgf = fibroblast growth factor; IGF2 = insulin-like growth factor 2

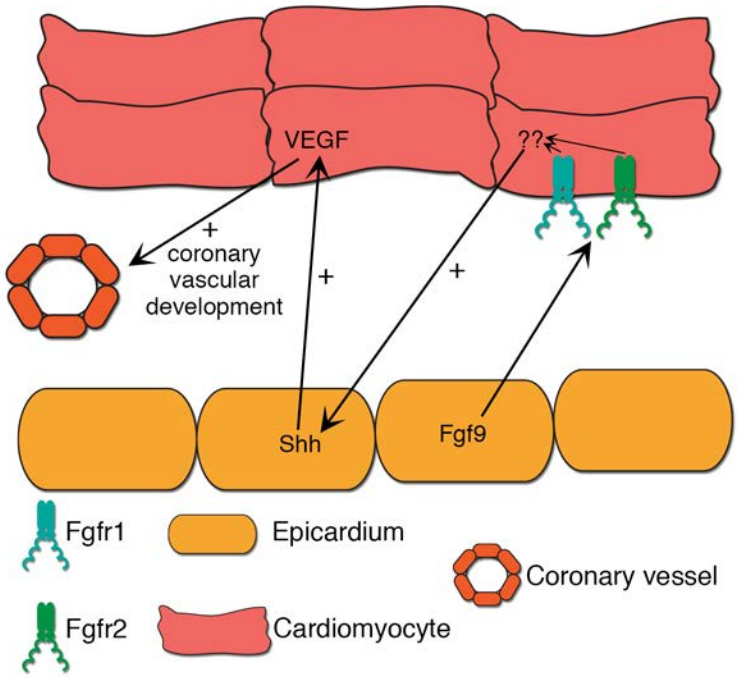

FIGURE 2.3. Sonic hedgehog-VEGF pathway crosstalk in coronary vascular development.
Crosstalk between the epicardium and myocardium regulates coronary vasculature development by the activation of the sonic hedgehog (Shh) and vascular endothelial growth factor (VEGF) pathways. Fgf9 signaling on the myocardium initiates this signaling cascade, however the intermediate player of this cascade is currently unknown. Fgf9 = fibroblast growth factor 9; Shh = sonic hedgehog; VEGF = vascular endothelial growth factor; FGFr1 = fibroblast growth factor receptor 1; Fgfr2 = fibroblast growth factor receptor 2

CHAPTER III: EPICARDIAL-DERIVED ADRENOMEDULLIN DRIVES CARDIAC HYPERPLASIA DURING EMBRYOGENESIS[1]

Overview

Background: Growth promoting signals from the epicardium are essential for driving myocardial proliferation during embryogenesis. In adults, these signals become reactivated following injury and promote angiogenesis and myocardial repair. Therefore, identification of such paracrine factors could lead to novel therapeutic strategies. The multi-functional peptide adrenomedullin (*Adm*=gene, AM=protein) is required for normal heart development. Moreover, elevated plasma AM following myocardial infarction offers beneficial cardioprotection and serves as a powerful diagnostic and prognostic indication of disease severity. **Results:** Here, we developed a new model of *Adm* over-expression by stabilizing the *Adm* mRNA through gene-targeted replacement of the endogenous 3' UTR. As expected, $Adm^{hi/hi}$ mice express three-times more AM than controls in multiple tissues, including the heart. Despite normal blood pressures, $Adm^{hi/hi}$ mice unexpectedly showed significantly enlarged hearts due to increased cardiac hyperplasia during development. The targeting vector was designed to allow for reversion to wildtype levels via Cre-mediated modification. Using this approach, we demonstrate that AM derived from the epicardium, but not the myocardium or cardiac fibroblast, is responsible for driving cardiomyocyte hyperplasia. **Conclusions:** AM is produced by the

[1]This chapter previously appeared as an article published in Developmental Dynamics and is reprinted with permission. The original citation is as follows: Wetzel-Strong SE, Li M, Klein KR, Nishikimi T, and Caron KM. (2014), Epicardial-derived adrenomedullin drives cardiac hyperplasia during embryogenesis. *Dev Dyn*. 243: 243-256. doi: 10.1002/dvdy.24065

epicardium and drives myocyte proliferation during development, thus representing a novel and clinically-relevant factor potentially related to mechanisms of cardiac repair after injury.

Introduction

Recently, many exciting connections between factors that regulate myocardial development and those that are elevated during myocardial injury have been appreciated (46). Central to these connections are the unique roles of the epicardium during embryogenesis and the newly emerging concept that the epicardium becomes reactivated—re-expressing fetal genes—during disease processes (68). For example, studies in zebrafish and mice have shown that the epicardium is required for maintenance of myocardial proliferation during embryogenesis through several growth promoting signaling pathways including Raldh2, Wt-1, IgF, FGF and b1 integrin (30, 47, 86, 102, 120). During cardiac injury, many of these same growth promoting factors become stimulated such that the potential of the epicardium to contribute to heart regeneration and repair is restored from its normally adult quiescent state (84, 233). Several recent studies have begun to elucidate the pleiotropic roles for epicardial-derived cells (EPDCs) in the formation of numerous cardiac cell types, including coronary endothelial and smooth muscle cells, cardiac fibroblasts, heart valves and perhaps even cardiomyocytes (46, 68). However, it is also evident that an important function of the epicardium is to secrete paracrine factors that promote angiogenesis, myocardial regeneration and cardiac fibroblast proliferation (52, 206). Therefore identifying new factors that exhibit these dual roles of supporting both embryonic and injured heart growth is a desirable and clinically promising area of research.

In this study, we find that adrenomedullin peptide, secreted from the epicardium, is a potent regulator of cardiomyocyte proliferation during embryogenesis. Since the discovery of adrenomedullin (protein = AM, gene = *Adm*) in 1993 (108), many diverse biological functions have been described for this small circulating peptide during development, normal physiology

and disease (25, 97). We, and others, have previously shown that genetic deletion of the highly conserved *Adm* gene in mice causes embryonic lethality at mid-gestation (24, 203, 204). The most prominent phenotype of *Adm*$^{-/-}$ embryos is their extreme hydrops fetalis, or interstitial edema, which we have attributed to a marked arrest of lymphatic endothelial cell proliferation and lymphangiogenesis at mid-gestation (59). However, the expression of *Adm*, although enriched in lymphatic endothelial cells, is not restricted. Indeed, the earliest and most robust expression of *Adm* can be observed in the heart at around e8.0 (24, 152, 153). Consequently, we found that *Adm*$^{-/-}$ mice also have small hearts characterized by enhanced trabeculation and a thin compact zone (24). Furthermore, loss of either the receptor for AM, calcitonin receptor-like receptor (*Calcrl*) (42), or the receptor modifying protein *Ramp2* (59) results in a phenocopy of the *Adm*$^{-/-}$ phenotype. Taken together, the highly conserved and robust cardiac phenotypes of mice with genetic deletion of AM signaling components demonstrates the essential function of AM in promoting embryonic heart development.

A multitude of clinical studies have also shown that circulating levels of AM are elevated two- to three-fold above basal levels during a variety of human disease conditions (97). Recently, the robust surge in plasma AM levels during cardiovascular disease is being used as a clinical diagnostic tool. The pro-hormone form of AM, mid regional pro-AM (MRpro-AM), is a highly effective clinical biomarker of patient prognosis following heart attack, providing greater sensitivity than traditional biomarkers such as atrial natriuretic peptide (ANP) and B-type natriuretic peptide (BNP) (48, 141, 142). In addition, AM also offers protection from cardiovascular disease. Several studies using mice haploinsufficient for *Adm*, have clearly demonstrated an exacerbation of cardiovascular disease with a reduction in basal levels of AM (20, 203), highlighting the importance of circulating AM in controlling the extent of damage. Additionally, animal studies examining the impact of AM infusion on cardiovascular disease progression have revealed a protective effect of AM on disease progression (170, 190). Furthermore, a limited number of studies performed in human patients have demonstrated that

infusion of AM after a cardiovascular incident is associated with a reduction in the degree of damage (98, 159, 166). However, since these studies have relied on the infusion of AM, it remains unclear whether the physiological 3-fold increase of circulating AM during cardiovascular disease has any direct or protective implications.

Therefore, we sought to develop a mouse model that recapitulates the plasma elevation of AM observed during human disease as a useful tool for elucidating the precise functions of AM in cardioprotection. Herein, we describe the successful generation of a novel mouse model of *Adm* over-expression that was intentionally designed to conserve the endogenous promoter regulatory elements of the gene, with the added capability of reversing the over-expression by Cre-LoxP strategies. Surprisingly, we discovered that these animals have enlarged hearts due to cardiac hyperplasia during development—a phenotype that was reversed when high AM levels from the epicardium were genetically restored to basal levels.

Results

Transcriptional and translational up-regulation of Adm expression in $Adm^{hi/hi}$ mice.

We recently described the generation of the $Adm^{hi/hi}$ mice by gene targeting techniques which allowed for the stabilization the *Adm* mRNA half-life by the bovine growth hormone 3′ untranslated region (UTR) (126). Previous *in vitro* studies predicted that this modification would stabilize the mRNA transcript of *Adm* by approximately 3.5-fold compared to the native transcript, while still allowing for endogenous regulation of *Adm* gene expression by its native 5′UTR promoter region (93). Here we show that *Adm* mRNA transcript levels, as measured by quantitative (q)RT-PCR, were statistically increased by approximately 3- to 15-fold in $Adm^{hi/hi}$ mice compared to wildtype control animals in ten different tissues at 4 months of age (**Figure 1A**). Moreover, a radioimmunoassay for total AM peptide levels revealed a statistically significant ~3-fold increase in AM peptide levels from kidney and lung extracts (**Figure 1B**). Analysis of circulating AM in the blood plasma of 4 month old animals by a fluorescent EIA

method also showed a significant 2- to 3-fold increase in *Adm*$^{hi/hi}$ animals compared to wildtype littermates (**Figure 1C**). Thus, the 3′UTR gene targeting approach successfully recapitulated the increases in *Adm* mRNA and peptide expression at a level that is comparable to that observed in human patients with cardiovascular disease and myocardial infarction.

***Enhanced Adm expression in developing heart of Adm*$^{hi/hi}$ mice.**

Previous studies have shown the developing embryonic mouse heart expresses *Adm* as early as e8.0 and this expression persists throughout development and into adulthood (24, 153). Using immunohistochemistry, we find that endogenous levels of AM peptide expression are localized to the epicardium, with very low levels of expression in the compact zone and trabeculae at e13.5 (**Figure 2A,C**). Similarly, *Adm*$^{hi/hi}$ mice showed this same spatiotemporal pattern, but as expected, using semi-quantitative imaging, we observed a robust and marked increase in AM expression from the epicardium and trabeculae compared to wildtype *Adm*$^{+/+}$ animals (**Figure 2B,D**). By assessing the integrated density of AM at the epicardium, we confirmed that *Adm*$^{hi/hi}$ embryos express higher levels of AM compared to wildtype controls (**Figure 2E**). We also confirmed that AM is expressed in the epicardium by staining adjacent sections for AM and cytokeratin (**Figure 2F,G**), which has been previously characterized as a marker of the epicardium (180, 236). This staining clearly demonstrates that AM is predominantly and robustly expressed in the epicardium, and to a much lesser extent in the myocardium. Another prominent feature of *Adm*$^{hi/hi}$ hearts that can be appreciated from these images is the apparently larger size of the ventricle compared to *Adm*$^{+/+}$ hearts viewed at the same magnification (compare **Figures 2A** and **2B**).

Adm*$^{hi/hi}$ *mice have enlarged, hyperplastic hearts.

Unexpectedly, we discovered that 2 month old *Adm*$^{hi/hi}$ mice had remarkably and visibly enlarged hearts compared to wildtype controls (**Figure 3A**). Heart weight to body weight

(HW:BW) ratios (**Figure 3B**), as well as heart weight to tibia length (HW:TL) ratios (**Figure 3C**) were significantly increased compared to wildtype control mice. Individual chamber dissections revealed that both ventricles and atria of *Adm*$^{hi/hi}$ hearts were significantly enlarged compared to those of littermates (**Figure 3D**).

Since either hypertrophic or hyperplastic mechanisms could contribute to enlargement of the heart, we used histological techniques to evaluate cardiomyocyte size and density. We found no difference in the cardiomyocyte cross-sectional area between wildtype and *Adm*$^{hi/hi}$ animals, suggesting that the enlarged hearts of *Adm*$^{hi/hi}$ animals were not hypertrophic (**Figure 4A**). This conclusion was further supported by quantitation of cardiomyocyte cellular density from wheat germ agglutinin stained sections, which also revealed no difference in cellular myocyte density between *Adm*$^{hi/hi}$ animals and wildtype controls (**Figure 4B,C**). Additionally, qRT-PCR analysis of the pro-hypertrophic genes, *Anp* and *Bnp,* showed no significant differences between wildtype and *Adm*$^{hi/hi}$ animals (*Anp* expression = 1.20±0.3 versus 1.87±0.3; *Bnp* expression = 1.07±0.2 versus 1.83±0.4 for wildtype and *Adm*$^{hi/hi}$, respectively), further confirming that *Adm*$^{hi/hi}$ hearts are not hypertrophied. Finally, using isolectin staining, we also found no significant differences in vascular morphology or density between *Adm*$^{hi/hi}$ animals and control animals (**Figure 4B,C**). Based on these analyses, it was evident that the *Adm*$^{hi/hi}$ hearts were enlarged due to hyperplasia, not hypertrophy—a conclusion that is further supported by the fact that *Adm*$^{hi/hi}$ mice do not have elevated blood pressures (**Figure 4D**).

Since *Adm* expression is prominently enriched in the heart during embryogenesis (Figure 2), we performed BrdU incorporation studies to quantitate the number of proliferating cells in the hearts of wildtype and *Adm*$^{hi/hi}$ embryos. We assessed proliferation at six different time points of embryonic development, and importantly found that *Adm*$^{hi/hi}$ embryos always had more BrdU-positive cells per normalized field compared to wildtype, with significant differences in five out of six time points (**Figure 5A** and **5B**). From this analysis, it is also interesting to note that the shape of the proliferation curve for *Adm*$^{hi/hi}$ animals recapitulates the shape of the curve

exhibited by wildtype animals (see Figure 5B), indicating that *Adm*$^{hi/hi}$ hearts are still appropriately responding to signals responsible for regulating proliferation rates during development.

To further confirm this developmental hyperplasia, we stained e12.5 hearts with phospho-Histone H3 (**Figure 5C**), a less prevalent proliferation marker, and the cardiomyocyte marker, cardiac troponin T (cTnT). Consistent with the BrdU staining, we found a statistically significant increase in the level of phospho-Histone H3 labeling in *Adm*$^{hi/hi}$ hearts compared to wildtype littermates (**Figure 5C**). Moreover, by co-staining with cTnT, we could easily identify the phospho-Histone H3-positive cells as cardiomyocytes, by identifying phospho-H3-positive nuclei that were surrounded by cTnT signal, as indicated by the asterisks in the 40x images in Figure 5C. Finally, we also compared the overall heart size of wildtype and *Adm*$^{hi/hi}$ animals at the level of the ventricular valves at e15.5 and as expected, the enhanced levels of proliferation in *Adm*$^{hi/hi}$ hearts resulted in a visible enlargement in the heart size of *Adm*$^{hi/hi}$ embryos (**Figure 5D**).

High AM drives the cardiomyocyte cell cycle.

Cyclins and cyclin dependent kinases are critical for maintaining normal cardiomyocyte proliferation during development. Therefore, we further confirmed the accelerated degree of proliferation in *Adm*$^{hi/hi}$ hearts by assessing protein levels of cyclin B_1 and cyclin D_1 by Western blotting of postnatal day 1 heart lysates. Our choice of postnatal day 1 tissue for these assays was based on the need to isolate sufficient amounts of protein for Western analysis but furthermore allowed us to interrogate whether the hyperplasia of *Adm*$^{hi/hi}$ animals persists through the end of the proliferative phase of cardiac development. This analysis revealed a significant elevation of both cyclin B_1 and cyclin D_1 protein in the hearts of *Adm*$^{hi/hi}$ pups compared to wildtype (**Figure 5E**), even during the early postnatal period. As in the late stages of embryonic heart development, the proliferation rates in *Adm*$^{hi/hi}$ hearts are modestly, but

significantly elevated compared to wildtype animals, further highlighting the responsiveness of proliferating cardiomyocytes in *Adm*$^{hi/hi}$ hearts to intrinsic regulators of the cell cycle.

To determine whether cells in *Adm*$^{hi/hi}$ hearts do indeed exit the cell cycle in a fashion comparable to wildtype animals, we also assessed proliferation in the hearts of 6-month old adult wildtype and *Adm*$^{hi/hi}$ animals by Ki67 staining. This analysis revealed that levels of proliferation are very low in the hearts of both wildtype and *Adm*$^{hi/hi}$ groups, and we found no significant difference in the degree of proliferation (data not shown), clearly demonstrating that the hyperplasia of *Adm*$^{hi/hi}$ animals is limited to the developmental period.

We sought to further confirm our *in vivo* data demonstrating that AM can act directly on cardiomyocytes to drive the cell cycle by treating HL-1 cells, a cardiomyocyte cell line, with AM peptide. We chose to use the HL-1 cell line since previous studies have demonstrated that these cells retain many properties of adult cardiomyocytes in culture, including: cardiomyocyte-specific currents, gene expression profiles resembling adult cardiomyocytes, and the presence of cardiomyocyte-specific structures, such as intercalated discs (36). Additionally, HL-1 cells have the ability to proliferate in culture without losing these cardiomyocyte characteristics (36), unlike isolated neonatal cardiomyocytes. Thus, we treated the HL-1 cell line with 1nM AM or vehicle in serum-free media and measured cell counts. After 72-hours of treatment, there were significantly more HL-1 cells in the AM-treated conditions compared to vehicle–treated cells (**Figure 5F**), indicating that AM can directly drive the proliferation of cardiomyocytes. These data, along with our *in vivo* data, clearly demonstrate first, that AM can act directly on cells to drive proliferation, and second, that elevated AM promotes cardiac hyperplasia.

Reversion of the Adm^{hi} allele to basal levels reverses the cardiac hyperplasia.

The design of our targeting vector intentionally included loxP sites flanking the bGH 3′UTR stabilizing element to allow for tissue- and time-dependent reversion of high *Adm* levels back to wildtype levels (**Figure 6A**). To confirm that this approach was effective, we crossed the

$Adm^{hi/+}$ mice to the CMV-Cre line (201) to generate mice with a wildtype *Adm* allele, as well as a modified Adm^{hi} allele, referred to as $Adm^{3'\Delta}$. $Adm^{3'\Delta}$ heterozygous mice were then intercrossed, at which point the CMV-Cre transgene was selected against, in order to generate homozygous $Adm^{3'\Delta/3'\Delta}$ mice. By qRT-PCR, we found that $Adm^{3'\Delta/3'\Delta}$ mice express *Adm* at levels comparable to wildtype littermates (**Figure 6B**), confirming that removal of the stabilizing bGH 3′UTR element results in a reversion of *Adm* levels to near basal levels.

Importantly, this genetic modification also reversed the cardiac hyperplasia phenotype of $Adm^{hi/hi}$ mice. At 2 months of age, we assessed the HW:BW ratios of wildtype, $Adm^{hi/hi}$, and $Adm^{3'\Delta/3'\Delta}$ mice. We found that $Adm^{3'\Delta/3'\Delta}$ mice had HW:BW ratios that were significantly smaller than $Adm^{hi/hi}$ mice, and indistinguishable from those of wildtype mice (**Figure 6C**). Together, these data demonstrate the feasibility of genetically reversing the Adm^{hi} allele to normal levels, which is also associated with a reversal of the $Adm^{hi/hi}$ cardiac hyperplasia phenotype.

AM derived from Wt1-positive cells promotes enhanced heart size of $Adm^{hi/hi}$ mice.

Our next goal was to use this genetic approach to identify the cellular source of AM that drives the observed cardiac hyperplasia during development. After confirming that we would be able to detect a decrease in HW:BW with a global reduction in *Adm* expression, we proceeded to cross the $Adm^{hi/hi}$ mice to several different Cre mouse lines to assess the contribution of *Adm* from different cell types within the heart with respect to organ growth.

We began by assessing the contribution of cardiomyocyte-derived AM because the myocardium can release growth factors to regulate heart growth and development (234). Therefore, we crossed the $Adm^{hi/hi}$ mice to two independent cardiomyocyte-specific Cre lines, the Nkx2.5-Cre (156) and αMHC-Cre (3) lines. At 2 months of age, we found there was no significant difference in the HW:BW ratio of $Adm^{hi/hi}$ and Nkx2.5-Cre+: $Adm^{3'\Delta/3'\Delta}$ mice (**Figure 7A**). Additionally, we found no difference in the HW:BW ratio of $Adm^{hi/hi}$ and αMHC-Cre+:

Adm$^{3'\Delta/3'\Delta}$ mice (data not shown). Together, these two independent cardiomyocyte-specific Cre lines clearly indicate that cardiomyocytes are not the cellular source of AM driving the heart growth during development.

Tomoda et al. found that the non-myocyte fraction of the rat heart expressed approximately 2.5 times more *Adm* than the myocyte fraction, suggesting that cardiac fibroblasts are a major source of AM in the heart (222). Therefore, we crossed the *Adm*$^{hi/hi}$ mice to the Fsp-Cre (13) mouse line to reduce *Adm* to wildtype levels in fibroblasts. Once again, we found there was no significant difference between *Adm*$^{hi/hi}$ and Fsp-Cre+:*Adm*$^{3'\Delta/3'\Delta}$ mice at 2 months of age (**Figure 7B**), suggesting that cardiac fibroblasts are not a major producer of AM during embryonic heart development.

Finally, we sought to determine whether AM derived from the epicardium contributed significantly to heart development because many studies have described the importance of the epicardium in secreting paracrine growth factors that regulate heart growth (120, 128, 138), and our data demonstrate that the epicardium is a major source of *Adm* expression during embryogenesis (Figure 2). By crossing the Wt1$^{GFPCre/+}$ (254) mice to the *Adm*$^{hi/hi}$ line, we were able to generate mice with reduced *Adm* in the epicardium (**Figure 7D**). In this case, we discovered that Wt1$^{GFPCre/+}$: *Adm*$^{3'\Delta/3'\Delta}$ mice had HW:BW ratios that were significantly lower that *Adm*$^{hi/hi}$ animals, and not significantly different from wildtype animals (**Figure 7C**). We also stained adjacent sections of the left ventricle from these animals for cytokeratin, to mark the epicardium, and AM (**Figure 7D**). We found that AM co-localized with cytokeratin expression in the epicardium, further confirming the expression and contribution of epicardial-derived AM in heart development. These images also reveal that AM expression of *Wt1*$^{GFPCre/+}$*:Adm*$^{3'\Delta/3'\Delta}$ mice is reduced in the epicardium compared to *Adm*$^{hi/hi}$ animals (**Figure 7E**) and is similar to wildtype littermates, thereby verifying that we successfully reduced AM expression in the epicardium of these animals, resulting in the normalization of heart size. Finally, to further corroborate these findings, we assessed *Adm* gene expression levels using RNA extracted from 2-month old left

ventricle samples from *Adm*$^{hi/hi}$ and *Wt1*$^{GFPCre/+}$*:Adm*$^{3'\Delta/3'\Delta}$ mice. This experiment revealed that *Adm* expression levels are significantly reduced to near baseline values in *Wt1*$^{GFPCre/+}$*:Adm*$^{3'\Delta/3'\Delta}$ mice compared to *Adm*$^{hi/hi}$ animals (**Figure 7F)**. Since Cre recombinase is expressed specifically in the pro-epicardium and epicardium in the *Wt1*$^{GFPCre/+}$ line (254), we concluded that a reduction in *Adm* expression level is due to a normalization of *Adm* expression levels specifically in the epicardium. Although *Adm* expression levels were still elevated over wildtype levels in *Wt1*$^{GFPCre/+}$*:Adm*$^{3'\Delta/3'\Delta}$ animals, it is important to recognize that this difference can be attributed to the fact that other cell types in the heart, including cardiomyocytes and fibroblasts, are still over-expressing *Adm*. Since we have demonstrated that a reduction of *Adm* levels in cardiomyocytes and fibroblasts fails to affect the HW:BW ratios (Figure 7A and 7B), these data indicate that the epicardium is a major source of *Adm* that promotes cardiac hyperplasia in the *Adm*$^{hi/hi}$ line.

Discussion

With this unique gene targeted mouse model, we have identified AM as a powerful regulator of cardiac growth during embryogenesis. Importantly, we have been able to demonstrate that AM secreted from epicardial cells is important for driving the cardiomyocyte cell cycle and promoting enlargement of the heart during embryogenesis. Considering the numerous and high profile clinical studies which link elevated plasma AM levels following myocardial infarction with both disease severity and cardioprotection, we consider that AM fulfills the characteristics of a newly recognized epicardial-derived growth factor that may play important roles in cardiac repair and regeneration.

Most importantly, the pharmacological targeting of AM signaling is readily achievable through small molecule agonists and antagonists capable of binding to the unique interface formed between the AM receptor, calcitonin receptor-like receptor and receptor activity modifying protein (RAMP) 2 (5). Indeed this receptor- RAMP paradigm is already being

exploited by the pharmaceutical industry for the treatment of migraine pain associated with CGRP signaling (50, 198). Therefore, while the delivery of AM peptide has some limitations as a treatment strategy for myocardial infarction, activation of AM signaling through its unique G protein-coupled receptor paradigm is attainable.

In the literature, a limited number of mouse models have been reported that display cardiac hyperplasia (27, 81, 100, 183, 188, 227). Many of these mutant animals die during the late embryonic development or the early postnatal period (81, 100, 183, 188), which contrasts with this *Adm*$^{hi/hi}$ model, which survives into adulthood. This difference can, perhaps, be attributed to the presence of additional cardiac defects in some lines or differences in how the heart is enlarged. For example, many of these mouse lines display other cardiac abnormalities in addition to cardiomyocyte hyperplasia, including: ventricular septal defects (81, 100, 183), double outlet right ventricles (100), and dilated atria (183, 188). The *Adm*$^{hi/hi}$ mice do not display additional cardiac defects, which potentially explains why these mice are viable. Moreover, several of the other reported mouse lines displaying cardiac hyperplasia display a reduction in the luminal space of the ventricle due to a robust increase in the space occupied by the trabeculi as well as a drastic increase in the thickness of the compact layer (81, 100, 183, 188). Since the degree of trabeculation between wildtype and *Adm*$^{hi/hi}$ animals appears similar, the lumens of the *Adm*$^{hi/hi}$ mice remain unobstructed, allowing for normal heart function and viability of the mice.

We found that a reduction of *Adm* in the epicardium through the use of the Wt1$^{GFPCre/+}$ mouse line resulted in a reversion of the HW:BW ratio back to wildtype levels, indicating that the cardiac hyperplasia phenotype of the *Adm*$^{hi/hi}$ mice is caused by enhanced epicardial-derived AM. Some studies have indicated that Wt1 is expressed in a subset of cardiomyocytes during embryonic development (193), and therefore, the *Wt1*$^{GFPCre/+}$ line may promote recombination directly in the cardiomyocytes. Additionally, other groups have suggested that epicardial cells may differentiate into cardiomyocytes (18, 254), and thus the recombined genes from the cross

to the *Wt1*$^{GFPCre/+}$ line may be transmitted to the cardiomyocyte lineage. Therefore, it is possible that additional recombination in cardiomyocytes through one of these two mechanisms is contributing to the reduction of the HW:BW ratio in *Wt1*$^{GFPCre/+}$*:Adm*$^{3'\Delta/3'\Delta}$ mice. However, our data from two independent cardiomyocyte-specific Cre lines showing no reduction in HW:BW with reduced levels of AM expression in cardiomyocytes suggests that the contribution of cardiomyocyte-derived AM to the developmental hyperplasia observed in the *Adm*$^{hi/hi}$ line is minimal.

Our conclusion that the epicardium is a major contributor of AM during heart development is further supported by the similarities between the heart phenotype of *Adm*$^{-/-}$ mice (24) and animals with a disrupted epicardium (115, 117, 128, 180). Specifically, one characteristic of animals lacking an epicardium or with disrupted growth factor secretion from the epicardium is a thin compact zone (115, 117, 128, 180), which was also observed in the *Adm*$^{-/-}$ mice (24). Although *Adm*$^{-/-}$ animals do not exhibit other cardiac defects that are sometimes described in other models with epicardial alterations, it is possible that AM acts independently or through different growth factors than those investigated to date. Additionally, it is possible that AM may play a role in the endocardium, as *Adm*$^{-/-}$ embryos also have abnormal trabeculation compared to wildtype littermates (24), and the endocardium has been implicated in the regulation of trabecular development (65, 72, 123, 150, 210). However, since the majority of the proliferation we observed in the hearts of *Adm*$^{hi/hi}$ hearts was localized to the compact zone and septum (see Figure 5C) and the development of these areas is largely regulated by the epicardium (67, 214), it seems likely that endocardial-derived AM contributes minimally to the observed cardiac hyperplasia.

Our current study does not excluded the possibility that AM may interact with other growth factors to promote cardiac hyperplasia in *Adm*$^{hi/hi}$ animals. To date, several epicardial-derived factors critical to compact zone proliferation have been identified. These factors include several members of the fibroblast growth factor (FGF) family (120), members of the insulin

growth factor (IGF) signaling cascade (128), as well as retinoic acid (RA) (28, 30, 149, 213) and erythropoietin (Epo) (213, 248). Presently, it remains unclear whether any interaction exists between AM and these factors in the heart to promote the cardiac hyperplasia observed in *Adm*$^{hi/hi}$ animals. Similar to AM, the FGFs and their corresponding receptors are widely expressed throughout the body during development and play an important role in regulating cellular growth in many organ systems (122). Although there have been very few studies investigating any relationship between AM and the FGFs, one recent study found that transgenic over-expression of FGF18 in the lung during the early postnatal development period promoted an increase in *Adm* expression (58), indicating the potential for crosstalk between these two signaling pathways; however, it is unknown whether a similar paradigm exists in the heart during embryonic development. Another potential mechanism by which the *Adm* signaling pathway may interact with other epicardial-derived signals is through the transactivation of FGF and IGF receptors. Guidolin et al. (75) have reported that AM may transactivate the VEGFR2 to promote angiogenesis in human vascular endothelial cells. Specifically, they found that the angiogenic properties of AM were dependent on the tyrosine kinase domain of the VEGFR2 receptor, (75) which suggests that other receptor tyrosine kinases, such as the FGF and IGF receptors, may be subject to transactivation by AM signaling. Furthermore, Cornish et al. (40) found that AM-induced proliferation of osteoblasts was inhibited with the loss of IGF-1R, indicating a potentially broader paradigm for crosstalk between AM signaling and receptor tyrosine kinases. Finally, several studies have demonstrated that Epo and RA are essential regulators of epicardial-derived growth factors (28, 30, 149, 213, 248). Although there is no data currently available that demonstrates a direct relationship between AM and Epo, both of these peptides are strongly induced by hypoxia through HIF-1α (54, 64), which may indicate parallel function. Finally, a limited number of studies have examined the relationship between AM and RA (116, 151). These studies have found that in macrophages (116) and vascular smooth

muscle cells (151), RA induced *Adm* expression, indicating that *Adm* may be induced by RA in the epicardium during cardiac development to regulate cardiomyocyte proliferation.

Future studies to elucidate these interactions are underway. For example, this *Adm* over-expression model will be useful for understanding the importance of AM elevation during disease, and with Cre-recombinase technology, we can begin to address in what tissues and at what times AM elevation is advantageous. Additionally, the role of AM during developmental processes of many organs, including the heart, lymphatic system, and other organ systems, can be studied more thoroughly due to the viability of these animals.

Experimental Procedures

Animals

Adm$^{hi/hi}$ mice were generated using standard gene targeting techniques, as described in detail in (126). Briefly, the targeting vector was designed to replace the endogenous 3′ untranslated region (UTR) with a stabilizing cassette that increases the *Adm* mRNA half-life. Additionally, loxP sites allow for the deletion of the stabilizing element and its replacement by an 80 bp of AU/U-rich element of the mouse *c-fos* gene (ARE) (Figure 6A). For genotyping, a 3-primer, PCR-based strategy was used: primer 1: 5′- AACCTTACACCTTGCTGAGACATTC-3′; primer 2: 5′- TTTATTAGGAAAGGACAGTGGGAGTG-3′; primer 3: 5′-CCCACATTCGTGTCAAACGCTAC-3′. Primers 1 and 3 amplify a 760-bp wildtype allele, while primers 2 and 3 amplify a 600-bp targeted allele. Mice used in these studies were either from a mixed genetic background or backcrossed to the C57Bl6 strain for over 9 generations. For all experiments, littermate animals were used as controls.

To generate mice with reduced *Adm* expression either globally or in specific cells types, *Adm*$^{hi/hi}$ mice were crossed with the following previously characterized Cre mouse lines: CMV-Cre (201), αMHC-Cre (3), Nkx2.5-Cre (156), Fsp-Cre (13), or Wt1$^{GFPCre/+}$ (254). The recombined *Adm*^{hi} allele was designated *Adm*$^{3'\Delta}$. Heart weight to body weight (HW:BW) ratios

were assessed at 2 months of age. All studies were approved by the Institutional Animal Care and Use Committee of UNC-CH.

Gene expression analysis

Adm gene expression was analyzed by quantitative (q)RT-PCR with the Mx3000P Real-Time PCR System from Stratagene. Primers for *Adm* amplification were 5′-GAGCGAAGCCCACATTCGT-3′ and 5′-GAAGCGGCATCCATTGCT-3′ and the probe sequence was 5′-FAM-CTACCGCCAGAGCATGAACCAGGG-TAMRA-3′. Primers for *Bnp* amplification were 5′-CTGCTGGAGCTGATAAGAGA-3′ and 5′-TGCCCAAAGCAGCTTGAGAT-3′ and the probe sequence was 5′-FAM-CTCAAGGCAGCACCCTCCGGG-TAMRA-3′. Taqman Gene Expression Assays for *Anp* and GAPDH were purchased from Applied Biosystems. Embryonic lung RNA from Ambion was used as calibrator. RNA was isolated from mouse tissues with Trizol and subsequently DNaseI treated. The ΔΔCt method was used to determine the relative levels of gene expression. Assays were repeated 3 times, each time with triplicates.

Measurement of AM peptide

Mouse AM was measured using a specific immunoradiometric assay kit (AM RIA, Shionogi) with some modifications, as previously reported (167, 169). Plasma levels of AM were measured by a fluorescent immunoassay (Phoenix Pharmaceuticals, FEK-010-08) following the manufacturer's protocol.

Adrenomedullin staining

Paraffin embedded left ventricle sections were blocked for 1 hour in 5% normal donkey serum at room temperature. Slides were then incubated with adrenomedullin antibody (Novus, NBP1-19731) overnight at room temperature. Slides were washed with PBS prior to incubation with secondary antibodies for 2 hours at room temperature.

Cytokeratin staining

Paraffin embedded tissues were subjected to three, 5 minute rounds of antigen retrieval in 10mM citric acid buffer/0.05% Tween 20. Slides were then blocked in 5% normal donkey

serum/0.1% Triton X at room temperature for 1 hour. Slides were incubated with diluted cytokeratin primary antibody (Dako, Z0622) overnight at room temperature. After washing slides with PBS, secondary antibody was applied for 2 hours at room temperature in the dark.

Capillary density and cardiomyocyte density assay

Paraffin embedded heart sections were blocked in 1%BSA/0.2% triton X-100 in PBS for one hour, then incubated with Isolectin B4 FITC conjugate (Sigma L2895, 1:200), Rhodamine wheat germ agglutinin (Vector Laboratories, RL-1022, 1:1000), and 1:1000 DAPI in 1%BSA in PBS for 2.5 hours at room temperature, then washed in PBS and rinsed with ddH2O.

Measurement of mean arterial pressure (MAP)

The MAP was assessed by the tail cuff method as previously described (114). Briefly, mice were acclimated to the restraint apparatus for two days prior to data collection. For three days following the acclimation period, blood pressure data were collected for each mouse. The data from the three days were then averaged together to generate the MAP value.

BrdU incorporation assay

Timed matings were performed between $Adm^{hi/+}$ males and females. Two hours prior to the dissection of the embryos, the pregnant female was injected with BrdU (0.1mg/g of BW) via tail vein injection. Embryos were carefully dissected and genotypes were determined from DNA extracted from either the yolk sac or the tail. Frozen sections of the heart were stained for BrdU using a diaminobenzidine (DAB)-based protocol.

Phospho-Histone H3 (Ser10) and cardiac troponin co-staining

Frozen e12.5 embryo heart sections were thawed overnight prior to antigen retrieval. Slides were blocked in 10% normal goat serum in 0.05M Tris buffer for 1 hour prior to applying primary phospho-Histone H3 antibody (Cell Signaling, 9701) and cardiac troponin T antibody (Thermo, MS-295-P) to slides overnight at 4°C. Slides were washed with three changes of 0.05M Tris buffer prior to incubating with fluorescent secondary antibody for 2 hours at room temperature in the dark.

Cyclin B_1 and cyclin D_1 Western blot

Hearts were dissected from postnatal day 1 pups and flash-frozen in liquid nitrogen. Protein was isolated from wildtype and *Adm*$^{hi/hi}$ hearts using standard procedures. Samples were denatured and run on NuPage Bis-Tris gels and proteins were transferred to PVDF membranes. Membranes were probed with cyclin B_1 (Rockland, 100-401-152), cyclin D_1 (Rockland, 100-401-153) and actin (Sigma, A4700) antibodies overnight at 4ºC. Membranes were incubated with secondary antibodies for 45minutes and imaged using a Li-Cor Odyssey CLx. Integrated density was assessed using ImageJ software.

Proliferation of HL-1 cells with AM treatment

HL-1 cells are a cardiomyocyte cell line first developed and characterized by Claycomb et al. in 1998 (36). When cultured in Claycomb media (Sigma, 51800C), supplemented with norepinephrine and L-glutamine, these cells retain many properties of cardiomyocytes, but, unlike isolated cardiomyocytes, will proliferate in culture (36). For this experiment, HL-1 cells were plated in fibronectin/gelatin-coated 24-well dishes at a density of 50,000 cells per well in serum-free media. Cells were allowed to adhere to the plates for 4 hours prior to treatment. At the time of treatment, the media was removed from each well and replaced with serum-free media containing either tissue culture-grade water as a vehicle control or 1nM AM (Phoenix Pharmaceuticals, 010-31). Total cell numbers in each well were counted using a Countess Automated Cell Counter. Each condition was performed in triplicate to allow for statistical analysis.

Statistics

Statistical analyses were performed with JMP software (SAS). One-way ANOVA was used to determine significance at $p < 0.05$. In all figures, error bars represent SEM.

Funding

AHA EIA 0940097N, NIH HL091973, HD060860, Burroughs Wellcome Fund to K.M.C. and AHA PRE11710002 to S.E.W-S.

Figures

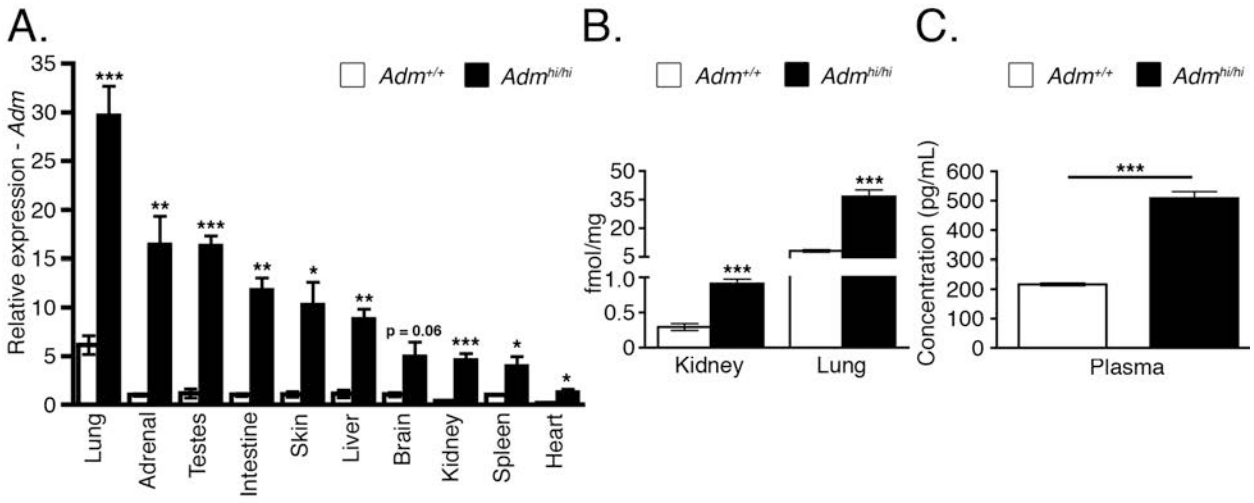

FIGURE 3.1. Transcriptional and translational up-regulation of *Adm*.
A. Quantitative RT-PCR analysis of *Adm* from wildtype and *Adm*$^{hi/hi}$ tissues (n = 3-10) at 4 months of age. **B.** Peptide levels of AM from 2- to 3-month old wildtype and *Adm*$^{hi/hi}$ lung and kidney as determined by a radioimmunoassay (n = 5-6). **C.** Plasma levels of AM from 4-month old wildtype and *Adm*$^{hi/hi}$ animals using a fluorescent immunoassay (n = 3). All values are ± SEM. *p<0.05, **p<0.01, ***p<0.001

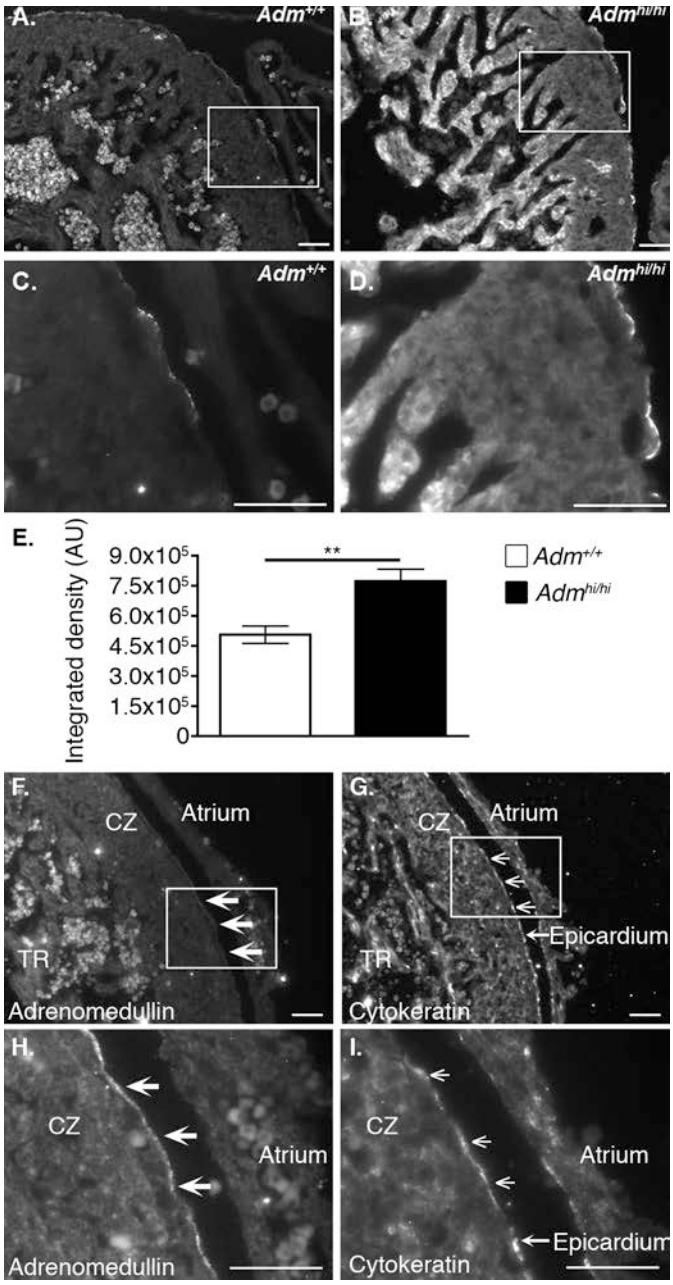

FIGURE 3.2. AM expression is localized to the developing epicardium and up-regulated in *Adm*$^{hi/hi}$ mice.

Immunofluorescence of AM peptide in heart sections of e13.5 embryos. **A.** and **C.** *Adm*$^{+/+}$ control mice. **B.** and **D.** *Adm*$^{hi/hi}$ mice. Images A & B were obtained with a 300 msec exposure, while images C and D were obtained with a 75 msec exposure. Boxes in A and B represent fields shown in panels C and D, respectively. **E.** The amount of AM expressed in the epicardium was assessed from panels C and D by measuring the integrated density of staining using Image J software. Data are expressed as arbitrary units (AU) of integrated density. Colocalization of AM peptide and the epicardial marker, cytokeratin. **F**. and **H.** Adrenomedullin staining. **G.** and **I.** cytokeratin staining. The white boxes on panels F and G indicate the fields presented in panels H and I, respectively. Filled arrow heads on panels F and H indicate areas of AM staining, while open arrow heads in panels G and I highlight areas positive for cytokeratin staining. TR = trabecular zone; CZ = compact zone. Scale bars = 50 mM. All values are ± SEM. **p<0.01

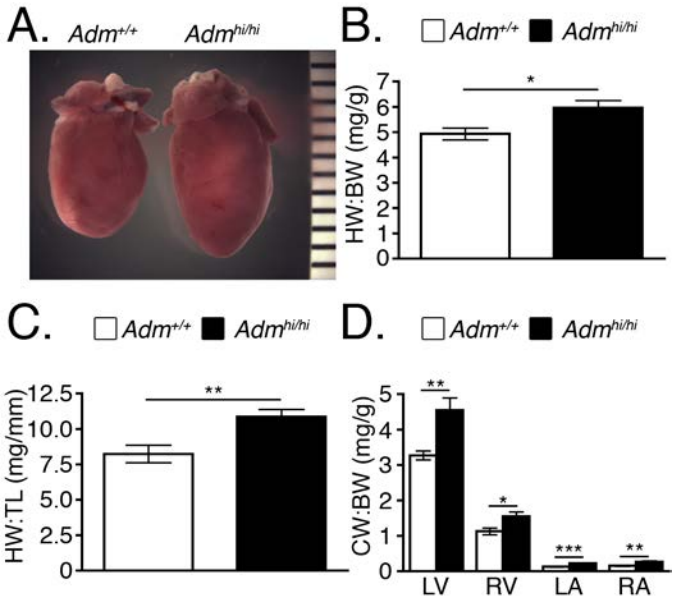

FIGURE 3.3. *Adm*$^{hi/hi}$ mice have larger hearts that wildtype littermates
A. Gross appearance of hearts from 9-week old male wildtype and *Adm*$^{hi/hi}$ mice. **B.** Heart weight to body weight (HW:BW) ratios were assessed at 2 months of age (n = 6-12). **C.** Heart weight to tibia length (HW:TL) ratios were assessed at 2-4 months of age (n = 6). **D.** The ratio of left ventricle (LV), right ventricle (RV), left atria (LA), and right atria (RA) to body weight was assessed at 2 months of age to obtain chamber weight to body weight (CW:BW) ratios (n = 6-11). All values are ± SEM. *p<0.05, **p<0.01, ***p<0.001

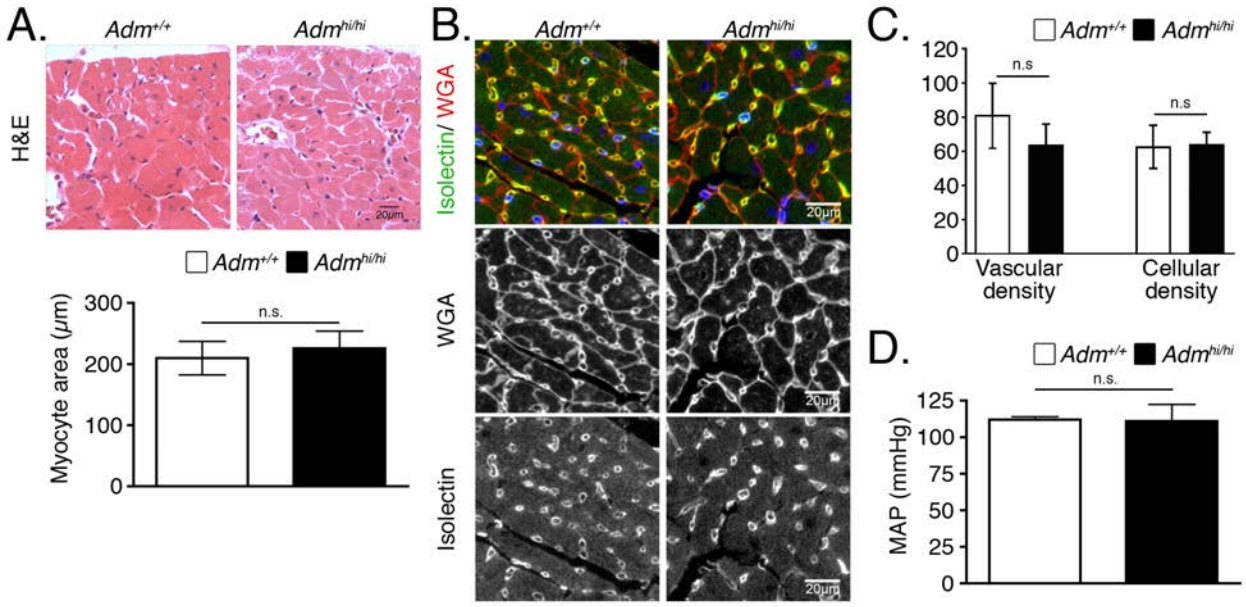

FIGURE 3.4. Hearts of *Adm*$^{hi/hi}$ mice are not hypertrophic.
A. Representative heart sections were stained with hematoxylin and eosin (H&E). The cardiomyocyte cross-sectional area was determined from 15 individual myocytes per animal (n=3). **B.** Representative heart sections were stained with isolectin **(green)**, wheat germ agglutinin (WGA) **(red)**, and DAPI **(blue)**. We have also included single channel views of the WGA and isolectin staining to aid in the visualization of the vascular and cellular density. **C.** Total numbers of vessels and cardiomyocytes were quantitated from images at 20x magnification (n = 3-8). Data shown here are representative of two independent experiments conducted by separate researchers. **D.** Mean arterial pressure (MAP) measurements assessed by tail cuff (n = 3-4). All values are ± SEM.

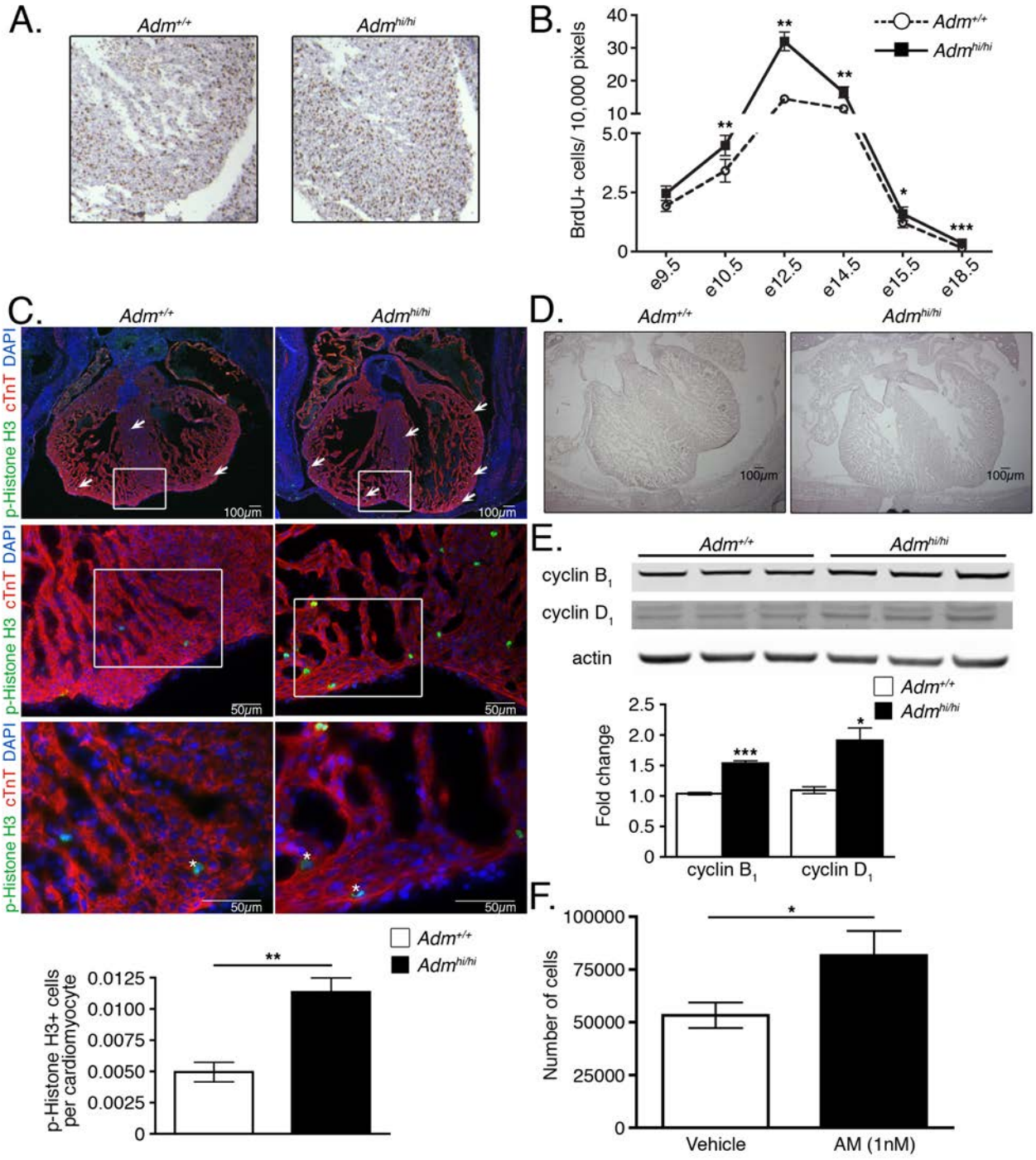

FIGURE 3.5. Enhanced proliferation of *Adm*$^{hi/hi}$ hearts during embryonic development. **A.** Representative images of wildtype and *Adm*$^{hi/hi}$ hearts at embryonic day e12.5 stained for BrdU. **B.** Quantitation of the total number of BrdU positive cells from wildtype and *Adm*$^{hi/hi}$ hearts throughout embryonic development normalized to the number of pixels in the image that were analyzed. **C.** Representative images of wildtype and *Adm*$^{hi/hi}$ hearts at embryonic day e12.5 stained with phospho-Histone H3 (p-Histone H3) **(green),** cardiac troponin T (cTnT) **(red)**, and

DAPI **(blue)**. The white boxes on the 4x (upper panels) and 20x (middle panels) images represent the areas magnified in the 20x and 40x (lower panels) images, respectively. Asterisks on 40x images indicate proliferating cardiomyocytes. The graph in the lower panel shows the number of phospho-Histone H3-positive cells per cardiomyocyte, which was determined by assessing three 20x magnification fields per animal (n=3). **D.** Low-power images of e15.5 wildtype and *Adm*$^{hi/hi}$ hearts showing differences in heart size. Scale bar = 100μm **E.** Representative Western blot for cyclin B_1 and cyclin D_1 normalized to actin. Each lane on the blot is loaded with protein lysates from individual postnatal day 1 pups. Differences in lane loading were accounted for by normalizing each cyclin band to the corresponding actin band for each lane. These numbers were then normalized to a wildtype sample to compute the fold change. **F.** Proliferation of the HL-1 cardiomyocyte cell line with AM treatment. HL-1 cells were treated in serum-free media for 72 hours with either vehicle or 1nM AM, prior to performing cell counts. Each condition was performed in triplicate. All values represent means ± SEM. *p<0.05, **p<0.01, ***p<0.001

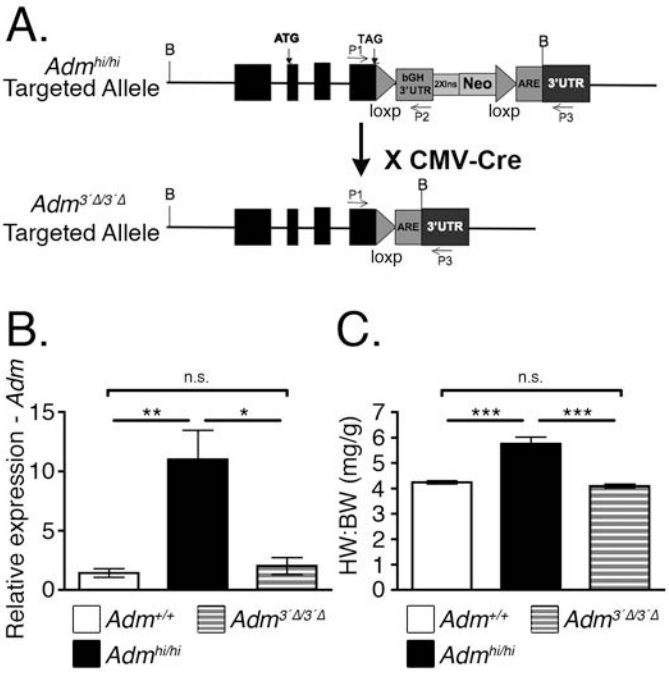

FIGURE 3.6. Mice with excised bGH 3′UTR have normal-sized hearts.
A. Gene targeting design indicating the location of loxP sites flanking the bovine growth hormone (bGH) 3′UTR segment. **B.** *Adm*$^{hi/+}$ mice were bred to the CMV-Cre line to globally excise the bGH 3′UTR fragment from the *Adm*^{hi} allele. This new allele is designated as *Adm*$^{3´Δ}$. After removing the Cre recombinase via breeding, *Adm* expression was assessed by qRT-PCR (n = 5-6). **C.** At 2-3 months of age, the heart weight to body weight (HW:BW) ratios of *Adm*$^{3´Δ/3´Δ}$ mice was compared to the HW:BW ratios of age-matched *Adm*$^{hi/hi}$ and wildtype mice (n = 5-7). All values represent means ± SEM. *p<0.05, **p<0.01, ***p<0.001

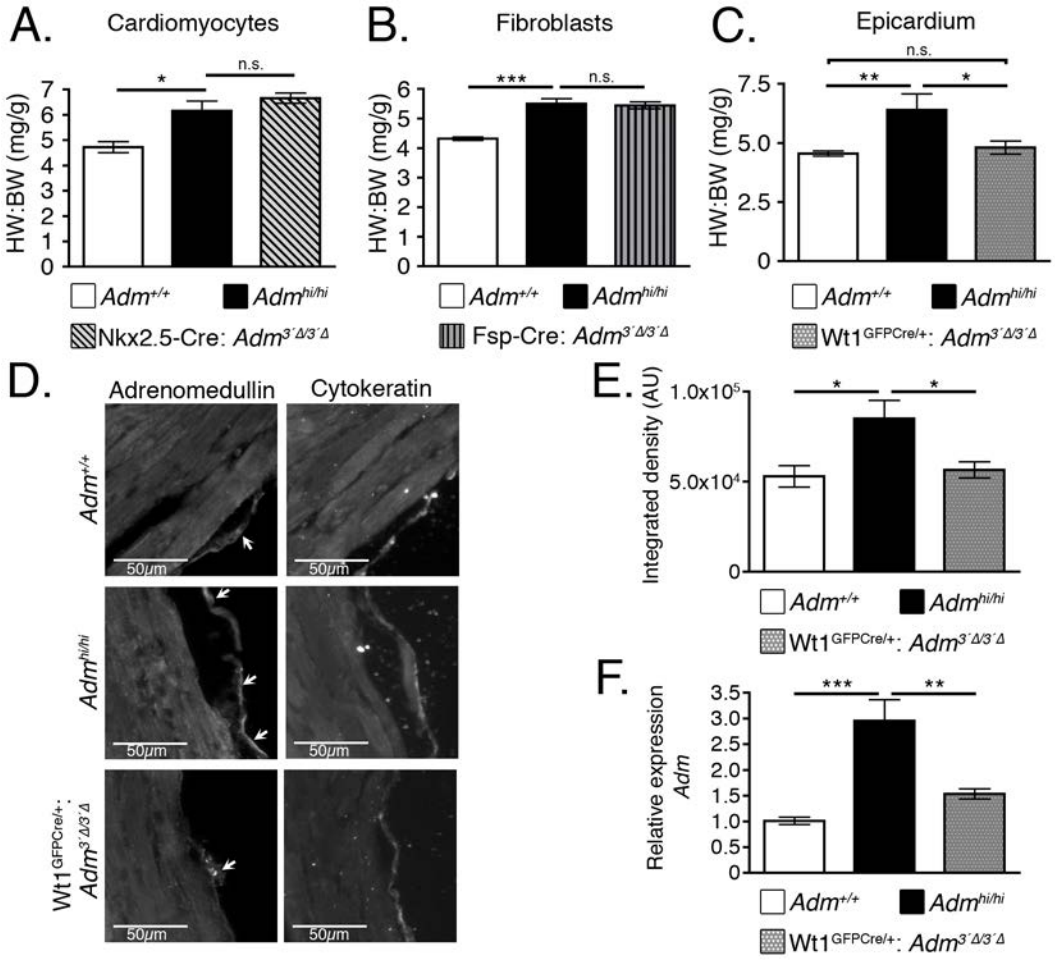

FIGURE 3.7. Epicardial-derived AM contributes to cardiac hyperplasia of *Adm*$^{hi/hi}$ mice. **A.** *Adm*$^{hi/hi}$ mice were crossed with the Nkx2.5-Cre mouse line to generate *Adm*$^{hi/hi}$ animals with wildtype levels of *Adm* in cardiomyocytes. Heart weight to body weight (HW:BW) ratios were assessed at 2 months of age (n = 4-8). **B.** *Adm*$^{hi/hi}$ mice were crossed to the Fsp-Cre mouse line to generate *Adm*$^{hi/hi}$ mice with wildtype levels of *Adm* in fibroblasts. Heart weight to body weight (HW:BW) ratios were assessed at 2 months of age (n = 4-10). **C.** *Adm*$^{hi/hi}$ mice were crossed with the Wt1$^{GFPCre/+}$ mouse line to generate *Adm*$^{hi/hi}$ mice with wildtype levels of *Adm* in the epicardium. At 2 months of age, heart weight to body weight (HW:BW) ratios were assessed (n = 3-6). **D.** Adjacent left ventricle sections from wildtype, *Adm*$^{hi/hi}$, and *Wt1*$^{GFPCre/+}$*:Adm*$^{3´Δ/3´Δ}$ mice were stained with adrenomedullin (left panels) and the epicardial marker, cytokeratin (right panels). Adrenomedullin and cytokeratin images were acquired with a 130 msec exposure for all images. Images were acquired at 20x magnification and the scale bar represents 50μm. **E.** The amount of AM expressed in the epicardium was assessed from the images in panel D by measuring the integrated density using Image J software. The data are presented as arbitrary units (AU) of integrated density. **F.** RNA extracted from 2-month old left ventricle samples was used to assess the relative expression levels of *Adm* by qRT-PCR. All values represent means ± SEM. *p<0.05, **p<0.01, ***p<0.001

CHAPTER IV: COHORT OF ESTROGEN-INDUCED MICRORNAS, INCLUDING THE NOVEL MIR-879, BALANCE ADRENOMEDULLIN EXPRESSION IN RESPONSE TO ESTROGEN SIGNALING[2]

Overview

Estrogen regulates the expression of many genes and has been correlated with differences in cardiac contraction; however the underlying mechanisms remain poorly defined. Adrenomedullin (*Adm* = gene; AM = protein) is a multi-functional peptide with inotropic actions. Previous studies have demonstrated that *Adm* expression is increased in the presence of estrogen, suggesting a relationship between AM and estrogen in cardiac contraction during physiological and pathological states. In this study, female mice in a mouse model of genetic *Adm* over-expression, referred to as $Adm^{hi/hi}$ mice, were found to express 60-times more *Adm* in the heart than wildtype littermates, which was greater than the 3-fold elevation of *Adm* observed in $Adm^{hi/hi}$ male hearts. This drastic elevation of *Adm* was correlated with an enhancement of cardiac function. Interestingly, ovariectomy reversed the dramatic over-expression of *Adm* and resulted in a reversion of heart function to wildtype levels. Since the 3′ untranslated region (UTR) of *Adm* was displaced to generate the $Adm^{hi/hi}$ line, the theory that estrogen-induced microRNAs normally down-regulate *Adm* levels in an estrogen-dependent fashion to prevent aberrant *Adm* over-expression in females was examined. Using a bioinformatic approach, it was determined that the mouse *Adm* 3′UTR contains many target sites for previously characterized estrogen-induced microRNAs. This study also determined that the novel microRNA, miR-879, is

[2]This work is currently in revision for publication in The American Journal of Physiology – Regulatory, Integrative and Comparative Physiology. Permission for re-printing will be obtained upon publication. Contributing authors include: Sarah E. Wetzel-Strong, Manyu Li, Scott T. Espenschied, and Kathleen M. Caron

another estrogen-induced microRNA that does in fact interact with the 3´UTR of *Adm* to destabilize the mRNA. Together, these studies revealed that estrogen-induced microRNAs play an important role in balancing *Adm* expression in females.

Introduction

The steroid hormone 17β-estradiol, referred to herein as estrogen, plays an important role in the regulation of gene transcription. Several mechanisms have been described by which estrogen can regulate gene expression. In the classical model of estrogen signaling, estrogen interacts with cytoplasmic estrogen receptor-alpha (ERα) or ER-beta (ERβ), resulting in translocation of the estrogen-ER complex to the nucleus (14). Once in the nucleus, the estrogen-ER complex can either interact directly with the DNA at estrogen response elements (ERE) (176) or the complex can interact with other transcription factors to indirectly regulate transcription (164, 242). Additionally, estrogen receptors bound to the plasma membrane can promote downstream signaling when activated by estrogen (179). Moreover, phosphorylation of estrogen receptors can result in ligand-independent activation and subsequent gene expression regulation (225). Finally, estrogen can interact with G protein-coupled estrogen receptor 1 (GPER), resulting in activation of downstream signaling and subsequent gene expression changes (56). Together, the multitude of pathways by which estrogen can influence cellular functions and gene transcription underscores the complexity of estrogen-mediated actions in physiological and pathological states.

For many years, researchers have recognized that differences exist between males and females with regards to cardiac function both in physiological and pathological scenarios (34, 62, 82, 135, 178). For instance, several studies have noted that healthy females have higher ejection fractions compared to age-matched males (34, 178). Interestingly, several studies have demonstrated that women are more likely to have heart failure with preserved ejection fraction

than men (62, 82), suggesting a role for female sex hormones in systolic heart function. In addition to the effect of female sex hormones on ejection fraction, work by Locati et al revealed that females are at increased risk for long QT syndrome (135), indicating that sex hormones might contribute to disease pathology. Animal studies have demonstrated that sex hormones, and in particular estrogen, can directly promote an increase in the QT interval (51, 196), confirming the sex-dependent differences observed in humans. Together, these findings, along with studies demonstrating that ERα and ERβ are expressed in endothelial cells (55), smooth muscle cells (192), cardiomyocytes and fibroblasts (73), underscore a widespread role for female sex hormones in the regulation of cardiac contraction.

Cardiomyocyte contraction is dependent on the generation of an action potential, which is regulated by the flow of ions between the cardiomyocyte and the extracellular space through ion channels. Thus, disruptions in normal ion flow, either by altered levels of the ion channels or mutations in the ion channel components, can impact cardiomyocyte contraction and heart function. In animal models of long QT syndrome, estrogen was found to decrease the levels of several potassium channels in the heart (51, 196), leading to the lengthening of the QT interval and arrhythmias. In humans, many ion channels in the heart are differentially regulated with sex, including the down-regulation of several potassium channels in the female heart (61). Together, these studies highlight the sex-dependent differences in cardiac function, mediated in part by differences in ion channel expression. Undoubtedly, a further understanding of the effects of estrogen on the cardiovascular system is necessary for developing effective therapeutics for women.

Recently, several groups have demonstrated that estrogen can regulate the expression of microRNAs (12, 26, 35, 172, 177). These short DNA fragments work primarily to repress gene expression by interacting with the 3´ untranslated region (3´UTR) to either prevent translation of the mRNA into protein or to promote degradation of the mRNA (11). Due to the tendency for families of microRNAs to target multiple genes within a particular network (148),

there has been a surge in interest regarding the role of microRNAs during cardiovascular disease, since therapies may be more effective if multiple components of a pathway can be targeted at one time.

Adrenomedullin (*Adm* = gene; AM = protein) is a secreted peptide with a multitude of functions (19, 24, 37, 87, 106, 108, 168, 231). Specifically in the heart, several groups have described an inotropic role for AM (87, 216, 217), although these findings have been controversial (88, 211). During many human disease conditions, including cardiovascular disease, circulating levels of AM in the plasma are significantly elevated above baseline levels (97). Thus, the inotropic role of AM (87, 216, 217), along with other cardioprotective properties (8, 20, 203), indicate that the observed elevation of AM in the plasma during cardiovascular disease most likely serves to mitigate the extent of damage. Interestingly, *Adm* expression is enhanced by estrogen through ERα-dependent mechanisms (240), indicating that AM signaling may represent a novel mechanism by which estrogen protects the hearts of females. In this study, the serendipitous discovery of drastic *Adm* over-expression in the heart of female $Adm^{hi/hi}$ mice was explored. Specifically, since the native *Adm* 3′UTR was displaced with the generation of the $Adm^{hi/hi}$ line, the possibility of estrogen-dependent negative regulation of *Adm* at the 3′UTR was examined.

Materials and Methods

Mice

The generation of $Adm^{hi/hi}$ mice has been documented previously (126, 245). Briefly, gene targeting techniques were used to insert the bovine growth hormone (bGH) 3´UTR upstream of the native *Adm* 3´UTR, thereby stabilizing the *Adm* mRNA. Mice used in these studies were either from a mixed genetic background (129S6/SvEv x C57Bl6/J) or backcrossed to the C57Bl6/J strain for over 9 generations. For all experiments, littermate animals were used

as controls. To assess the impact of endogenous estrogen on expression levels of *Adm* wildtype animals from the 129S6/SvEv background, referred to as SvEV, were utilized. Ovariectomized C57Bl6/J females and intact controls during estrus and diestrus were used to assess the impact of endogenous estrogen on expression of *Eig121l* and *miR-879*.

Ovariectomy was performed to remove the influence of endogenous hormones on gene expression. Mice were 21- to 28-days old at the time of ovariectomy. Mice were anesthetized with avertin (400-500 mg/kg/body weight) and placed on a warm heating pad to maintain body temperature throughout the surgical procedure. Hair was removed from the abdomen and a small <1 cm incision was made through the abdominal wall about 1 cm to the left of the spinal cord. The ovary was exteriorized and placed on a sterile drape. Silk sutures were used to ligate the oviduct and anterior connective tissue prior to excising the ovary. The body wall was then sutured with dissolvable sutures and wound clips were used to close the skin. The procedure was repeated on the animal's right side. Wound clips are removed 4-5 days after surgery and 4 weeks later the ovariectomized mice were used in experiments.

Transthoracic echocardiography was performed on $Adm^{hi/hi}$ and littermate wildtype mice under anesthesia (3% isoflurane) with a VisualSonics Vevo770 high-resolution imaging system.

All studies were approved by the Institutional Animal Care and Use Committee at the University of North Carolina at Chapel Hill.

Gene expression analysis

Gene expression was analyzed by quantitative (q)RT-PCR with the Mx3000P Real-Time PCR System from Stratagene. *Adm* (RefSeq ID: NM_009627.1) gene expression was assessed using primers and a probe described previously (245). Taqman Gene Expression Assays for *EIG121L* (RefSeq ID: NM_172706.3, cat# 4351372), *miR-879* (RefSeq ID: NR_030537.1, cat# 4427975), *Gapdh* (RefSeq ID: NM_001289726.1, cat# 4308313) and *snoRNA-202* (cat# 4427975), were purchased from Applied Biosystems. Samples were assessed three times in triplicate. Relative levels of gene expression were determined using the $\Delta\Delta$Ct method.

Plasmids, mutagenesis, transfection, and luciferase assay

700-bp of the 3´UTR region of the *mAdm* gene (112 bp after Adm stop codon) was cloned into the Xba I site of pGL3-Promoter Vector (Promega, E1761). The QuikChange® II Site-Directed Mutagenesis Kit from Stratagene was used to introduce specific point mutations in the miR-25 and miR-879 binding sites. MicroRNA-25 (AM17100-PM10584), microRNA-879 (AM17100-PM12276), and a scrambled negative control microRNA (AM4611) were ordered from Ambion. HEK293T cells were transfected with 10nM microRNAs, 250ng/ml plasmids, and 5ng/ml *Renilla* luciferase (*Rluc*) reporter vectors using Lipofectamine 2000 (Invitrogen, 11668-027) in accordance with the manufacturer's protocol. 48h after transfection, the cells were lysed and luciferase activities were measured with the Dual-Glo luciferase assay system (Promega, E2920).

Statistics

Statistical analyses were performed with JMP software (SAS). One-way ANOVA was used to determine significance at $p < 0.05$. In all figures, error bars represent SEM.

Results

Dramatic, estrogen-dependent increase of Adm in female Adm$^{hi/hi}$ heart

Previous studies have characterized the generation of the *Adm* over-expression model (126), referred to as *Adm$^{hi/hi}$* mice, as well as the developmental (245) and reproductive phenotypes (126) observed in this line. These mice were generated by the gene-targeted insertion of the stable bovine growth hormone (bGH) 3′UTR upstream of the unstable native *Adm* 3′UTR (126), thereby resulting in accumulation of *Adm* mRNA and increased expression. Through this approach, 5′UTR regulatory elements remain unchanged, thereby preventing disruption of the native regulatory elements of *Adm*. This approach, however, does disrupt the native 3′UTR regulatory elements with the insertion of the bGH 3′UTR. When the expression

levels of *Adm* in female tissues were compared to the levels previously reported in males (245), similar degrees of *Adm* over-expression in the adrenal gland, reproductive organs, intestine, skin, liver, brain, kidney and spleen were observed between the two sexes (**Figure 1A**). However, upon examination of *Adm* expression in the heart, a dramatic 60-fold increase in *Adm* was observed in $Adm^{hi/hi}$ female hearts relative to wildtype littermates (**Figure 1A**). This 60-fold increase in expression was reduced to a 4-fold increase of expression with ovariectomy of female animals, which is comparable to the increase observed in male $Adm^{hi/hi}$ mice (245). Previous studies by Watanabe et al. (240) using ovariectomized mice demonstrated that *Adm* is regulated by estrogen through ERα-dependent mechanisms; however, since these experiments were performed using estrogen infusion, it remains unclear whether endogenous changes in estrogen can promote detectable differences in *Adm* expression. This study revealed a dramatic, estrogen-dependent increase in *Adm* expression in $Adm^{hi/hi}$ females suggesting that shifting levels of endogenous estrogen with the different phases of the estrus cycle are capable of regulating *Adm* expression. Therefore, an assessement of *Adm* expression levels from heart and uterus samples of wildtype 129S6/SvEv, abbreviated as SvEV, female mice in either diestrus or estrus, the low and high phases of the estrus cycle, respectively was conducted. This approach revealed a modest, but significant increase of *Adm* transcript levels in the hearts and uteri of estrus females compared to diestrus females (**Figure 1B**), indicating that changes in endogenous estrogen levels can modulate *Adm* expression *in vivo*.

Enhanced contractility of $Adm^{hi/hi}$ females is reversed with ovariectomy

Several studies have suggested that AM has inotropic properties in the heart (87, 217), prompting an investigation of any potential functional consequences resulting from this 60-fold increase in cardiac *Adm*. To do this, cardiac function was determined using echocardiography. As the results in Table 1 demonstrate, $Adm^{hi/hi}$ females have enhanced heart function, as indicated by an increase in both the ejection fraction and fractional shortening, compared to

wildtype littermates, consistent with the published inotropic properties of AM. Additionally, ovariectomy of females prior to the onset of puberty reverted the heart function of *Adm*$^{hi/hi}$ females to wildtype levels, indicating that the robust cardiac over-expression of *Adm* was responsible for the enhanced function. No significant differences were noted in the internal chamber dimensions, indicating that *Adm*$^{hi/hi}$ females do not have dilated left ventricles. Finally, assessment of male cardiac function by echocardiography revealed no significant difference in ejection fraction between wildtype and *Adm*$^{hi/hi}$ males (42.42±5.49 vs. 42.19±3.04), indicating that a three- to four-fold increase of cardiac AM is insufficient for altering cardiac function.

Estrogen drives the expression of miR-879, which targets the Adm 3´UTR

Under basal conditions, *Adm* expression levels differ in a sex-dependent manner in the heart, highlighting the importance of estrogen-regulation of endogenous *Adm*. Compared to the expression of *Adm* in the hearts of wildtype males (data previously published in reference (245)), intact wildtype females express significantly more *Adm*. This sex-dependent difference in *Adm* expression in wildtype animals, however, is only about 5-fold; not the 50-fold difference observed between *Adm*$^{hi/hi}$ males (reported in reference (245)) and intact *Adm*$^{hi/hi}$ females. Consistent with notion that estrogen mediates *Adm* expression in an estrogen-dependent manner in the heart, ovariectomization of wildtype females results in *Adm* expression levels indistinguishable from wildtype males; while ovariectomization of *Adm*$^{hi/hi}$ females results in a 4-fold elevation of *Adm* expression over wildtype animals, which is comparable to the difference observed between male wildtype and *Adm*$^{hi/hi}$ mice (245). Together, these data suggested that estrogen acts on both the 5′UTR and 3′UTR of *Adm* to provide fine-tuned control of *Adm* expression in response to hormonal cues. Therefore, the hypothesis was put forth that estrogen-induced microRNAs target *Adm* to decrease expression levels in the heart in the presence of estrogen and that by inserting the bGH 3´UTR upstream of the native *Adm* 3´UTR, this important regulatory process had been disrupted. In support of this hypothesis, several

groups have identified microRNAs that are indeed induced by estrogen (12, 26, 35, 172, 177), and so, the 3´UTR of *Adm* was examined for any predicted target sites of microRNAs that are up-regulated by estrogen. Of the 54 microRNAs that are predicted to target the mouse *Adm* 3´UTR, 15 of these predicted target sites were for estrogen-induced microRNAs (**Figure 2A**). During this analysis, a target site for the poorly characterized microRNA, miR-879, was noticed in the *Adm* 3´UTR. This particular microRNA was of interest because it is located within a gene called estrogen-induced gene 121-like, abbreviated as *Eig121l*. Currently, very little is known about *Eig121l* and miR-879, so the regulation of *Eig121l* and miR-879 by estrogen was interrogated. Using RNA extracted from heart lysates of ovariectomized, diestrus, and estrus females, the relative expression of *Eig121l* and miR-879 were assessed by qRT-PCR. This experiment revealed that with increasing levels of endogenous estrogen, the expression of *Eig121l* (**Figure 2B**) and miR-879 (**Figure 2C**) increased significantly, indicating that *Eig121l* and the residing microRNA, miR-879, are regulated by estrogen.

MicroRNA-879 destabilizes Adm through its predicted target site

Having confirmed that miR-879 is up-regulated by endogenous estrogen in the heart, the next objective was to determine whether this microRNA can indeed interact with the 3´UTR of *Adm* to reduce transcript levels. To accomplish this, the luciferase gene within the pGL3-promoter vector was stabilized with 700 base pairs of the mouse *Adm* 3´UTR, labeled as Adm700;native (**Figure 3A**), thereby allowing for the use of the relative amount of luciferase luminescence as a read-out of *Adm* gene stability. To demonstrate that miR-879 works through the predicted target site in the *Adm* 3´UTR, two vectors were generated in which separate single point mutations were created within the predicted target site for miR-879, designated as Adm700;miR-879^{m1} and Adm700;miR-879^{m2} (**Figure 3A**). Additionally, a vector was created with a single point mutation in the predicted target site for miR-25, the positive control of *Adm* de-stabilization for this experiment, represented as Adm700;miR25^{m1} (**Figure 3A**). The reason for

selecting this microRNA as a positive control was two-fold; first, miR-25 is the most highly conserved microRNA to target the *Adm* 3´UTR, and second, miR-25 is also regulated by estrogen (26), further supporting the hypothesis that estrogen-driven microRNAs help balance *Adm* expression in the female heart. As shown in Figure 3B, transfection with the Adm700;native vector and either miR-879 or miR-25 resulted in a significant reduction in the amount of luciferase luminescence normalized to the total amount of Renilla luminescence, indicating that both microRNAs can act on the *Adm* 3´UTR to destabilize expression. This approach also demonstrated that these microRNAs were acting specifically through the predicted target sites, since transfection of the mutated vectors along with the proper microRNA did not alter the relative luminescence (**Figure 3B**).

Discussion

Based on the findings in this study, a balanced model of the regulation of *Adm* by estrogen is proposed (**Figure 4**). To summarize, previous studies have demonstrated that *Adm* expression is up-regulated by estrogen through ERα (240). This study indicates that under normal circumstances, estrogen drives the expression of a cohort of microRNAs, including miR-879, that target the *Adm* 3´UTR, resulting in balanced *Adm* expression. In the case of the $Adm^{hi/hi}$ mice, the introduction of the bGH 3´UTR most likely displaced the native target sites for these estrogen-induced microRNAs, rendering them ineffective in balancing the positive transcriptional force of estrogen from the 5′UTR of *Adm*, resulting in dramatic over-expression of *Adm* in the female heart. This study also found that this dramatic over-expression of *Adm* had physiological consequences, including enhanced contractility of the cardiomyocytes. Although this study cannot rule out the possibility that the modification of the *Adm* 3′UTR with the generation of the $Adm^{hi/hi}$ line has altered the responsiveness of the promoter due to displacement of repressive cis-acting elements, the large number of estrogen-induced

microRNAs that target the *Adm* 3′UTR indicates an important role for estrogen-induced microRNAs in *Adm* gene regulation. Additionally, results from the luciferase assay revealed that modification of even one base pair within the predicted target site for the estrogen-induced microRNA miR-25 severely reduced *Adm* expression, indicating that this microRNA may play a critical role in the regulation of *Adm*, although this requires further study.

The fine-tuned balance of gene expression levels by microRNAs has emerged as a powerful and pervasive mechanism for controlling numerous biological processes from early development to pathological disease progression (2, 205). Indeed, the coordinated expression of microRNAs in response to cellular and physiological stimuli can be exploited in order to control both positive and negative regulatory factors within a biological pathway or signaling cascade (148). Thus, microRNAs can provide a buffer against large and detrimental variations in gene expression in response to (patho)physiological stimuli, such as estrogen. This study has revealed the importance of this type of balanced gene regulation for a particular cardioprotective, estrogen-regulated gene, *Adm*, in the heart. Considering that it has been notoriously difficult to identify the downstream target genes of estrogen signaling that account for sex differences in cardiovascular disease susceptibility and progression (139), it seemed possible that similar microRNA regulatory mechanisms might be in place for other estrogen-regulated target genes with important roles in cardiovascular disease.

To test this theory, other targets of miR-879 were examined using the microRNA.org database, and it was immediately noted that the *Kcnj2* gene, encoding the Kir2.1 potassium channel, was one of the top ten genes predicted to be down-regulated by miR-879. *Kcnj2* is highly expressed in the heart (189) and contains species-conserved ERα binding sites within its promoter. Importantly, mutations in this gene are associated with Andersen syndrome (long QT syndrome type-7), of which a symptom is ventricular arrhythmia (226). Therefore, the cardiac

function of miR-879 is likely to extend to additional target genes with roles in cardiac conductance and cardiovascular disease, and this will be an exciting area for future study.

It is noteworthy that numerous potassium and cardiac conductance ion channels are significantly down-regulated in female hearts compared to males at the basal state (61). However, the regulatory mechanisms contributing to these sex differences in gene expression have yet to be explained. Therefore, the 3´UTRs of the cardiac conductance ion channels identified by Gaborit et al. as reduced in female hearts compared to males (61) were examined for binding sites of microRNAs that are positively regulated by estrogen (26). This analysis also included KCNA5, a potassium channel differentially expressed with sex (17, 51), and KCND2, a potassium channel associated with long QT syndrome in mice (10). Interestingly, all of the ion channels analyzed contained four or more target sites, and half contained ten or more target sites, for microRNAs that are up-regulated by estrogen. The genes identified with a high proportion of target sites for estrogen-regulated microRNAs were *ABCC4*, *KCNJ11*, *KCNE1*, *GJA1*, *KCNA5*, and *KCND2*. Therefore, future studies to elucidate the molecular networks that underlie the sex-dependent differences in ion channel gene expression in the heart should include an assessment of estrogen-regulated microRNAs.

Finally, considering that the inotropic properties of AM on cardiomyocytes has been controversial (87, 88, 211, 217), the comparison of the contractile function in intact and ovariectomized $Adm^{hi/hi}$ female mice herein helps to clarify the effects of AM dosage on cardiac contractility. This study found that the modest, but physiologically relevant 4-fold increase of AM in ovariectomized $Adm^{hi/hi}$ females did not alter cardiac function whereas, in intact $Adm^{hi/hi}$ females, estrogen drives *Adm* expression to levels 60 times greater than wildtype counterparts, which in turn significantly enhances cardiac function. With regard to the period immediately following the onset of myocardial infarction, it is therefore possible that the robust, yet transient increases in AM, through the action of HIF-1 (64), may occur in order to help sustain cardiac function. But then, how persistently elevated plasma AM can ultimately be correlated to poor

patient survival remains curious. It also remains under-studied whether the clinically-diagnostic plasma levels of AM in cardiovascular disease differ between men and women. The results from this study highlight the importance of carefully considering hormonal status when evaluating AM during cardiovascular disease. Results from this work underscore the importance of carefully evaluating estrogen-regulated genes and pathways, including microRNAs, as underlying factors contributing to sex differences in cardiovascular disease susceptibility and progression.

Perspectives and Significance

Hormonal signals, including estrogen, mediate gene expression changes that contribute to sex-dependent differences in physiological and pathological states. In this study, displacement of the native *Adm* 3′UTR in the generation of the $Adm^{hi/hi}$ mouse line led to the serendipitous appreciation of the important role played by estrogen-induced microRNAs in the regulation of *Adm*. Additionally, this study alludes to the presence of tissue-specific regulatory networks of microRNAs, as the 60-fold elevation of *Adm* observed in $Adm^{hi/hi}$ females was restricted to the heart. Given the elevation of plasma AM levels during human disease (97), and the cardioprotective properties of AM (20, 78, 170, 173, 203), future studies should examine the implications of this dramatic elevation of AM on cardiovascular pathology following an insult. Additionally, further work investigating the relative levels of estrogen-induced microRNAs across tissues should be conducted to enhance the understanding of the complex networks regulating *Adm* expression. Finally, further exploration into the role of estrogen-induced microRNAs in the regulation of cardiac ion channels should be investigated as a potential mechanism underlying sex-dependent differences in diseases involving cardiac contraction.

Financial Support

Supported by an American Heart Association Established Investigator Award and NIH/NHLBI RO1 HL901973 to K.M.C., as well as AHA PRE11710002 to S.E.W.-S.

Figures

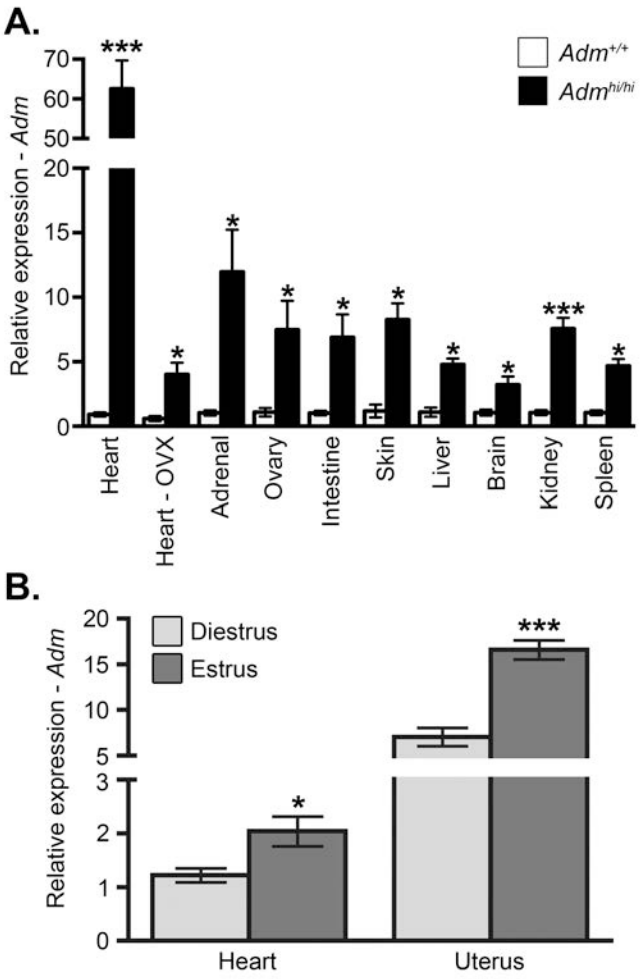

Figure 4.1. *Adm* expression is drastically up-regulated in the heart in an estrogen-dependent manner.
A. Quantitative RT-PCR (qRT-PCR) analysis for *Adm* from $Adm^{+/+}$ and $Adm^{hi/hi}$ intact females normalized to calibrator. Additionally, *Adm* expression was analyzed by qRT-PCR in the hearts of ovariectomized (OVX) $Adm^{+/+}$ and $Adm^{hi/hi}$ female mouse hearts and normalized to calibrator. **B.** qRT-PCR analysis of *Adm* levels from wildtype SvEV heart and uterus samples isolated during diestrus and estrus. All values represent means±SEM. *p<0.05, ***p<0.0001

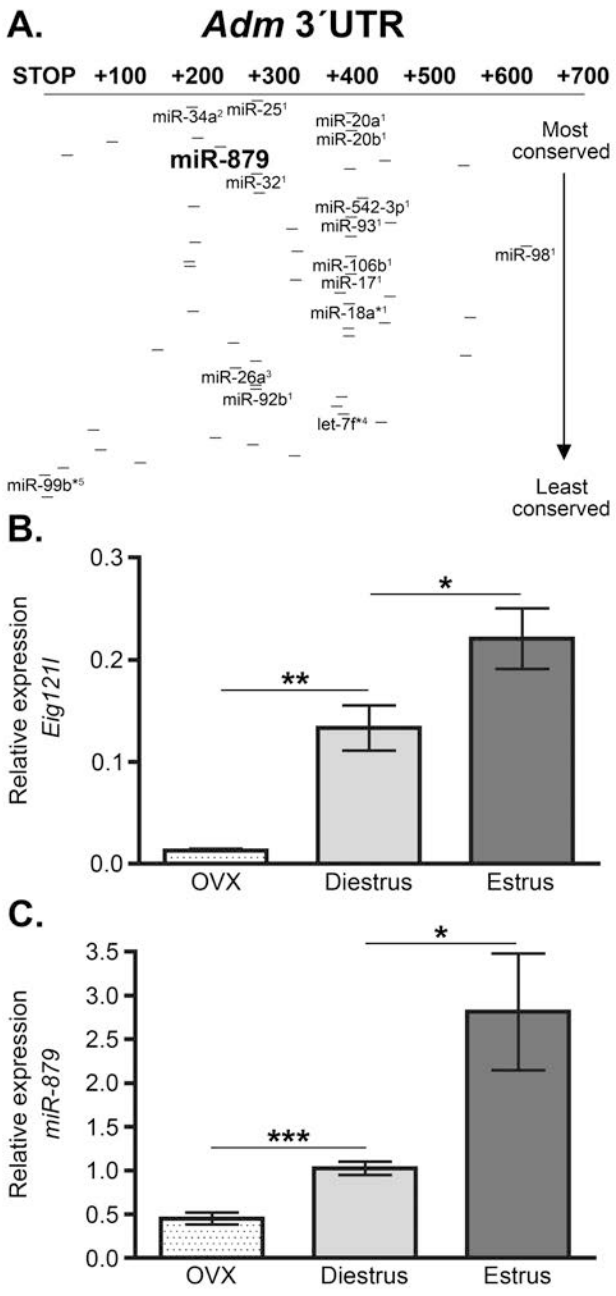

Figure 4.2. Regulation of *Adm* by estrogen-regulated microRNAs.
A. Schematic of the microRNA binding sites located in the *M. musculus* 3´UTR of *Adm* as identified by the MicroCosm Targets database (http://www.ebi.ac.uk/enright-srv/microcosm/htdocs/targets/v5/). Lines indicate microRNA binding sites, while bold microRNA names indicate estrogen-regulated microRNAs. [1]Castellano L et al. (2009); [2]Chung TKH et al. (2009); [3]Pan Q et al. (2007); [4]Bhat-Nakshatri P et al. (2009); [5]Nothnick WB et al. (2010). **B.** qRT-PCR analysis for *Eig121l* from ovariectomized (OVX), diestrus, and estrus C57Bl6/J female hearts normalized to mouse calibrator. **C.** qRT-PCR analysis of miR-879 expression from the hearts of ovariectomized (OVX), diestrus, and estrus C57Bl6/J females. Expression of miR-879 was normalized to sno-202 and relative expression was calculated using the ΔΔCT method. All values are means±SEM. *p<0.05, **p<0.001, ***p<0.0001

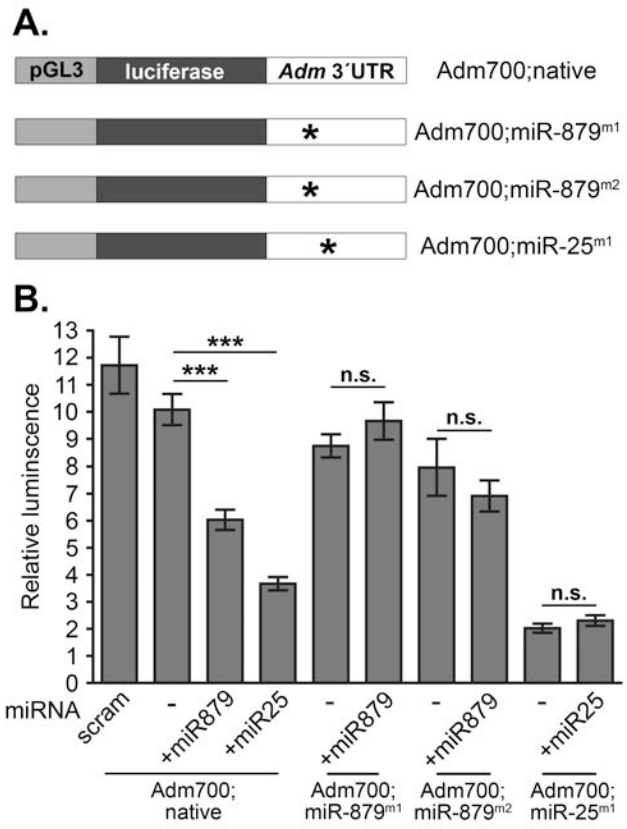

Figure 4.3. Estrogen-regulated microRNA-879 negatively regulates *Adm* expression. **A.** Graphical representation of luciferase vectors used for assessing regulation of *Adm* by microRNAs. Adm700;native refers to the modified pGL3-promoter vector in which luciferase expression was stabilized by 700-bp of the mouse *Adm* 3´UTR. Two separate sets of point mutations were made to the predicted miR-879 target sites in the Adm700 construct and are designated as Adm700;miR-879^{m1} and Adm700;miR-879^{m2}. Additionally, the target site for miR-25 was mutated and is designated Adm700;miR-25^{m1}. Asterisks indicate location of point mutations. **B.** Relative luminescence was calculated by normalizing luciferase luminescence to Renilla luminescence. Scram refers to the scrambled negative control. All values represent means±SEM. ***p<0.0001

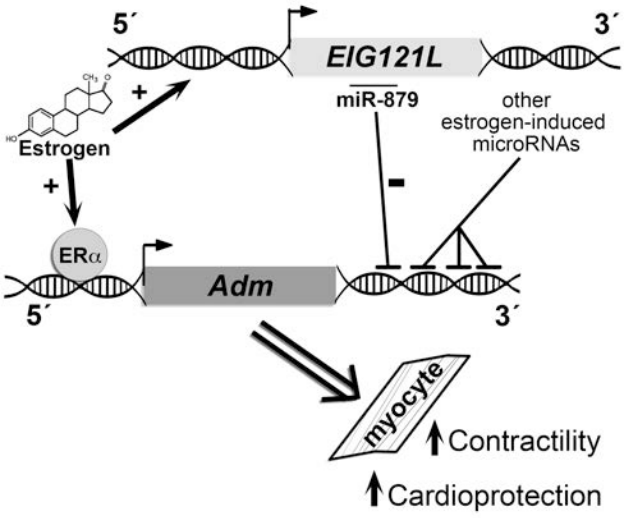

Figure 4.4. Model of *Adm* regulation and physiology.
ERα, estrogen receptor-α; *Adm*, adrenomedullin; *Eig121l*, estrogen-induced gene 121-like; miR-879, microRNA-879.

Table

	Adm$^{+/+}$ ♀	*Adm*$^{hi/hi}$ ♀	*Adm*$^{+/+}$-OVX	*Adm*$^{hi/hi}$-OVX
N	6	6	8	9
MAP (mmHg)	124.68±5.68	114.25±23.78	ND	ND
Heart Rate	505.67±6.38	471.4±15.64	505±15.98	477.22±14.73
LVED, d(mm)	3.83±0.07	4.17±0.15	3.94±0.14	3.62±0.18†
LVED, s(mm)	3.01±0.04	2.98±0.12	3.03±0.1	2.81±0.13
LVPW, d(mm)	0.7±0.03	0.73±0.04	0.73±0.03	0.76±0.04
LVPW, s(mm)	0.92±0.04	1.01±0.02	0.97±0.04	0.92±0.04
LV%FS	20.32±1.49	27.65±1.47*	21.36±1.02	22.1±1.41†
LV%EF	41.97±2.63	53.63±2.33*	43.78±1.74	45.15±2.38†
LV Vol; d (μl)	66.26±2.67	80.82±6.65	70.76±5.87	61.53±7.14
LV Vol; s (μl)	38.24±1.4	37.34±3.66	39.58±3.15	33.14±3.63
CO (ml/min)	14.24±1.44	20.36±1.85*	15.78±1.82	13.37±1.82†

Table 4.1. Blood pressure and echocardiogram data.
MAP, mean arterial pressure; LVED, left ventricular end diameter; LVPW, left ventricle posterior wall; %FS, percent fractional shortening; %EF, percent ejection fraction; CO, cardiac output. * $p<0.05$ compared to *Adm*$^{+/+}$ females; † $p<0.05$ compared to *Adm*$^{hi/hi}$ females.

CHAPTER V: ADRENOMEDULLIN OVER-EXPRESSION DOES NOT ALTER PATHOLOGY IN RENIN TRANSGENIC MODEL OF CHRONIC HYPERTENSION[3]

Introduction

Cardiovascular disease continues to be a leading cause of mortality in developed countries despite improved efforts to educate the public about lifestyle changes that can minimize risk. Hypertension affects nearly a third of adults in the United States (66) and is a major risk factor for more severe cardiovascular complications in the future if not controlled. In addition to changes to exercise routines and restricting sodium intake, individuals with hypertension may be prescribed a number of pharmaceutical drugs in an attempt to rein in blood pressure levels, including: diuretics, beta-blockers, ACE inhibitors, vasodilators, and blockers for the AngII receptor. Many of the existing therapies target the renin-angiotensin aldosterone system (RAAS), since chronic over-activation of this system causes fluid retention, and thus hypertension. Although these drugs help control blood pressure for many individuals, for some, blood pressure remains elevated despite aggressive treatment with several different drugs, a condition termed drug-resistant hypertension (224). Therefore, there is a great need to develop additional therapeutics that target factors external to the RAAS to improve blood pressure control and reduce the risk of heart disease and stroke.

Adrenomedullin (*Adm* = gene; AM = protein) is a small, widely expressed peptide with many cardioprotective properties. Several studies performed both *in vitro* and *in vivo* have demonstrated that AM has vasodilatory (108), inotropic (87), anti-fibrotic (168), and anti-hypertrophic (140, 231) functions. Together, these functions suggest a beneficial role for AM in the cardiovascular system, particularly during disease. In fact, several studies to date have

[3]Contributing authors include: Sarah E. Wetzel-Strong and Kathleen M. Caron

indicated that AM is indeed a cardioprotective peptide (20, 203). Studies using *Adm* heterozygous mice have revealed a worsening of cardiovascular disease in a sex-specific manner compared to animals with wildtype levels of AM (20), indicating the importance of this peptide in modulating injury during disease. Additionally, several groups have infused AM into animals and humans during cardiovascular disease and have noted a beneficial effect on blood pressure and prognosis (98, 157-159, 166, 228). However, it remains unclear whether genetic up-regulation of AM alters cardiovascular disease progression. Finally, a limited number of studies have found associations between various *Adm* polymorphisms and hypertension risk (90, 112), indicating a potential direct role for AM in disease progression.

Until recently, accurately measuring circulating levels of AM in the blood has posed a significant challenge due to the affinity of AM for its binding partner, complement factor H (CFH) (184), as well as its short half life (146). To circumvent these problems, an assay has been developed to measure circulating levels of mid-regional pro-AM (MR-proAM) (155). This stable peptide fragment is produced in equal proportions to AM during the cleavage process that occurs to produce mature AM (155), and therefore is a reliable read-out of AM circulating in the plasma. Measurement of MR-proAM during many human disease conditions have revealed that in many instances, including during cardiovascular disease, plasma levels of AM are elevated above baseline levels (97). Recently, clinicians have been exploring the usefulness of plasma MR-proAM levels as a biomarker for disease severity (31, 48, 101, 111, 142). With regards to cardiovascular disease, several studies have indicated that MR-proAM levels are a useful biomarker of cardiovascular disease severity (48, 142). In fact, these studies have revealed that MR-proAM may be a better biomarker than traditional cardiovascular biomarkers, such as BNP, by allowing for better stratification of patient risk and prediction of mortality following patient discharge (142). These findings clearly highlight the clinical significance of AM during human disease; supporting previous work performed using animal models.

Given the clear importance of AM as a protective peptide during cardiovascular disease, we were interested in determining whether genetic over-expression of *Adm* at levels comparable to the elevation observed in human patients with cardiovascular disease offered any further protection. To address this question, we crossed the *Adm* over-expression line (*Adm*$^{hi/hi}$), which has a three-fold elevation in circulating levels of AM in the plasma and a three- to 15-fold elevation in *Adm* gene expression within tissues compared to wildtype controls (245), to the renin transgenic mouse line, abbreviated as RenTgMK. The RenTgMK line is a well-characterized model of chronic hypertension (21-23), in which a modified version of the renin gene is constitutively expressed from the liver, resulting in persistent activation of the renin-angiotensin aldosterone system (RAAS). We then performed cardiovascular phenotyping on male *RenTgMK*:*Adm*$^{+/+}$ and *RenTgMK*:*Adm*$^{hi/hi}$ mice to assess differences in cardiomyocyte hypertrophy, cardiac function, and cardiac fibrosis.

Methods

Animals

Adm$^{hi/hi}$ animals, maintained on a C57Bl6/J background, used for these studies were generated as previously described (126, 245) and crossed to the established RenTgMK line, maintained on a 129S6/SvEv (21). Genotyping was performed by PCR using previously described primers (23, 126). For these studies, male mice were maintained on a mixed C57Bl6/J x 129S6/SvEv background and studied at 2-, 3-, 6-, and 8-months of age. Control animals utilized in this study were wildtype and *Adm*$^{hi/hi}$ age-matched animals maintained on a mixed C57Bl6/J x 129S6/SvEv background. Conscious echocardiograms were performed at 6- and 8-month of age by the Rodent Advanced Surgical Models Core lab at the University of North Carolina. Echocardiogram data was analyzed using Vevo2.2 software. All experiments were approved by the Institutional Animal Care and Use Committee of the University of North Carolina at Chapel Hill.

Gene expression analysis

Left ventricular tissue was collected and stored at -80°C in RNAlater (Ambion, AM7021) prior to RNA extraction. RNA was isolated from the ventricle tissue by a TriZol-chloroform extraction. Subsequently, the RNA was treated with DNaseI to degrade contaminating genomic DNA (Promega, M6101) prior to reverse transcription by M-MLV as described in the manufacturer's protocol (Invitrogen, 28025-013). Gene expression was then assessed by quantitative reverse transcription (qRT)-PCR with the StepOne Plus Real-Time PCR system by Life Technologies. Primer and probe sequences for *Calcrl*, *Ramp1*, *Ramp2*, and *Ramp3*, have been previously described (41, 42, 127). Pre-designed primer/probe assay-on-demand sets from Applied Biosystems were used to assess *Nppa* (Applied Biosystems, Mm01255747_g1) and *Col1a1* (Applied Biosystems, Mm00801666_g1) expression. Primer and probe sets for *Gapdh* (Applied Biosystems, 430813), Mouse eukaryotic translation elongation factor 1 alpha 1 (Meef) (8), *B2m* (Applied Biosystems, Mm00437762_m1), and *Polr2a* (Applied Biosystems, Mm00839493_m1) were used for internal housekeeping controls. Relative levels of gene expression were determined by the ΔΔCt method.

Organ weight ratios

Prior to dissection, the animal was weighed and the body weight was recorded. The total weight of both kidneys was measured after dissection to obtain kidney weight. The chambers of the heart were dissected apart so that the left ventricle remained intact and individual chamber weights were recorded. The total heart weight was obtained by adding together the individual chamber weights. Tibias were also dissected and the length was measured using calipers. Kidney, heart, and chamber weights were normalized to body weight as well as tibia length to generate organ ratios.

Histology

The left ventricle was cut in half along its axis and the right half (when the septum was facing up), was fixed in 4% paraformaldehyde overnight. After fixation, samples were embedded

in paraffin and 5μm sections were cut. Staining for hematoxylin and eosin (H&E) as well as Picrosirius red were performed following established protocols.

Cardiomyocyte cross-sectional area analysis

Left ventricle sections stained with H&E were used to assess cardiomyocyte cross-sectional area. For each animal, three distinct areas in the outer free wall of the ventricle, in which the cardiomyocytes were primarily oriented in a cross-sectional fashion, were randomly selected and imaged at 25x magnification. Using ImageJ software, the area of five cross-sectional cardiomyocytes was measured per field to generate the average cardiomyocyte cross-sectional area.

Quantitation of perivascular and interstitial fibrosis

Perivascular and interstitial fibrosis were quantitated from left ventricle sections stained with Picrosirius Red. To assess perivascular fibrosis, images of three coronary vessels in cross-section were obtained for each animal at 25x magnification. Then, using ImageJ software, the total thickening area, which includes the area of the fibrosis, intima layer, and lumen, was determined. Additionally, the intima and lumen area was measured to allow for determination of the fibrotic and intima areas individually through calculations. Finally, the lumen area was measured to account for vessel size. To determine the degree of interstitial fibrosis, images of the interstitial fibrosis near the apex of the left ventricle were obtained at 10x magnification. Using ImageJ software, a threshold analysis was performed to calculate the percent area of fibrosis. Briefly, the channels of the image were split. The area of fibrosis was determined by performing a threshold analysis of the green channel, as the Picrosirius red staining is most pronounced in this channel. Next, the total area of tissue present in the image was determined by performing a threshold analysis of the tissue visible in the blue channel and the percent area of collagen was calculated.

Statistical analysis

Statistical significance was determined by performing a two-tailed student's t-test using GraphPad Prism software. Values of $p<0.05$ were considered significant. All values shown on graphs in figures represent the means±SEM.

Results

Over-expression of Adm does not alter left ventricle hypertrophy

We began assessing cardiomyocyte hypertrophy by determining heart weight to body weight (HW:BW) and left ventricle to body weight (LV:BW) ratios because hypertrophy increases the overall mass of the left ventricle. However, since *Adm*$^{hi/hi}$ animals have increased HW:BW and LV:BW ratios at baseline due to cardiac hyperplasia during embryonic development (245), we represented these ratios as the percent change for the RenTgMK groups over the appropriate RenTgMK-negative controls. As expected, the hearts of both RenTgMK groups were visibly enlarged compared to non-RenTgMK controls. Notably, the hearts of *RenTgMK*:*Adm*$^{hi/hi}$ animals were extremely enlarged due to the combination of baseline cardiac hyperplasia in the *Adm*$^{hi/hi}$ line(reported in (245) and cardiomyocyte hypertrophy due to sustained activation of the RAAS. However, with this analysis, we found that there was no difference in the percent increase for either the HW:BW (**Figure 1A**) or LV:BW (**Figure 1B**) ratios between *RenTgMK*:*Adm*$^{+/+}$ and *RenTgMK*:*Adm*$^{hi/hi}$ animals. Together, these results indicate that hypertrophy is occurring at the same rate between *RenTgMK*:*Adm*$^{+/+}$ and *RenTgMK*:*Adm*$^{hi/hi}$ animals. Additionally, we recorded the weights of the kidneys, lung, and liver. When these organ weights were normalized to body weight, we found that *RenTgMK*:*Adm*$^{hi/hi}$ mice had significantly larger kidneys at 8 months of age (**Figure 1C**); however, lung (**Figure 1D**) and liver (**Figure 1E**) weights did not differ with genotype.

To further confirm that cardiomyocyte hypertrophy is similar between *RenTgMK*:*Adm*$^{+/+}$ and *RenTgMK*:*Adm*$^{hi/hi}$ mice, we measured the cross-sectional area of cardiomyocytes from

H&E stained sections of the left ventricle (**Figure 2A**). This analysis revealed that the cardiomyocyte cross-sectional areas of *RenTgMK*:*Adm*$^{+/+}$ and *RenTgMK*:*Adm*$^{hi/hi}$ mice were elevated compared to non-RenTgMK controls (**Figure 2B**), although not significantly. Finally, we assessed the gene expression levels of *Nppa* in left ventricular tissue, as elevated *Nppa* levels are indicative of hypertrophy. From this analysis, we found that *RenTgMK*:*Adm*$^{+/+}$ and *RenTgMK*:*Adm*$^{hi/hi}$ mice had elevated expression of *Nppa* compared to the corresponding animals negative for the renin transgene (**Figure 2C, D, and E**), however, there was no appreciable difference between the two RenTgMK groups. These data indicate that although the hearts of RenTgMK mice are hypertrophied, over-expression of *Adm* does not ameliorate this hypertrophy.

Perivascular and interstitial cardiac fibrosis are unchanged with Adm over-expression

In response to chronic pressure overload, fibrotic changes occur in the heart to provide structural support to the vessels and myocardium. Previous studies have found that AM can have anti-fibrotic effects (168), leading us to ask whether *Adm* over-expression attenuates the perivascular and interstitial fibrosis that occur in the RenTgMK model of chronic hypertension. To begin, we assessed the degree of perivascular fibrosis using left ventricle sections stained with Picorsirius Red (**Figure 3A**). As shown in Figure 5B, we measured the total area of vessel thickening, the intima layer area, and the area of the lumen. Using these measurements, we calculated the total thickening (**Figure 3C**), as well as the fibrotic (**Figure 3D**) and intima (**Figure 3E**) areas relative to the lumen size. Although these analyses did not reveal a difference in the degree of perivascular fibrosis between *RenTgMK*:*Adm*$^{+/+}$ and *RenTgMK*:*Adm*$^{hi/hi}$ mice **(Figure 3C, D, and E**), these results are confounded by the fact that animals positive for the renin transgene did not exhibit enhanced perivascular fibrosis compared to animals lacking the transgene.

In addition to assessing changes in perivascular fibrosis, we also used sections stained with Picrosirius red to determine whether differences exist in the degree of interstitial fibrosis (**Figure 4A**). Using a threshold analysis to determine the percent area of fibrosis for a given area of tissue, we found that the degree of interstitial fibrosis did not differ between *RenTgMK*:*Adm*$^{+/+}$ and *RenTgMK*:*Adm*$^{hi/hi}$ male mice (**Figure 4B**). Similar to what was observed for the perivascular fibrosis, the RenTgMK animals did not display increased fibrosis compared to non-renin transgene controls, even in advanced stages of the disease in contrast to what has been previously reported for this model, making it impossible to draw an accurate conclusion from these results. Finally, we assessed gene expression levels of *Col1a1* as a measure of collagen production, and thus a read out of fibrosis. From this analysis, we found that the relative expression of *Col1a1* was not significantly different for any group analyzed at 2 months (**Figure 4C**), 3 months (**Figure 4D**), 6 months (**Figure 4E**), and 8 months (**Figure 4F**), reflecting the Picrosirius red findings.

Over-expression of Adm does not alter cardiac function in renin transgene model

Finally, we assessed the impact of *Adm* over-expression on cardiac function in the RenTgMK model of chronic hypertension by performing echocardiography. As shown in Table 1, we did not detect any significant differences in cardiac function between *RenTgMK*:*Adm*$^{+/+}$ and *RenTgMK*:*Adm*$^{hi/hi}$ males, although by 8-months of age, we observed a trend for reduced heart function in *RenTgMK*:*Adm*$^{hi/hi}$ mice. This trend for decreased cardiac function can be attributed to a non-significant trend in dilation of the left ventricles of *RenTgMK*:*Adm*$^{hi/hi}$ mice at 8-months of age. Consistent with our data indicating no difference in the degree of left ventricular hypertrophy, we found no significant difference in wall thickness between *RenTgMK*:*Adm*$^{+/+}$ and *RenTgMK*:*Adm*$^{hi/hi}$ animals, although both groups had wall thicknesses that were significantly greater than age-matched non-RenTgMK+ controls. Together, these results indicate that *Adm* over-expression does not alter heart function in chronic hypertension,

and lends further support to the conclusion that hypertrophy is not altered by *Adm* over-expression in this model.

Discussion

In this study, we sought to determine the impact of constitutive three-fold elevation of AM in the context of chronic hypertension through the use of genetic mouse models. We found that AM over-expression did not alter the progression of cardiomyocyte hypertrophy in the renin transgenic model of chronic hypertension. Additionally, AM over-expression also did not alter the degree of fibrosis with disease progression. However, it is important to note that perivascular and interstitial fibrosis did not increase with advancing disease in the *RenTgMK: Adm*$^{+/+}$ animals as previously described by Caron et al (21). Finally, AM over-expression did not significantly alter cardiac function, although we did observe a trend for reduced heart function in *RenTgMK: Adm*$^{hi/hi}$ animals compared to *RenTgMK: Adm*$^{+/+}$ controls. Although these results seem to indicate that AM over-expression does not confer additional cardioprotection during chronic hypertension, the altered disease progression observed in *RenTgMK: Adm*$^{+/+}$ animals underscores the need to interpret the findings of this study cautiously.

Initial studies characterizing the RenTgMK line describe a progressive worsening of cardiac and kidney dysfunction with advancing age (20, 21, 23). Specifically, the degree of interstitial and perivascular fibrosis observed in the hearts of *RenTgMK: Adm*$^{+/+}$ mice increases progressively, with significant fibrotic plaques observed in the left ventricle wall by six- to eight-months of age (23). In this study, both *RenTgMK: Adm*$^{+/+}$ and *RenTgMK: Adm*$^{hi/hi}$ animals at six- and eight-months of age failed to display any noticeable increase in left ventricular fibrosis compared to non-RenTgMK-positive groups. There are several possibilities that could explain this lack of disease progression. For instance, it is possible that we acquired the incorrect RenTg line, and were therefore characterizing either the RenTgKC or RenTgARE lines. Studies by Caron et al (23) demonstrated that the RenTgKC and, in particular, the RenTgARE lines

present with a milder degree of hypertension, and thus, present with milder cardiac and kidney pathologies. Therefore, PCR primers were designed to allow for detection of either the MK sequence, which is present only in the RenTgMK line, or the ARE sequence, present only in the RenTgARE line, in order to determine the RenTg line utilized in the lab. From this approach, it was determined that the RenTg line used in these studies was, in fact, the RenTgMK line, therefore ruling out the possibility that we had inadvertently conducted these experiments in a less severe model of hypertension. Additionally, it is possible that the mixed genetic background utilized in this study has introduced a genetic modifier that has altered fibrosis progression. Other groups have demonstrated genetic background can alter the extent of fibrosis, cardiomyocyte hypertrophy, and inflammation in response to pressure overload on the heart (9). Therefore, it is likely that we inadvertently changed the genetic factors responsible for promoting cardiac fibrosis in the RenTgMK line by introducing the C57Bl6/J strain into this cross.

Previous studies have found that in the context of chronic hypertension, cardiomyocyte hypertrophy is exacerbated with a 50% reduction in AM (20), indicating that AM is an anti-hypertrophic peptide. Therefore, we might have expected to observe a reduction in cardiomyocyte area with AM over-expression. One potential explanation for the lack of difference in cardiomyocyte hypertrophy between *RenTgMK: Adm*$^{+/+}$ and *RenTgMK: Adm*$^{hi/hi}$ mice is that wildtype levels of AM are necessary to protect against exacerbated hypertrophy, but additional AM is unable to overcome the hypertrophic response to pressure overload. Some studies have identified AM as a vasodilatory peptide (108), and therefore it might be expected that AM over-expression could suppress cardiac hypertrophy by reducing blood pressure. However, previous work with the *Adm*$^{hi/hi}$ mice reveals that blood pressure is unchanged in this model of AM over-expression (245). Given that we did not observe a difference in cardiac hypertrophy, it is unlikely that blood pressure differences exist between *RenTgMK: Adm*$^{+/+}$ and *RenTgMK: Adm*$^{hi/hi}$ mice.

The observed trend for reduced cardiac function in the *RenTgMK: Adm*$^{hi/hi}$ mice is curious since *in vitro* and *in vivo* studies have generally suggested that AM exhibits inotropic properties (87, 216, 217). One possibility is that the hyperplastic hearts of the *Adm*$^{hi/hi}$ line (245) exhibit a decline in function with advancing age, independent of any overlaying cardiovascular disease. Although cardiac hyperplasia has been described in several mouse models (27, 81, 100, 183, 188, 227), the majority of these lines die due to a myriad of additional cardiac defects. However, Chaudhry et al (27) found that over-expression of cyclin A2 resulted in viable mice with hyperplastic hearts. Interestingly, at eight-months of age, the transgenic mice had a small, but significant decrease in cardiac function compared to wildtype controls (27), indicating that a similar phenomenon may occur in the *Adm*$^{hi/hi}$ mice. In support of this theory, male *Adm*$^{hi/hi}$ mice on a mixed 129S6/SvEv x C57Bl6/J background show a mild reduction in cardiac function compared to wildtype littermate controls at eight-months of age (Table 1); however this trend was not as pronounced as the trend observed between *RenTgMK: Adm*$^{+/+}$ and *RenTgMK: Adm*$^{hi/hi}$ mice. Thus, further longer-term studies are required to determine the underlying cause of the observed functional differences in aging *Adm*$^{hi/hi}$ animals.

Although the data presented here seem to indicate that AM over-expression does not alter disease progression in the context of chronic hypertension, additional studies need to be conducted to definitively define the effect of AM over-expression during this disease. One way to address this question is through the infusion of AngII via osmotic minipumps into wildtype and *Adm*$^{hi/hi}$ animals. Through this approach, hypertension can be achieved without introducing the confounding variable of a mixed genetic background. Additionally, this approach allows animals to develop normally before the onset of hypertension in adulthood, thereby more closely mimicking the human condition. Another potential approach that could be utilized is a renal artery clip model (70). This approach promotes an increase in AngII production by the kidney, ultimately leading to hypertension. Since this is a surgical model of hypertension, mixed genetic backgrounds can be avoided. However, as with any surgical model, the variability between

animals is greater due to slight differences in the surgical procedure on each animal, such as clip placement in this instance. Therefore, large numbers of animals would be required to accurately detect any differences attributed to genotype. Finally, to address the effect of pressure overload specifically on the heart, transaortic constriction could be performed. Although this approach is not a model of hypertension, and therefore cannot be used to draw conclusions regarding the role of elevated AM during human hypertension, this approach does allow for an assessment of the influence of AM over-expression on cardiac changes following an increase in load on the left ventricle. This approach could provide conclusive insight regarding the effect of AM over-expression on cardiomyocyte hypertrophy, as well as the impact on cardiac fibrosis.

In conclusion, this study attempted to decipher the effect of AM over-expression on disease progression in chronic hypertension. Presumably due to the mixed genetic background of the animals used for these experiments, disease pathologies did not progress as anticipated in *RenTgMK: Adm*$^{+/+}$ control animals, thereby making it difficult to draw conclusions from these findings. However, it seems likely that AM over-expression may have a minimal impact on cardiomyocyte hypertrophy, although this finding needs verification. Additionally, it appears that AM over-expression promotes a reduction in cardiac function, especially with advancing age. However, the explanation for this observation remains elusive and warrants closer study. Together, the results from this study indicate that over-expression of AM during hypertension may, at best, be minimally beneficial.

Financial Support

This work was supported by a pre-doctoral fellowship to SEW-S from the American Heart Association (12PRE1171002).

Figures

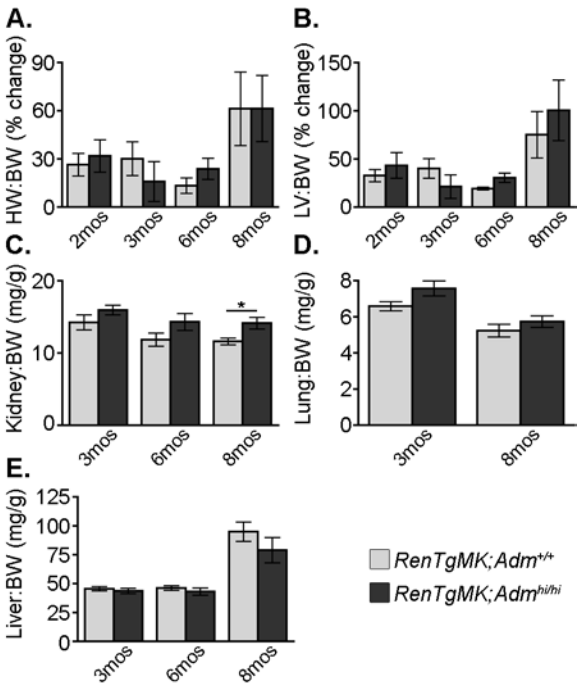

Figure 5.1. Heart and organ ratios of *RenTgMK;Adm*$^{+/+}$ and *RenTgMK;Adm*$^{hi/hi}$ males over time.

A. Heart weight to body weight ratios (HW:BW) represented as a percent change compared to corresponding non-RenTgMK+ controls. **B.** Left ventricle to body weight ratios (LV:BW) represented as the percent change compared to appropriate non-RenTgMK+ controls. **C.** Kidney weight to body weight ratios. **D.** Lung weight to body weight ratios. **E.** Liver weight to body weight ratios.

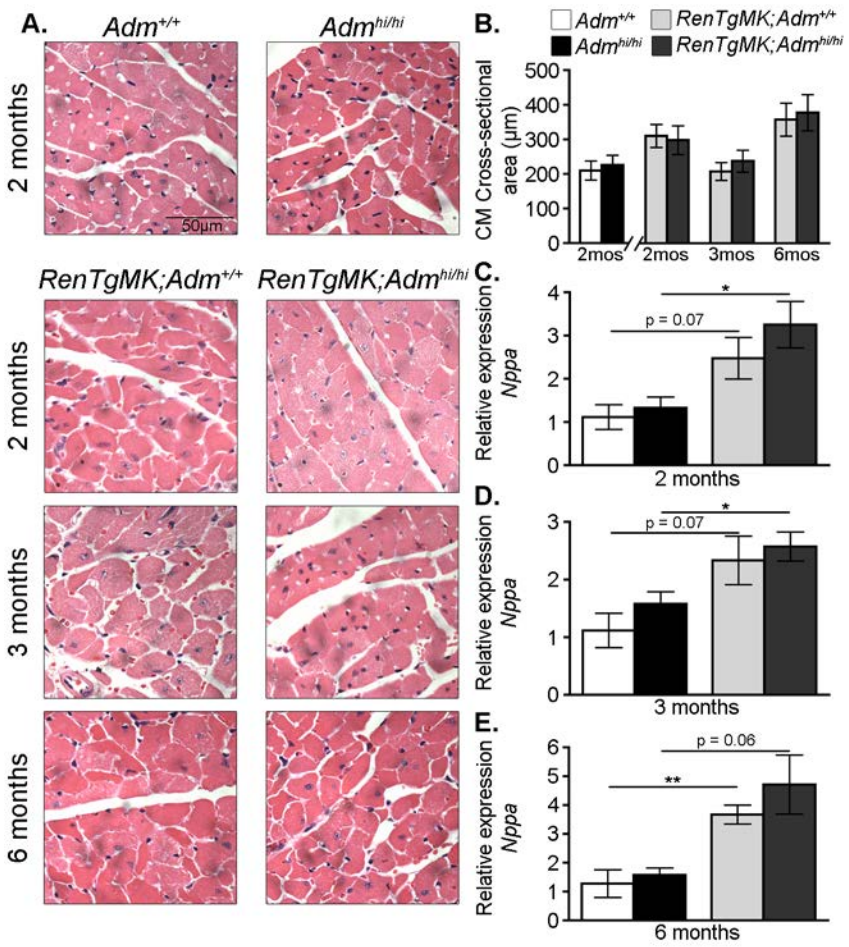

Figure 5.2. Over-expression of *Adm* does not alter the degree of cardiomyocyte hypertrophy.
A. Representative images of H&E stained sections of the left ventricle used for measuring cardiomyocyte cross-sectional area. All images obtained at 40x magnification. **B.** The cardiomyocyte (CM) cross-sectional area was determined by measuring the area of 15 cardiomyocytes per animal from H&E stained sections (n = 3-6). **C.** Quantitative RT-PCR (qRT-PCR) was performed using RNA isolated from the left ventricle of 2-month old animals. Relative expression of *Nppa* was determined by normalizing to the housekeeping gene *B2m* using the ΔΔCT method. **D.** Relative expression of *Nppa* from left ventricle samples of 3-month old animals. **E.** Relative expression of *Nppa* from left ventricle samples of 6-month old animals.

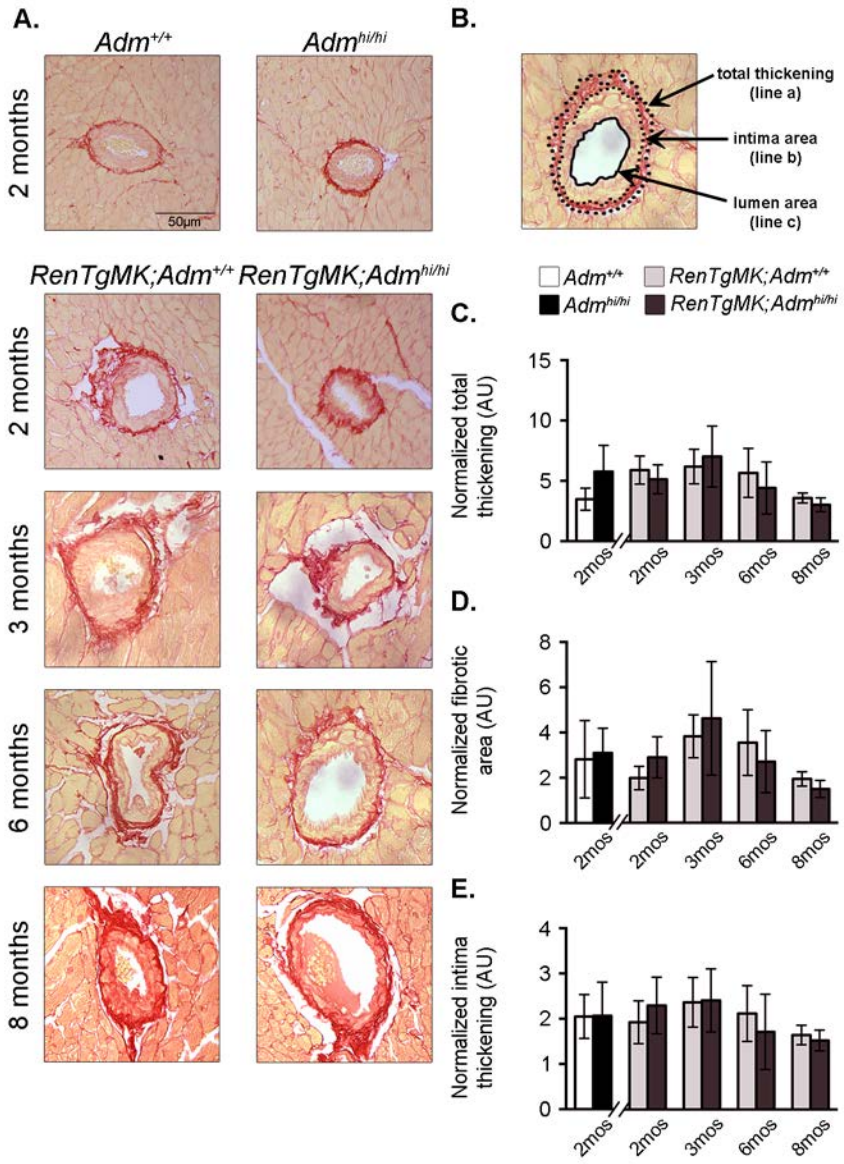

Figure 5.3. Perivascular fibrosis does not differ with *Adm* over-expression.
A. Representative images of coronary vessels stained with Picrosirius Red. All images obtained at 25x magnification. **B.** Schematic demonstrating areas measured for quantitation. **C.** The normalized total thickening was determined by subtracting the total thickening (line a shown in panel B) from the lumen area (line c in panel B) and dividing by the lumen size (line c in panel B). Three vessels were measured from each animal for this analysis (n = 3-7). **D.** The normalized fibrotic area was determined by subtracting the measured total thickening area (line a in panel B) from the measured intima area (line b in panel B) and dividing by the lumen area (line c in panel B). For this analysis, three vessels were measured from each animal (n = 3-7). **E.** The normalized intima thickening was determined by subtracting the intima area measurement (line b in panel B) from the lumen area (line c in panel B) and dividing by the lumen area (line c in panel B). Three vessels were measured from each animal (n = 3-7).

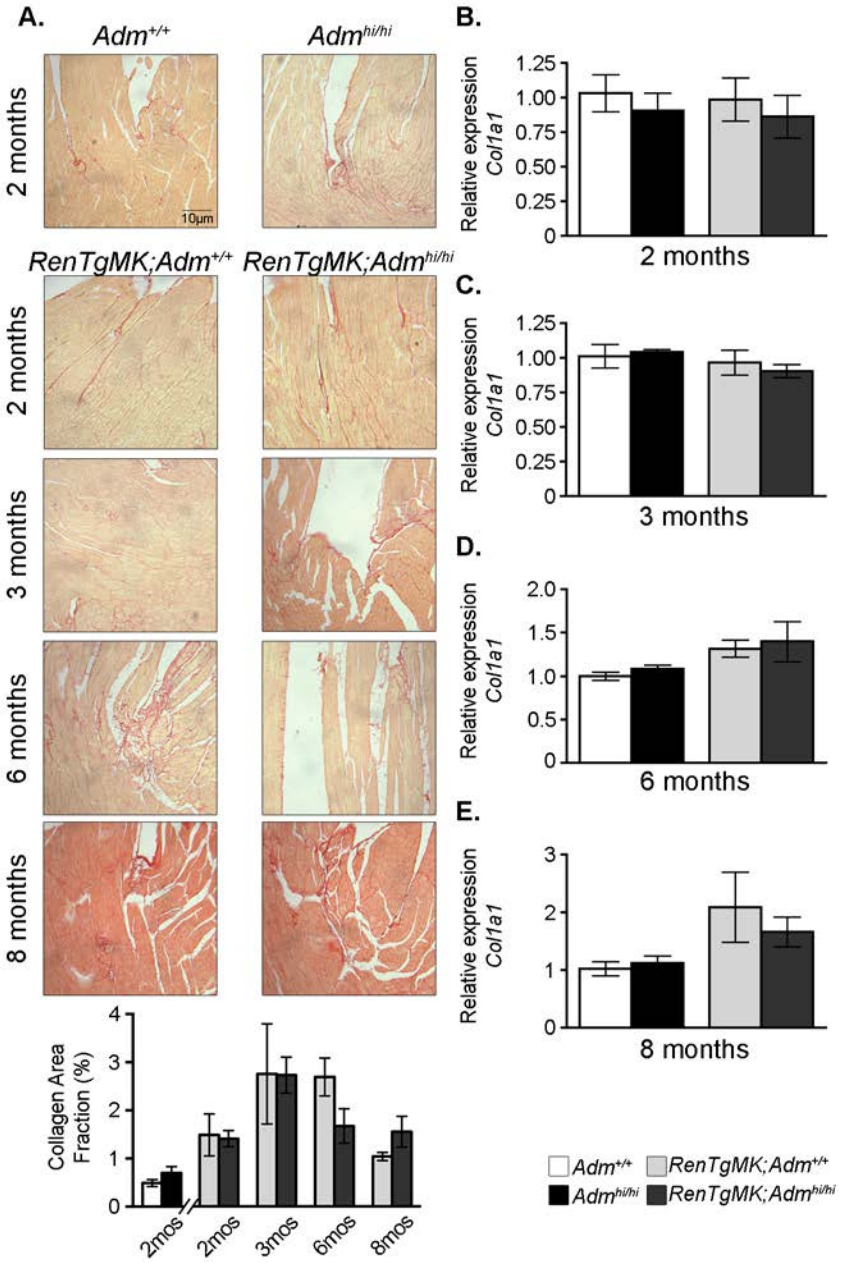

Figure 5.4. *Adm* over-expression does not alter the degree of interstitial fibrosis within the left ventricle.

A. Representative images of interstitial fibrosis at the apex of the left ventricle visualized with Picrosirius Red staining. All images obtained at 10x magnification. The collagen area fraction was determined by performing a threshold analysis using ImageJ software using 10x images of fibrosis at the apex of the left ventricle. **B.** Relative expression of *Col1a1* in the left ventricle of 2-month old males was determined by qRT-PCR. **C.** Relative expression levels of *Col1a1* from left ventricle samples of 3-month old males. **D.** Relative expression of *Col1a1* in the left ventricle from 6-month old males. **E.** Relative expression of *Col1a1* in the left ventricle of 8-month old males.

Table

Age	6 months				8 months			
Genotype	*Adm*$^{+/+}$	*Adm*$^{hi/hi}$	*RenTgMK;Adm*$^{+/+}$	*RenTgMK;Adm*$^{hi/hi}$	*Adm*$^{+/+}$	*Adm*$^{hi/hi}$	*RenTgMK;Adm*$^{+/+}$	*RenTgMK;Adm*$^{hi/hi}$
n	3	4	6	4	4	3	5	6
IVS;s (mm)	2.05±0.04	1.84±0.09	2.49±0.12*	2.47±0.04*	1.76±0.12	1.62±0.03	2.32±0.08*	2.03±0.12
IVS;d (mm)	1.38±0.14	1.30±0.12	1.83±0.08*	1.74±0.05*	1.20±0.05	1.15±0.07	1.62±0.04*	1.42±0.08
LVID;s (mm)	1.62±0.27	2.34±0.22	1.23±0.17	1.29±0.19*	2.00±0.19	2.27±0.21	1.70±0.20	2.63±0.34
LVID;d (mm)	2.99±0.27	3.77±0.34	2.74±0.24	2.80±0.30	3.68±0.13	3.71±0.20	3.26±0.18	4.22±0.35
LVPW;s (mm)	1.63±0.22	1.44±0.03	2.34±0.13*	2.18±0.09*	1.66±0.05	1.43±0.05	2.03±0.04*	2.01±0.11*
LVPW;d (mm)	1.26±0.22	1.00±0.05	1.73±0.08*	1.56±0.04*	1.05±0.07	1.03±0.05	1.40±0.12*	1.44±0.11*
%EF	79±4.47	69±1.86	88±2.05	85±4.57*	78±3.66	70±3.21	80±3.63	68±4.93
%FS	47±4.45	38±1.52	56±2.77	54±5.03*	46±3.18	39±2.51	48±3.68	38±4.13

Table 5.1. Echocardiograph data from 6- and 8-month males.
IVS – interventricular septum; LVID – left ventricle internal diameter; LVPW – left ventricle posterior wall; %EF – percent ejection fraction; %FS – percent fractional shortening; -s – systole; -d – diastole * $p<0.05$ compared to corresponding age-matched non-RenTgMK+ group

CHAPTER VI: CONCLUSIONS AND FUTURE DIRECTIONS

Summary

In summary, the results and conclusions from these studies further elucidate the role of AM in cardiac development. Specifically, the role of epicardial-derived AM in cardiac development has been demonstrated, opening many interesting avenues of future study. Additionally, these studies have highlighted the importance of estrogen-induced microRNAs in the balance of *Adm* expression in the female heart, and potentially reveal one mechanism underlying sex-dependent differences in cardiovascular health. Finally, studies presented in this dissertation have begun to assess the effect of physiologically elevated AM levels on cardiovascular health during chronic hypertension; although further studies in this area need to be conducted to definitively assess the impact of AM in this context to remove the confounding effect of mouse strain.

Current State of the Cardiovascular Field

Epicardium during cardiac development and regeneration

Although much advancement has been made in delineating the function of the epicardium during cardiac development, further studies into the signaling mechanisms regulating these processes are needed. One recent study in zebrafish has demonstrated that a heartbeat is essential for proper epicardium formation (185). Specifically, this study found that in zebrafish, a heartbeat is required for migration of epicardial cells to the heart from the PEO and for expansion of the epicardium over the heart surface after the initial seeding of epicardial cells (185). Further studies investigating the signaling pathways that are activated by the contracting myocardium to regulate migration are warranted.

Several studies have demonstrated that the epicardium plays an important role in the development of the conduction system (255) and the cardiac valves (244). Although the epicardium does not appear to directly contribute to the formation of the atrioventricular (AV) conduction axis (1), studies have demonstrated that EPDCs contribute to the formation of the annulus fibrosus (244, 255). The annulus fibrosus is responsible for insulating the ventricular walls from the electrical impulses fired in the atria to prevent premature contraction of the ventricles. Therefore, studies further investigating the relationship between epicardium formation, conduction diseases and arrhythmias may prove fruitful. In addition, lineage-tracing studies have determined that EPDCs replace the endocardial-derived fibroblasts in the AV lateral cushions (244). Further studies into the signaling mechanisms regulating this process and the potential implications in adulthood are still needed.

Unlike mammals, the heart of adult zebrafish can regenerate after injury (71, 186), and the epicardium has been implicated in the repair process (85, 103, 238, 251). Since scar formation negatively impacts long-term prognosis after injury, there has been a recent surge of interest in clarifying the mechanisms underlying this regenerative potential and translating these findings into mammals. Recently, Zhao et al (251) have determined that Notch signaling activation in the epicardium and endocardium is essential for cardiomyocyte proliferation in the compact zone. Specifically, this study determined that loss of Notch signaling resulted in scar formation, rather than regeneration, reflecting the wound healing process that occurs in other vertebrates (251). Interestingly, this study found that the epicardium still becomes activated with the loss of Notch signaling and that coronary regeneration is unaffected, indicating that regeneration is not prevented in this context by inadequate vascularization in the injured zone (251). However, this study revealed that cardiomyocyte proliferation is extremely sensitive to the amount of Notch signaling as over-activation of the Notch pathway also impaired regeneration (251). Several studies have suggested a link between AM and the Notch signaling pathway in the vasculature (118, 134, 162, 250); however, it remains unclear whether AM is up- or

downstream of Notch. Therefore, further studies investigating the mechanisms regulating Notch signaling in the epicardium and the potential role of AM in this process are warranted.

Other studies have indicated that ECM deposition by the epicardium is critical for zebrafish cardiac regeneration (238). Additionally, this study found that injury induced the expression of a fibronectin receptor in cardiomyocytes, highlighting the importance of fibronectin deposition for proper repopulation of the injured site by cardiomyocytes (238). Further studies regarding the mechanisms underlying the role of ECM in cardiomyocyte proliferation and the removal of ECM after regeneration may be valuable. Finally, Huang et al found that IGF signaling plays an important role in the regenerative process of zebrafish hearts (85), in addition to the previously described role during normal cardiac development (128). Therefore, it will be interesting to determine if other epicardial-derived growth factors involved in normal cardiac development can also contribute to cardiac regeneration.

Role of the epicardium during cardiovascular disease

Although advancements in modern medicine have enhanced survival following myocardial infarction, scar formation in the heart remains an unsolved problem, ultimately leading to complications later in life. Unsurprisingly, there has been a surge in interest to heal the scarred tissue either through repopulation of the injured area with stem cells or by other regenerative mechanisms. Since some studies have suggested that the epicardium may be a source of cardiac stem cells (131) and zebrafish studies have demonstrated a critical role for the epicardium in cardiac regeneration (85, 103, 238, 251), several groups have focused on determining the potential of the epicardium for repair following injury.

Recent work by Bollini et al (15) has investigated whether activated epicardial cells are similar to EPDCs generated during embryonic development. This study found that adult EPDCs exhibit a great degree of diversity (15). For instance, some of these EPDCs express markers of cardiac progenitor cells, while others appear to be programmed for a mesenchymal lineage

(15). This study also found that the surface markers of embryonic EPDCs differ from adult EPDCs in several ways (15), including increased expression of several stem cell and mesenchymal cell markers, such as Sca-1, CD45, CD44, and CD90. This indicates that distinct signaling mechanisms may be involved in the derivation of EPDCs at different stages of life and following injury. These findings underscore the challenges faced by researchers attempting to regenerate the adult heart from the activated epicardium and highlight the need to identify the signaling mechanisms determining EPDC fate.

A limited number of studies have sought to identify activators of epicardial genes following epicardial reactivation after an injury. One recent study by Huang et al (84) has identified an important role for C/EBP transcription factors in the regulation of *Raldh2* and *Wt1* expression during embryonic development and adult disease. Interestingly, this study found that suppression of C/EBP action resulted in improved heart function following myocardial infarction (84). This study also found a significant reduction in fibrosis and inflammation with the inhibition of C/EBP in the epicardium, which may contribute to the improved heart function (84). Further work uncovering the underlying mechanisms by which C/EBP suppression protects the heart would be interesting and could potentially uncover useful therapeutic targets.

Sex-dependent differences in cardiovascular health

Recent studies have sought to advance the understanding of the mechanisms underlying sex-dependent differences in cardiovascular disease. These studies are of utmost importance in order to elucidate the reasons behind the unpredictability of hormone replacement therapy (HRT) in menopausal women. Recent clinical trials have indicated that inhibition of PDE5 may offer protection in various cardiovascular diseases (57, 197, 218). However, recent work by Sasaki et al (200) has revealed that estrogen is essential for the therapeutic effectiveness of PDE5-mediated compounds in females. This finding highlights the complicated nature of treating cardiovascular disease in women, especially after the onset of menopause.

Interestingly, this study also found that while estrogen enhanced the effectiveness of the PDE5 inhibitor, sildenafil, in male mice, estrogen was not required in males to achieve therapeutic benefit (200), highlighting the differences that exist between the sexes in terms of hormone signaling.

Recently, investigators have also become interested in determining the role of hormones in male cardiac health. One recent study by Le et al (121) sought to determine the impact testosterone and estrogen in both sexes following myocardial infarction. Overall, hormones were detrimental to male cardiac health, primarily due to increased apoptosis (121). Interestingly, estrogen administration to males exacerbated infarct size, despite the fact that ERα and ERβ are expressed at similar levels in male and female hearts (121). This study, however, did not assess levels of GPR30, a membrane-bound GPCR that is capable of binding estrogen and promoting downstream signaling (6), which may account for the differing effect of estrogen between males and females. In summary, this study provides some insight regarding the role of hormones in damage following myocardial infarction between the sexes; however, further studies are required to fully elucidate the complex pathways involved in these processes.

Finally, the roles of several other pathways in mediating cardioprotection in females have been explored. For example, the suppression of reactive oxygen species (ROS) generation by estrogen has been suggested to be one mechanism by which female hearts are protected from damage in the context of ischemia-reperfusion injury (104). Recent work by Liu et al (133) has further elucidated the mechanisms underlying estrogen-mediated suppression of ROS generation. Specifically, this study found that estrogen increased the movement of phosphorylated p38β mitogen-activated protein kinase (p38β MAPK) into the mitochondria (133). Once in the mitochondria, p38β MAPK interacts with MnSOD, a member of the superoxide dismutase family, to activate it and thereby decrease ROS formation (133). Other studies have demonstrated that AM, which can be induced by estrogen (240), can offer

cardioprotection from ischemia-reperfusion injury by reducing ROS formation (105). Together, these, and many other studies, highlight the importance of estrogen in the reduction of ROS generation, which ultimately contributes to protection of the female heart upon re-oxygenation of the cardiac tissue. From these studies, it may be possible to generate therapeutics to reduce ROS generation in males and menopausal females following ischemia-reperfusion to mitigate cardiac damage.

Future Directions

Experiments related to AM signaling during cardiac development

One possible area of future study involves further exploration into the role of AM during cardiac development. Previous work by the Caron lab found that loss of CLR from endothelial cells through the use of Tie2-Cre mice(59) resulted in embryonic demise during mid-gestation with a phenotype similar to mice globally lacking CLR (42). Although this study clearly demonstrates the importance of endothelial AM signaling for proper lymphatic development, it remains unclear whether AM signaling on the epicardium, endocardium, or endothelial cells of the heart contribute to the observed cardiac defects as Tie2, the promoter driving Cre in the previously described study, is expressed in all of these cell populations (239).

In order to address this question, the *Calcrl*$^{fl/fl}$ line could be crossed to the *Wt1*$^{tm1(EGFP/cre)Wtp}$*/J* line, abbreviated as Wt1-Cre, to remove CLR specifically from the proepicardium and epicardium. Once this cross has been established, the first thing to determine is whether epicardial-specific loss of CLR is compatible with life. Therefore, several litters of animals can be generated to assess the number of *Wt1-Cre: Calcrl*$^{fl/fl}$ animals that survive to birth and beyond. Next, timed matings should be performed to assess cardiac morphology throughout development, regardless of whether *Wt1-Cre: Calcrl*$^{fl/fl}$ animals are viable. If it is found that these animals are not surviving to birth, the timed matings can also be used to determine at what developmental stage the embryos are dying. This genetic cross will

allow for the determination of the role of AM signaling on the epicardium during development, and might also permit an evaluation of the relative contribution of the lymphatic and cardiovascular abnormalities to embryonic demise.

In addition to examining the contribution of AM signaling on the epicardium to cardiac development, future studies can be conducted to determine whether AM over-expression alters the expression of growth factors or their respective receptors either in the epicardium or the myocardium to contribute to the cardiac hyperplasia observed in the *Adm*$^{hi/hi}$ line. To begin, RNA-seq could be performed on embryonic cardiomyocyte and epicardial cell samples from wildtype and *Adm*$^{hi/hi}$ animals to assess whether AM over-expression changes the expression levels of any growth factors or receptors. This approach will allow for the identification of interesting pathways in a rapid fashion and minimize the chance of overlooking important contributors to cardiac hyperplasia in this model. If this approach identifies growth factor pathways that are altered with AM over-expression, these gene expression changes can be individually verified by qRT-PCR. Upon confirming changes in gene expression, the role of these pathways in AM-driven cardiac hyperplasia can be determined through inhibition or activation of these pathways *in vitro* and *in vivo*.

In the event that AM over-expression is found to increase expression of one or more growth factors in epicardial cells, the contribution of these individual growth factors on AM-mediated cardiac hyperplasia can be assessed in several ways. First, the growth factor of interest can be knocked down by shRNA in epicardial cells from wildtype and *Adm*$^{hi/hi}$ animals. The supernatant from wildtype and *Adm*$^{hi/hi}$ epicardial cells treated with and without shRNA can then be applied to either isolated neonatal cardiomyocytes, myocyte-like cells lines, or embryonic heart cultures and the effect on proliferation can be assessed. It is important to characterize the degree of knockdown achieved, since many of these growth factors have previously been demonstrated to be essential for proper cardiac growth and development (128, 138, 234). Therefore, if the knockdown is too efficient, it may be difficult to assess whether the

increased growth factor expression is driving the hyperplasia observed in *Adm*$^{hi/hi}$ animals. One possible way to circumvent this problem is to treat knockdown cells with increasing concentrations of the growth factor to determine the effect on proliferation. It may also be interesting to cross the *Adm*$^{hi/hi}$ line to mouse lines lacking the growth factor of interest and assessing cardiovascular development in animals heterozygous for the particular growth factor in the presence of AM over-expression. The hope with this approach is that AM over-expression will not promote an increase in growth factor levels above those observed in wildtype animals to determine the contribution of this growth factor over-expression on cardiac hyperplasia in the *Adm*$^{hi/hi}$ line. Alternatively, the growth factor receptors could be pharmacologically inhibited in cultures of cardiomyocytes, prior to treatment with epicardial cell supernatant from wildtype and *Adm*$^{hi/hi}$ embryos. In the scenario in which AM over-expression is found that change the expression profile of growth factor receptors, an approach similar to that described above can be utilized. Briefly, this possibility can be investigated by applying chemical inhibitors of these receptors to cardiomyocyte cultures treated with supernatant from either wildtype or *Adm*$^{hi/hi}$ epicardial cultures and the effect on proliferation can be determined. Additionally, cardiac development can be assessed in animals that are heterozygous for these receptors and over-express AM in a complimentary approach to determine the effect of signaling through these receptors on AM-mediated cardiac hyperplasia.

Another mechanism by which AM may indirectly promote cardiac hyperplasia is through receptor transactivation. Several groups have demonstrated that GPCRs can activate receptor tyrosine kinases (RTK) and that it is the signaling downstream of the activated RTK that produces the observed outcomes (45). In order to determine whether RTK transactivation is occurring with AM treatment, epicardial and cardiomyocyte cell cultures could be treated with either vehicle or AM. Upon treatment with AM, protein could be collected from these cells and assayed for RTK phosphorylation. Commercial kits, such as the Mouse Phospho-Receptor Tyrosine Kinase Array from R&D Systems, allow users to assess the phosphorylation status of

many RTKs at one time, thereby minimizing the time, number of samples, and reagents needed to thoroughly investigate the possibility of RTK activation. If this experiment identifies one or more RTKs that are activated by AM, several experiments can be conducted to determine how this activation is occurring. To date, studies have characterized several ways in which GPCRs can transactivate RTKs (reviewed in (246)). One mode of RTK transactivation occurs when GPCR activation triggers the activation of metalloproteases within the cell, resulting in the release of sequestered growth factor precursors. These released growth factors can then act on the appropriate RTK to promote activation of the signaling cascade (187). The remaining two modes of RTK transactivation do not include activation of the RTK by the native ligand. Instead, activation of the GPCR can either promote downstream signaling that results in RTK phosphorylation (44), and thus activation, or a complex can form between the activated GPCR and the RTK, resulting in RTK activation (144). To test whether growth factor precursors are being released to activate the RTK, an inhibitor of the RTK can be added to the cells along with AM treatment, and phosphorylation of the RTK can be assessed. In order to determine whether signaling downstream of CLR promotes RTK phosphorylation, cells treated with AM can also be treated with chemical inhibitors of downstream signaling molecules and RTK phosphorylation can be assessed. Finally, in order to determine whether CLR is directly interacting with the RTK to promote activation, immunoprecipitation could be performed, utilizing a tagged version of CLR, since reliable antibodies are not commercially available for this receptor.

Finally, in addition to the interaction of AM with CLR and RAMP2 or RAMP3, it is possible that AM may also act through additional receptor complexes to modulate some aspects of cardiac development. For instance, recent work by Klein et al (110) has suggested that the chemokine receptor CXCR7 can function as a decoy receptor for AM. Therefore, it is possible that AM is interacting with CXCR7 and potentially eliciting downstream changes via alternative signaling pathways. Recent studies have shown that activation of other chemokine receptors, such as Ccr7, results in an inhibition of Wnt signaling (249). Since Wnt signaling can activate

the transcription of genes involved in cell proliferation, it is possible that a similar mechanism occurs when AM interacts with CXCR7 as a means of regulating cardiac proliferation. To test this possibility, *in vitro* studies can be performed to determine whether AM treatment in the presence or absence of CXCR7 alters β–catenin localization. Additionally, cells could be treated with Wnt pathway inhibitors, and the effect of AM over-expression or CXCR7 loss on cell proliferation could be assessed.

Experiments related to the regulation of Adm by estrogen-induced microRNAs

Further exploration into the mechanisms underlying the regulation of *Adm* by estrogen-induced microRNAs represents another interesting avenue of future research. The results presented in this dissertation indicate that regulation of *Adm* by estrogen-induced microRNAs may be largely confined to the heart. This finding raises several questions, including: how do the profiles of estrogen-induced microRNAs differ between the heart and other estrogen-responsive tissues, and which estrogen-induced microRNAs are responsible for regulating *Adm* expression in the heart. In order to address these questions, several experiments could be conducted. First, using RNA extracted from several tissues, the effect of estrogen on microRNA expression levels could be assessed by microarray. For this experiment, female mice would be subjected to ovariectomy before sexual maturation and divided into two groups; a control group receiving vehicle injections and a group injected with β–estradiol. This experimental approach allows for the conclusive determination of estrogen's effect on microRNA expression across different tissues without the confounding variable of changing progesterone levels, which occurs in cycled females (76). Once the profile of estrogen-induced microRNAs that are differentially expressed in the female heart is established, additional studies can be conducted to evaluate the relative importance of each of these remaining microRNAs in the regulation of *Adm* expression. One approach to determining the relative importance of each microRNA would be to

treat isolated neonatal cardiomyocytes with the microRNAs of interest and determine the relative decrease in *Adm* gene expression by qRT-PCR. From this approach, one would predict that the largest reduction in *Adm* gene expression would occur with the microRNA or group of microRNAs that are most critical for regulating *Adm* expression. Finally, confirmation of these findings could be obtained by performing the converse experiment. In this set-up, the microRNAs of interest could be silenced with siRNAs, and the expression of *Adm* could be assessed, only this time, an up-regulation of *Adm* would be expected.

In addition to pursuing further mechanistic studies, additional work can be conducted to investigate the effect of dramatic up-regulation of *Adm* in the heart in the context of cardiovascular disease progression. Human studies have noted that the onset of menopause results in an increased number of cardiovascular risk factors, increasing the likelihood of a cardiovascular incident (43). Given the many cardioprotective properties of AM (20, 77, 78, 105, 107, 165, 170, 171, 173, 203), it seems plausible that elevated levels of AM in females may offer protection in the context of cardiovascular disease. One approach that could be used to test whether the dramatic elevation of *Adm* in the female heart is cardioprotective is by challenging female wildtype and $Adm^{hi/hi}$ mice with ischemia-reperfusion injury and assessing disease pathology. Since *Adm* levels differ with changing levels of estrogen during the estrus cycle (reported in Chapter IV), it is important to ensure that females are cycled and analyzed at the same point in the estrus cycle. Additionally, since *Adm* transcript levels are elevated by 60-fold in the female $Adm^{hi/hi}$ heart (see Chapter IV), it may be interesting to also compare disease progression between intact and ovariectomized females. Finally, if intact $Adm^{hi/hi}$ females are found to be better protected against ischemia-reperfusion injury compared to ovariectomized $Adm^{hi/hi}$ females, the role of estrogen in this response could be determined by infusing estrogen into ovariectomized mice by osmotic minipump, and again, assessing cardiovascular pathologies.

Finally, studies could be conducted to further explore the relationship between *Adm* and other genes targeted by the same cohort of estrogen-induced microRNAs during cardiovascular disease. For these studies, female mice lacking either expression of several estrogen-induced microRNAs predicted to target the *Adm* 3′UTR could be generated and subjected to ischemia-reprefusion. Then, qRT-PCR could be used to assess the expression levels of *Adm* and other genes that share a high proportion of the knocked out microRNAs in the heart. One would expect that *Adm* expression levels would be elevated in the knockout animals compared to wildtype controls due to the loss of estrogen-dependent negative regulation of *Adm*, recapitulating what is observed in the $Adm^{hi/hi}$ female heart. Once the expression profiles of the related genes are determined, experiments can then be conducted to uncover the roles played by each gene in any observed differences in disease progression. Special focus should be paid to ion channels, as well as cell junction proteins, as highlighted in the discussion section of Chapter IV.

Experiments pertaining to epicardial-derived AM in cardiovascular disease

Another potential area of study involves investigating the role of AM, in particular the function of epicardial-derived AM, during ischemic injury of the heart. Given the many protective properties of AM (19, 37, 60, 106, 108, 140, 168, 231), there has been much interest in determining the cardioprotective potential of AM. Several studies have demonstrated that AM does offer some cardioprotection as a 50% reduction of AM results in worsened cardiovascular disease (20, 203). These findings have led researchers to ask whether over-expression of AM enhances protection of the heart following injury. To date, several studies have over-expressed AM either by infusion or adeno-associated virus (AAV) in animals and assessed disease following ischemia-reperfusion injury (78, 125, 170, 237, 243). These studies have largely found that AM over-expression does offer a modest degree of protection. However, these studies have been unable to address the effect of a physiologically-relevant 3-fold elevation in AM on

prognosis following ischemic injury. Additionally, as our recent work has determined that the epicardium is a major contributor of AM in the heart (245), the contribution of epicardial-derived AM on cardioprotection remains unknown. This last point is of particular interest given the reactivation of the epicardium following injury to the adult heart (**Figure 1**).

These questions can readily be addressed using genetic mouse models available in the lab. In order to address the effect of a genetic 3-fold elevation of AM, $Adm^{hi/hi}$ mice can be subjected to permanent ligation of the left anterior descending (LAD) artery. By opting to perform a permanent ligation of the artery, potential differences in reperfusion injury due to the antioxidant effect of AM (19, 105) can be avoided, thereby allowing for a more robust evaluation of the effect of AM over-expression on infarct size. This approach could also minimize the number of animals needed to assess the impact of AM over-expression on ischemic injury due to increased reproducibility of the area at risk (AAR). In the future, ischemia-reperfusion studies can also be performed to assess the role of elevated AM during reperfusion injury and to more closely mimic the human condition after coronary artery bypass surgery.

In order to assess whether genetic over-expression of AM offers cardioprotection following myocardial infarction, several parameters need to be evaluated. Several studies have indicated that AM enhances contractility (87, 216, 217) making it prudent to assess the impact of AM status on heart function. Therefore, baseline echocardiograms should be obtained for wildtype and $Adm^{hi/hi}$ animals prior to permanent ligation of the LAD artery. Then, echocardiograms can be performed 5-, 10-, and 15-days post-surgery on surviving animals to determine whether heart function is improved with AM over-expression. Another major factor that contributes to long-term prognosis following myocardial infarction is the extent of tissue damage in the vulnerable area. Therefore, a thorough examination of infarct size following ligation needs to be conducted to determine if AM over-expression reduces infarct size relative to wildtype animals. In order to confidently assess the impact of AM over-expression on infarct size, it is necessary to determine the percentage of the area at risk (AAR) that is infarcted.

Commonly, the AAR is determined by perfusing the heart with Evans blue dye, which will stain all perfused tissue, leaving the AAR unstained. After identification of the AAR, the tissue can be stained with triphenyl tetrazolium chloride (TTC) to identify the infarcted tissue. The reduction of TTC by metabolically active tissues results in the production of a red byproduct, while deceased tissue within the infarct is unable to catalyze this reduction resulting in a pale coloration of dead tissue within the infarcted region. By comparing the infarct area to the AAR for wildtype and $Adm^{hi/hi}$ animals, it can be determined whether AM reduces infarct size. In addition to quantifying the infarct area, the effect of AM over-expression on cell death can be assessed by TUNEL and cleaved caspase-3 staining to corroborate the TTC staining findings. By using both of these staining methods, total cell death can be assessed with TUNEL staining, while the contribution of apoptosis to the observed cell death can be determined with cleaved caspase-3 staining.

After determining the effect of AM over-expression on infarct size and cell death, it would be interesting to determine whether scar formation is altered with AM over-expression. Following the initial wave of cell death after an ischemic event, scar formation begins to stabilize the damaged area of the heart. Some studies have indicated that AM has an anti-fibrotic effect (168), so it is possible that AM over-expression in this model will results in reduced deposition of ECM and, thus, a reduction in scar formation. To establish whether AM reduces the degree of fibrosis following myocardial infarction, sections of the infarcted zone of the heart can be stained with Picrosirius Red to identify collagen fibers and the degree of fibrosis can be quantitated. Further support for any changes observed in fibrosis from histological assessment can be garnered by assessing changes in the expression of fibrosis-related genes, such as *Col1a1* and *TGF-β1*, by qRT-PCR. Inflammation also plays an important role in wound healing and therefore, should also be considered in this model. In order to quickly assess whether inflammatory differences exist, histological sections stained with H&E can be examined to determine the extent of inflammation. If differences are observed, immunohistochemistry can be

utilized to identify the immune cells present in the wound to deduce whether the composition of inflammatory cells within the wound varies with AM expression status.

Finally, some groups have demonstrated that the epicardium becomes reactivated following an injury such as myocardial infarction (52, 130, 252). During this reactivation, epicardial cells proliferate and undergo EMT to produce fibroblasts (252). It has also been suggested that the resulting EPDCs can secrete pro-angiogenic factors, thus promoting revascularization of the infarcted region (252). Prior studies have established that AM can promote angiogenesis (60, 106), and therefore, AM over-expression may improve revascularization of the infarct zone. This possibility can be addressed by staining heart sections with a marker of vascular endothelial cells, such as PECAM-1, and quantitating the number of vessels in the regions surrounding the infarct as well as within the infarcted zone. Work from our lab has revealed a proliferative role for AM in some scenarios (245). To determine whether AM over-expression increases proliferation of the activated epicardium, heart sections could be stained with phospho-Histone H3, a marker of mitosis, along with a marker of the epicardium, such as cytokeratin (180, 236), and the number of cells positive for both markers could be quantitated. Lastly, the effect of AM on EMT of the EPDCs can be assessed with immunohistochemistry. Specifically, heart sections of the infarcted region can be stained with a marker of epithelial cells, such as cytokeratin or E-cadherin (94), and a marker of mesenchymal cells, such as vimentin or FSP-1 (94), to identify cells transitioning from an epithelial phenotype to a mesenchymal fate. Together, these proposed experiments thoroughly characterize the effect of AM on cardiac repair following a myocardial infarction.

In addition to characterizing the effect of globally elevated AM on cardiac repair following a myocardial infarction, another interesting area of future study lies in determining the contribution of epicardial-derived AM in this process. When the $Adm^{hi/hi}$ line was generated, the stabilizing bGH 3′UTR was flanked with loxP sites (126). Thus, in the presence of Cre recombinase, the stabilizing 3′UTR is removed and *Adm* expression is re-stabilized by the

native 3′UTR, resulting in wildtype levels of AM (245). Therefore, the epicardial-specific Wt1-Cre line could be used to specifically reduce AM to wildtype levels in the epicardium, while maintaining AM over-expression in all other tissues. With these mice, we can then perform the experiments described above to determine which, if any, of these phenotypes are driven by AM produced by the epicardium.

Together, the studies proposed here would further our understanding of the function of AM during cardiac development. Additionally, these studies would advance our knowledge of the signaling pathways through which AM elicits its actions during development. Finally, these studies would also begin to address questions regarding the effect of a 3-fold elevation of AM during human cardiovascular disease and explore the possibility of exploiting this pathway for cardiac regeneration following injury.

Figures

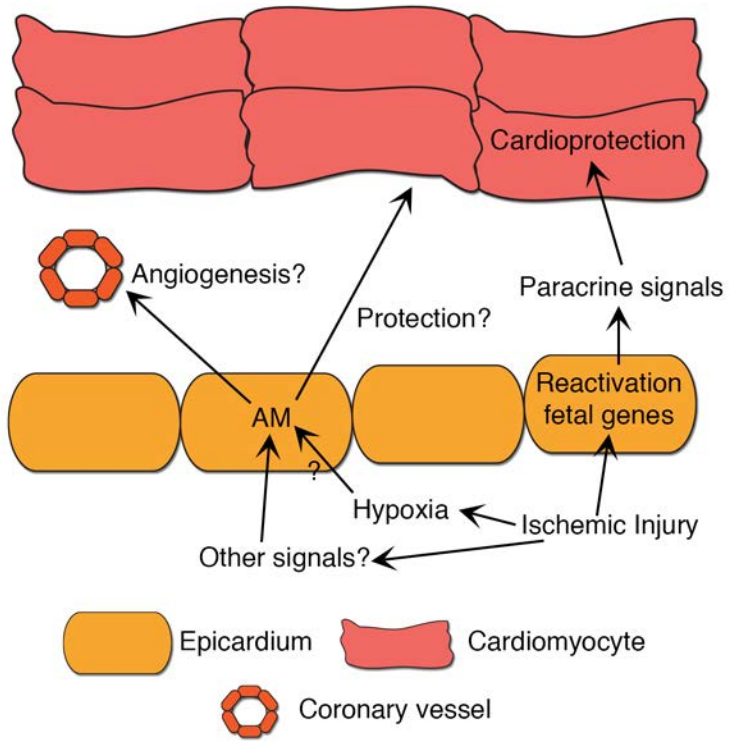

Figure 6.1. Epicardial reactivation following ischemic injury.
Upon ischemic injury, the fetal gene program is reactivated in the epicardium. Expression of AM could potentially be increased in the epicardium by hypoxia following ischemic injury of the heart. Given that AM is elevated following injury to the human heart and the many protective properties of AM, this may represent a novel mechanism of protection, although the underlying mechanisms have yet to be characterized.

REFERENCES

1. **Aanhaanen WT, Mommersteeg MT, Norden J, Wakker V, de Gier-de Vries C, Anderson RH, Kispert A, Moorman AF, and Christoffels VM**. Developmental origin, growth, and three-dimensional architecture of the atrioventricular conduction axis of the mouse heart. *Circ Res* 107: 728-736, 2010.

2. **Abdellatif M**. Differential expression of microRNAs in different disease states. *Circ Res* 110: 638-650, 2012.

3. **Agah R, Frenkel PA, French BA, Michael LH, Overbeek PA, and Schneider MD**. Gene recombination in postmitotic cells. Targeted expression of Cre recombinase provokes cardiac-restricted, site-specific rearrangement in adult ventricular muscle in vivo. *J Clin Invest* 100: 169-179, 1997.

4. **Allaker RP, Zihni C, and Kapas S**. An investigation into the antimicrobial effects of adrenomedullin on members of the skin, oral, respiratory tract and gut microflora. *FEMS Immunol Med Microbiol* 23: 289-293, 1999.

5. **Archbold JK, Flanagan JU, Watkins HA, Gingell JJ, and Hay DL**. Structural insights into RAMP modification of secretin family G protein-coupled receptors: implications for drug development. *Trends Pharmacol Sci* 32: 591-600, 2011.

6. **Ariazi EA, Brailoiu E, Yerrum S, Shupp HA, Slifker MJ, Cunliffe HE, Black MA, Donato AL, Arterburn JB, Oprea TI, Prossnitz ER, Dun NJ, and Jordan VC**. The G protein-coupled receptor GPR30 inhibits proliferation of estrogen receptor-positive breast cancer cells. *Cancer Res* 70: 1184-1194, 2010.

7. **Baek ST, and Tallquist MD**. Nf1 limits epicardial derivative expansion by regulating epithelial to mesenchymal transition and proliferation. *Development* 139: 2040-2049, 2012.

8. **Barrick CJ, Lenhart PM, Dackor RT, Nagle E, and Caron KM**. Loss of receptor activity-modifying protein 3 exacerbates cardiac hypertrophy and transition to heart failure in a sex-dependent manner. *Journal of molecular and cellular cardiology* 52: 165-174, 2012.

9. **Barrick CJ, Rojas M, Schoonhoven R, Smyth SS, and Threadgill DW**. Cardiac response to pressure overload in 129S1/SvImJ and C57BL/6J mice: temporal- and background-dependent development of concentric left ventricular hypertrophy. *American journal of physiology Heart and circulatory physiology* 292: H2119-2130, 2007.

10. **Barry DM, Xu H, Schuessler RB, and Nerbonne JM**. Functional knockout of the transient outward current, long-QT syndrome, and cardiac remodeling in mice expressing a dominant-negative Kv4 alpha subunit. *Circ Res* 83: 560-567, 1998.

11. **Bartel DP**. MicroRNAs: genomics, biogenesis, mechanism, and function. *Cell* 116: 281-297, 2004.

12. **Bhat-Nakshatri P, Wang G, Collins NR, Thomson MJ, Geistlinger TR, Carroll JS, Brown M, Hammond S, Srour EF, Liu Y, and Nakshatri H**. Estradiol-regulated microRNAs control estradiol response in breast cancer cells. *Nucleic acids research* 37: 4850-4861, 2009.

13. **Bhowmick NA, Chytil A, Plieth D, Gorska AE, Dumont N, Shappell S, Washington MK, Neilson EG, and Moses HL**. TGF-beta signaling in fibroblasts modulates the oncogenic potential of adjacent epithelia. *Science* 303: 848-851, 2004.

14. **Bjornstrom L, and Sjoberg M**. Mechanisms of estrogen receptor signaling: convergence of genomic and nongenomic actions on target genes. *Mol Endocrinol* 19: 833-842, 2005.

15. **Bollini S, Vieira JM, Howard S, Dube KN, Balmer GM, Smart N, and Riley PR**. Re-activated adult epicardial progenitor cells are a heterogeneous population molecularly distinct from their embryonic counterparts. *Stem cells and development* 23: 1719-1730, 2014.

16. **Bomberger JM, Parameswaran N, Hall CS, Aiyar N, and Spielman WS**. Novel function for receptor activity-modifying proteins (RAMPs) in post-endocytic receptor trafficking. *J Biol Chem* 280: 9297-9307, 2005.

17. **Brouillette J, Rivard K, Lizotte E, and Fiset C**. Sex and strain differences in adult mouse cardiac repolarization: importance of androgens. *Cardiovasc Res* 65: 148-157, 2005.

18. **Cai CL, Martin JC, Sun Y, Cui L, Wang L, Ouyang K, Yang L, Bu L, Liang X, Zhang X, Stallcup WB, Denton CP, McCulloch A, Chen J, and Evans SM**. A myocardial lineage derives from Tbx18 epicardial cells. *Nature* 454: 104-108, 2008.

19. **Cao YN, Kuwasako K, Kato J, Yanagita T, Tsuruda T, Kawano J, Nagoshi Y, Chen AF, Wada A, Suganuma T, Eto T, and Kitamura K**. Beyond vasodilation: the antioxidant effect of adrenomedullin in Dahl salt-sensitive rat aorta. *Biochem Biophys Res Commun* 332: 866-872, 2005.

20. **Caron K, Hagaman J, Nishikimi T, Kim HS, and Smithies O**. Adrenomedullin gene expression differences in mice do not affect blood pressure but modulate hypertension-induced pathology in males. *Proc Natl Acad Sci U S A* 104: 3420-3425, 2007.

21. **Caron KM, James LR, Kim HS, Knowles J, Uhlir R, Mao L, Hagaman JR, Cascio W, Rockman H, and Smithies O**. Cardiac hypertrophy and sudden death in mice with a genetically clamped renin transgene. *Proc Natl Acad Sci U S A* 101: 3106-3111, 2004.

22. **Caron KM, James LR, Kim HS, Morham SG, Sequeira Lopez ML, Gomez RA, Reudelhuber TL, and Smithies O**. A genetically clamped renin transgene for the induction of hypertension. *Proc Natl Acad Sci U S A* 99: 8248-8252, 2002.

23. **Caron KM, James LR, Lee G, Kim HS, and Smithies O**. Lifelong genetic minipumps. *Physiological genomics* 20: 203-209, 2005.

24. **Caron KM, and Smithies O**. Extreme hydrops fetalis and cardiovascular abnormalities in mice lacking a functional Adrenomedullin gene. *Proc Natl Acad Sci U S A* 98: 615-619, 2001.

25. **Caron KM, and Smithies O**. Multiple roles of adrenomedullin revealed by animal models. *Microsc Res Tech* 57: 55-59, 2002.

26. **Castellano L, Giamas G, Jacob J, Coombes RC, Lucchesi W, Thiruchelvam P, Barton G, Jiao LR, Wait R, Waxman J, Hannon GJ, and Stebbing J**. The estrogen receptor-alpha-induced microRNA signature regulates itself and its transcriptional response. *Proc Natl Acad Sci U S A* 106: 15732-15737, 2009.

27. **Chaudhry HW, Dashoush NH, Tang H, Zhang L, Wang X, Wu EX, and Wolgemuth DJ**. Cyclin A2 mediates cardiomyocyte mitosis in the postmitotic myocardium. *J Biol Chem* 279: 35858-35866, 2004.

28. **Chen J, Kubalak SW, and Chien KR**. Ventricular muscle-restricted targeting of the RXRalpha gene reveals a non-cell-autonomous requirement in cardiac chamber morphogenesis. *Development* 125: 1943-1949, 1998.

29. **Chen S, Lu X, Zhao Q, Wang L, Li H, and Huang J**. Association of adrenomedullin gene polymorphisms and blood pressure in a Chinese population. *Hypertension research : official journal of the Japanese Society of Hypertension* 36: 74-78, 2013.

30. **Chen T, Chang TC, Kang JO, Choudhary B, Makita T, Tran CM, Burch JB, Eid H, and Sucov HM**. Epicardial induction of fetal cardiomyocyte proliferation via a retinoic acid-inducible trophic factor. *Dev Biol* 250: 198-207, 2002.

31. **Chen YX, and Li CS**. Prognostic value of adrenomedullin in septic patients in the ED. *The American journal of emergency medicine* 31: 1017-1021, 2013.

32. **Cheung BM, Ong KL, Tso AW, Leung RY, Cherny SS, Sham PC, Lam TH, and Lam KS**. Plasma adrenomedullin level is related to a single nucleotide polymorphism in the adrenomedullin gene. *Eur J Endocrinol* 165: 571-577, 2011.

33. **Christoffels VM, Grieskamp T, Norden J, Mommersteeg MT, Rudat C, and Kispert A**. Tbx18 and the fate of epicardial progenitors. *Nature* 458: E8-9; discussion E9-10, 2009.

34. **Chung AK, Das SR, Leonard D, Peshock RM, Kazi F, Abdullah SM, Canham RM, Levine BD, and Drazner MH**. Women have higher left ventricular ejection fractions than men independent of differences in left ventricular volume: the Dallas Heart Study. *Circulation* 113: 1597-1604, 2006.

35. **Chung TK, Cheung TH, Huen NY, Wong KW, Lo KW, Yim SF, Siu NS, Wong YM, Tsang PT, Pang MW, Yu MY, To KF, Mok SC, Wang VW, Li C, Cheung AY, Doran G, Birrer MJ, Smith DI, and Wong YF**. Dysregulated microRNAs and their predicted targets associated with endometrioid endometrial adenocarcinoma in Hong Kong women. *Int J Cancer* 124: 1358-1365, 2009.

36. **Claycomb WC, Lanson NA, Jr., Stallworth BS, Egeland DB, Delcarpio JB, Bahinski A, and Izzo NJ, Jr.** HL-1 cells: a cardiac muscle cell line that contracts and retains phenotypic characteristics of the adult cardiomyocyte. *Proc Natl Acad Sci U S A* 95: 2979-2984, 1998.

37. **Clementi G, Caruso A, Cutuli VM, Prato A, Mangano NG, and Amico-Roxas M**. Antiinflammatory activity of adrenomedullin in the acetic acid peritonitis in rats. *Life Sci* 65: PL203-208, 1999.

38. **Combs MD, Braitsch CM, Lange AW, James JF, and Yutzey KE**. NFATC1 promotes epicardium-derived cell invasion into myocardium. *Development* 138: 1747-1757, 2011.

39. **Cormier-Regard S, Nguyen SV, and Claycomb WC**. Adrenomedullin gene expression is developmentally regulated and induced by hypoxia in rat ventricular cardiac myocytes. *J Biol Chem* 273: 17787-17792, 1998.

40. **Cornish J, Grey A, Callon KE, Naot D, Hill BL, Lin CQ, Balchin LM, and Reid IR**. Shared pathways of osteoblast mitogenesis induced by amylin, adrenomedullin, and IGF-1. *Biochem Biophys Res Commun* 318: 240-246, 2004.

41. **Dackor R, Fritz-Six K, Smithies O, and Caron K**. Receptor activity-modifying proteins 2 and 3 have distinct physiological functions from embryogenesis to old age. *J Biol Chem* 282: 18094-18099, 2007.

42. **Dackor RT, Fritz-Six K, Dunworth WP, Gibbons CL, Smithies O, and Caron KM**. Hydrops fetalis, cardiovascular defects, and embryonic lethality in mice lacking the calcitonin receptor-like receptor gene. *Mol Cell Biol* 26: 2511-2518, 2006.

43. **Dallongeville J, Marecaux N, Isorez D, Zylbergberg G, Fruchart JC, and Amouyel P**. Multiple coronary heart disease risk factors are associated with menopause and influenced by substitutive hormonal therapy in a cohort of French women. *Atherosclerosis* 118: 123-133, 1995.

44. **Dalton GD, and Howlett AC**. Cannabinoid CB1 receptors transactivate multiple receptor tyrosine kinases and regulate serine/threonine kinases to activate ERK in neuronal cells. *Br J Pharmacol* 165: 2497-2511, 2012.

45. **Daub H, Weiss FU, Wallasch C, and Ullrich A**. Role of transactivation of the EGF receptor in signalling by G-protein-coupled receptors. *Nature* 379: 557-560, 1996.

46. **Degenhardt K, Singh MK, and Epstein JA**. New approaches under development: cardiovascular embryology applied to heart disease. *J Clin Invest* 123: 71-74, 2013.

47. **del Monte G, Casanova JC, Guadix JA, MacGrogan D, Burch JB, Perez-Pomares JM, and de la Pompa JL**. Differential Notch signaling in the epicardium is required for cardiac inflow development and coronary vessel morphogenesis. *Circ Res* 108: 824-836, 2011.

48. **Dhillon OS, Khan SQ, Narayan HK, Ng KH, Struck J, Quinn PA, Morgenthaler NG, Squire IB, Davies JE, Bergmann A, and Ng LL**. Prognostic value of mid-regional pro-adrenomedullin levels taken on admission and discharge in non-ST-elevation myocardial infarction: the LAMP (Leicester Acute Myocardial Infarction Peptide) II study. *J Am Coll Cardiol* 56: 125-133, 2010.

49. **Di Meglio F, Castaldo C, Nurzynska D, Romano V, Miraglia R, Bancone C, Langella G, Vosa C, and Montagnani S**. Epithelial-mesenchymal transition of epicardial mesothelium is a source of cardiac CD117-positive stem cells in adult human heart. *Journal of molecular and cellular cardiology* 49: 719-727, 2010.

50. **Doods H, Arndt K, Rudolf K, and Just S**. CGRP antagonists: unravelling the role of CGRP in migraine. *Trends Pharmacol Sci* 28: 580-587, 2007.

51. **Drici MD, Burklow TR, Haridasse V, Glazer RI, and Woosley RL**. Sex hormones prolong the QT interval and downregulate potassium channel expression in the rabbit heart. *Circulation* 94: 1471-1474, 1996.

52. **Duan J, Gherghe C, Liu D, Hamlett E, Srikantha L, Rodgers L, Regan JN, Rojas M, Willis M, Leask A, Majesky M, and Deb A**. Wnt1/betacatenin injury response activates the epicardium and cardiac fibroblasts to promote cardiac repair. *EMBO J* 31: 429-442, 2012.

53. **Eto T, Kato J, and Kitamura K**. Regulation of production and secretion of adrenomedullin in the cardiovascular system. *Regul Pept* 112: 61-69, 2003.

54. **Fandrey J, Pagel H, Frede S, Wolff M, and Jelkmann W**. Thyroid hormones enhance hypoxia-induced erythropoietin production in vitro. *Experimental hematology* 22: 272-277, 1994.

55. **Favre J, Gao J, Henry JP, Remy-Jouet I, Fourquaux I, Billon-Gales A, Thuillez C, Arnal JF, Lenfant F, and Richard V**. Endothelial estrogen receptor {alpha} plays an essential role in the coronary and myocardial protective effects of estradiol in ischemia/reperfusion. *Arterioscler Thromb Vasc Biol* 30: 2562-2567, 2010.

56. **Filardo EJ, Quinn JA, Bland KI, and Frackelton AR, Jr.** Estrogen-induced activation of Erk-1 and Erk-2 requires the G protein-coupled receptor homolog, GPR30, and occurs via trans-activation of the epidermal growth factor receptor through release of HB-EGF. *Mol Endocrinol* 14: 1649-1660, 2000.

57. **Fisher PW, Salloum F, Das A, Hyder H, and Kukreja RC**. Phosphodiesterase-5 inhibition with sildenafil attenuates cardiomyocyte apoptosis and left ventricular dysfunction in a chronic model of doxorubicin cardiotoxicity. *Circulation* 111: 1601-1610, 2005.

58. **Franco-Montoya ML, Boucherat O, Thibault C, Chailley-Heu B, Incitti R, Delacourt C, and Bourbon JR**. Profiling target genes of FGF18 in the postnatal mouse lung: possible relevance for alveolar development. *Physiological genomics* 43: 1226-1240, 2011.

59. **Fritz-Six KL, Dunworth WP, Li M, and Caron KM**. Adrenomedullin signaling is necessary for murine lymphatic vascular development. *J Clin Invest* 118: 40-50, 2008.

60. **Fujii T, Nagaya N, Iwase T, Murakami S, Miyahara Y, Nishigami K, Ishibashi-Ueda H, Shirai M, Itoh T, Ishino K, Sano S, Kangawa K, and Mori H**. Adrenomedullin enhances therapeutic potency of bone marrow transplantation for myocardial infarction in rats. *American journal of physiology Heart and circulatory physiology* 288: H1444-1450, 2005.

61. **Gaborit N, Varro A, Le Bouter S, Szuts V, Escande D, Nattel S, and Demolombe S**. Gender-related differences in ion-channel and transporter subunit expression in non-diseased human hearts. *Journal of molecular and cellular cardiology* 49: 639-646, 2010.

62. **Galvao M, Adhere Scientific Advisory Committee Investigators C, and Study G**. Reshaping our perception of the typical hospitalized heart failure patient: a gender analysis of data from the ADHERE Heart Failure Registry. *The Journal of cardiovascular nursing* 20: 442-450, 2005.

63. **Gangula PR, Zhao H, Supowit SC, Wimalawansa SJ, Dipette DJ, Westlund KN, Gagel RF, and Yallampalli C**. Increased blood pressure in alpha-calcitonin gene-related peptide/calcitonin gene knockout mice. *Hypertension* 35: 470-475, 2000.

64. **Garayoa M, Martinez A, Lee S, Pio R, An WG, Neckers L, Trepel J, Montuenga LM, Ryan H, Johnson R, Gassmann M, and Cuttitta F**. Hypoxia-inducible factor-1 (HIF-1) up-regulates adrenomedullin expression in human tumor cell lines during oxygen deprivation: a possible promotion mechanism of carcinogenesis. *Mol Endocrinol* 14: 848-862, 2000.

65. **Gassmann M, Casagranda F, Orioli D, Simon H, Lai C, Klein R, and Lemke G**. Aberrant neural and cardiac development in mice lacking the ErbB4 neuregulin receptor. *Nature* 378: 390-394, 1995.

66. **Gillespie CD, Hurvitz KA, Centers for Disease C, and Prevention**. Prevalence of hypertension and controlled hypertension - United States, 2007-2010. *Morbidity and mortality weekly report Surveillance summaries* 62 Suppl 3: 144-148, 2013.

67. **Gittenberger-de Groot AC, Vrancken Peeters MP, Bergwerff M, Mentink MM, and Poelmann RE**. Epicardial outgrowth inhibition leads to compensatory mesothelial outflow tract collar and abnormal cardiac septation and coronary formation. *Circ Res* 87: 969-971, 2000.

68. **Gittenberger-de Groot AC, Winter EM, Bartelings MM, Goumans MJ, DeRuiter MC, and Poelmann RE**. The arterial and cardiac epicardium in development, disease and repair. *Differentiation* 84: 41-53, 2012.

69. **Glubb DM, McHugh PC, Deng X, Joyce PR, and Kennedy MA**. Association of a functional polymorphism in the adrenomedullin gene (ADM) with response to paroxetine. *Pharmacogenomics J* 10: 126-133, 2010.

70. **Goldblatt H, Lynch J, Hanzal RF, and Summerville WW**. Studies on Experimental Hypertension : I. The Production of Persistent Elevation of Systolic Blood Pressure by Means of Renal Ischemia. *The Journal of experimental medicine* 59: 347-379, 1934.

71. **Gonzalez-Rosa JM, Martin V, Peralta M, Torres M, and Mercader N**. Extensive scar formation and regression during heart regeneration after cryoinjury in zebrafish. *Development* 138: 1663-1674, 2011.

72. **Grego-Bessa J, Luna-Zurita L, del Monte G, Bolos V, Melgar P, Arandilla A, Garratt AN, Zang H, Mukouyama YS, Chen H, Shou W, Ballestar E, Esteller M, Rojas A, Perez-Pomares JM, and de la Pompa JL**. Notch signaling is essential for ventricular chamber development. *Developmental cell* 12: 415-429, 2007.

73. **Grohe C, Kahlert S, Lobbert K, Stimpel M, Karas RH, Vetter H, and Neyses L**. Cardiac myocytes and fibroblasts contain functional estrogen receptors. *FEBS Lett* 416: 107-112, 1997.

74. **Guadix JA, Ruiz-Villalba A, Lettice L, Velecela V, Munoz-Chapuli R, Hastie ND, Perez-Pomares JM, and Martinez-Estrada OM**. Wt1 controls retinoic acid signalling in embryonic epicardium through transcriptional activation of Raldh2. *Development* 138: 1093-1097, 2011.

75. **Guidolin D, Albertin G, Spinazzi R, Sorato E, Mascarin A, Cavallo D, Antonello M, and Ribatti D**. Adrenomedullin stimulates angiogenic response in cultured human vascular endothelial cells: Involvement of the vascular endothelial growth factor receptor 2. *Peptides* 29: 2013-2023, 2008.

76. **Guttenberg I**. Plasma levels of "free" progestin during the estrous cycle in the mouse. *Endocrinology* 68: 1006-1009, 1961.

77. **Hamid SA, and Baxter GF**. A critical cytoprotective role of endogenous adrenomedullin in acute myocardial infarction. *Journal of molecular and cellular cardiology* 41: 360-363, 2006.

78. **Hamid SA, Totzeck M, Drexhage C, Thompson I, Fowkes RC, Rassaf T, and Baxter GF**. Nitric oxide/cGMP signalling mediates the cardioprotective action of adrenomedullin in reperfused myocardium. *Basic Res Cardiol* 105: 257-266, 2010.

79. **Hatcher CJ, Diman NY, Kim MS, Pennisi D, Song Y, Goldstein MM, Mikawa T, and Basson CT**. A role for Tbx5 in proepicardial cell migration during cardiogenesis. *Physiological genomics* 18: 129-140, 2004.

80. **Hattori Y, Murakami Y, Atsuta H, Minamino N, Kangawa K, and Kasai K**. Glucocorticoid regulation of adrenomedullin in a rat model of endotoxic shock. *Life Sci* 62: PL181-189, 1998.

81. **Heallen T, Zhang M, Wang J, Bonilla-Claudio M, Klysik E, Johnson RL, and Martin JF**. Hippo pathway inhibits Wnt signaling to restrain cardiomyocyte proliferation and heart size. *Science* 332: 458-461, 2011.

82. **Hellermann JP, Jacobsen SJ, Reeder GS, Lopez-Jimenez F, Weston SA, and Roger VL**. Heart failure after myocardial infarction: prevalence of preserved left ventricular systolic function in the community. *American heart journal* 145: 742-748, 2003.

83. **Ho E, and Shimada Y**. Formation of the epicardium studied with the scanning electron microscope. *Dev Biol* 66: 579-585, 1978.

84. **Huang GN, Thatcher JE, McAnally J, Kong Y, Qi X, Tan W, DiMaio JM, Amatruda JF, Gerard RD, Hill JA, Bassel-Duby R, and Olson EN**. C/EBP transcription factors mediate epicardial activation during heart development and injury. *Science* 338: 1599-1603, 2012.

85. **Huang Y, Harrison MR, Osorio A, Kim J, Baugh A, Duan C, Sucov HM, and Lien CL**. Igf Signaling is Required for Cardiomyocyte Proliferation during Zebrafish Heart Development and Regeneration. *PLoS One* 8: e67266, 2013.

86. **Ieda M, Tsuchihashi T, Ivey KN, Ross RS, Hong TT, Shaw RM, and Srivastava D**. Cardiac fibroblasts regulate myocardial proliferation through beta1 integrin signaling. *Developmental cell* 16: 233-244, 2009.

87. **Ihara T, Ikeda U, Tate Y, Ishibashi S, and Shimada K**. Positive inotropic effects of adrenomedullin on rat papillary muscle. *Eur J Pharmacol* 390: 167-172, 2000.

88. **Ikenouchi H, Kangawa K, Matsuo H, and Hirata Y**. Negative inotropic effect of adrenomedullin in isolated adult rabbit cardiac ventricular myocytes. *Circulation* 95: 2318-2324, 1997.

89. **Ishii Y, Garriock RJ, Navetta AM, Coughlin LE, and Mikawa T**. BMP signals promote proepicardial protrusion necessary for recruitment of coronary vessel and epicardial progenitors to the heart. *Developmental cell* 19: 307-316, 2010.

90. **Ishimitsu T, Hosoya K, Tsukada K, Minami J, Futoh Y, Ono H, Ohrui M, Hino J, Kangawa K, and Matsuoka H**. Microsatellite DNA polymorphism of human adrenomedullin gene in normotensive subjects and patients with essential hypertension. *Hypertension* 38: 9-12, 2001.

91. **Ishimitsu T, Tsukada K, Minami J, Ono H, Ohrui M, Hino J, Kangawa K, and Matsuoka H**. Microsatellite DNA polymorphism of human adrenomedullin gene in type 2 diabetic patients with renal failure. *Kidney Int* 63: 2230-2235, 2003.

92. **Jenkins SJ, Hutson DR, and Kubalak SW**. Analysis of the proepicardium-epicardium transition during the malformation of the RXRalpha-/- epicardium. *Developmental dynamics : an official publication of the American Association of Anatomists* 233: 1091-1101, 2005.

93. **Kakoki M, Tsai YS, Kim HS, Hatada S, Ciavatta DJ, Takahashi N, Arnold LW, Maeda N, and Smithies O**. Altering the expression in mice of genes by modifying their 3' regions. *Developmental cell* 6: 597-606, 2004.

94. **Kalluri R, and Weinberg RA**. The basics of epithelial-mesenchymal transition. *J Clin Invest* 119: 1420-1428, 2009.

95. **Kapas S, Catt KJ, and Clark AJ**. Cloning and expression of cDNA encoding a rat adrenomedullin receptor. *J Biol Chem* 270: 25344-25347, 1995.

96. **Kapas S, and Clark AJ**. Identification of an orphan receptor gene as a type 1 calcitonin gene-related peptide receptor. *Biochem Biophys Res Commun* 217: 832-838, 1995.

97. **Karpinich NO, Hoopes SL, Kechele DO, Lenhart PM, and Caron KM**. Adrenomedullin Function in Vascular Endothelial Cells: Insights from Genetic Mouse Models. *Current hypertension reviews* 7: 228-239, 2011.

98. **Kataoka Y, Miyazaki S, Yasuda S, Nagaya N, Noguchi T, Yamada N, Morii I, Kawamura A, Doi K, Miyatake K, Tomoike H, and Kangawa K**. The first clinical pilot study of intravenous adrenomedullin administration in patients with acute myocardial infarction. *Journal of cardiovascular pharmacology* 56: 413-419, 2010.

99. **Kennedy SP, Sun D, Oleynek JJ, Hoth CF, Kong J, and Hill RJ**. Expression of the rat adrenomedullin receptor or a putative human adrenomedullin receptor does not correlate with adrenomedullin binding or functional response. *Biochem Biophys Res Commun* 244: 832-837, 1998.

100. **Kerkela R, Kockeritz L, Macaulay K, Zhou J, Doble BW, Beahm C, Greytak S, Woulfe K, Trivedi CM, Woodgett JR, Epstein JA, Force T, and Huggins GS**. Deletion of GSK-3beta in mice leads to hypertrophic cardiomyopathy secondary to cardiomyoblast hyperproliferation. *J Clin Invest* 118: 3609-3618, 2008.

101. **Khan SQ, O'Brien RJ, Struck J, Quinn P, Morgenthaler N, Squire I, Davies J, Bergmann A, and Ng LL**. Prognostic value of midregional pro-adrenomedullin in patients with acute myocardial infarction: the LAMP (Leicester Acute Myocardial Infarction Peptide) study. *J Am Coll Cardiol* 49: 1525-1532, 2007.

102. **Kikuchi K, Holdway JE, Major RJ, Blum N, Dahn RD, Begemann G, and Poss KD**. Retinoic acid production by endocardium and epicardium is an injury response essential for zebrafish heart regeneration. *Developmental cell* 20: 397-404, 2011.

103. **Kim J, Wu Q, Zhang Y, Wiens KM, Huang Y, Rubin N, Shimada H, Handin RI, Chao MY, Tuan TL, Starnes VA, and Lien CL**. PDGF signaling is required for epicardial function and blood vessel formation in regenerating zebrafish hearts. *Proc Natl Acad Sci U S A* 107: 17206-17210, 2010.

104. **Kim JK, Pedram A, Razandi M, and Levin ER**. Estrogen prevents cardiomyocyte apoptosis through inhibition of reactive oxygen species and differential regulation of p38 kinase isoforms. *J Biol Chem* 281: 6760-6767, 2006.

105. **Kim SM, Kim JY, Lee S, and Park JH**. Adrenomedullin protects against hypoxia/reoxygenation-induced cell death by suppression of reactive oxygen species via thiol redox systems. *FEBS Lett* 584: 213-218, 2010.

106. **Kim W, Moon SO, Sung MJ, Kim SH, Lee S, So JN, and Park SK**. Angiogenic role of adrenomedullin through activation of Akt, mitogen-activated protein kinase, and focal adhesion kinase in endothelial cells. *Faseb J* 17: 1937-1939, 2003.

107. **Kita T, Tokashiki M, and Kitamura K**. Aldosterone antisecretagogue and antihypertensive actions of adrenomedullin in patients with primary aldosteronism. *Hypertension research : official journal of the Japanese Society of Hypertension* 33: 374-379, 2010.

108. **Kitamura K, Kangawa K, Kawamoto M, Ichiki Y, Nakamura S, Matsuo H, and Eto T**. Adrenomedullin: a novel hypotensive peptide isolated from human pheochromocytoma. *Biochem Biophys Res Commun* 192: 553-560, 1993.

109. **Kitamura K, Kato J, Kawamoto M, Tanaka M, Chino N, Kangawa K, and Eto T**. The intermediate form of glycine-extended adrenomedullin is the major circulating molecular form in human plasma. *Biochem Biophys Res Commun* 244: 551-555, 1998.

110. **Klein KR, Karpinich NO, Espenschied ST, Willcockson HH, Dunworth WP, Hoopes SL, Kushner EJ, Bautch VL, and Caron KM**. Decoy Receptor CXCR7 Modulates Adrenomedullin-Mediated Cardiac and Lymphatic Vascular Development. *Developmental cell* 30: 528-540, 2014.

111. **Klip IT, Voors AA, Anker SD, Hillege HL, Struck J, Squire I, van Veldhuisen DJ, and Dickstein K**. Prognostic value of mid-regional pro-adrenomedullin in patients with heart failure after an acute myocardial infarction. *Heart* 97: 892-898, 2011.

112. **Kobayashi Y, Nakayama T, Sato N, Izumi Y, Kokubun S, and Soma M**. Haplotype-based case-control study revealing an association between the adrenomedullin gene and proteinuria in subjects with essential hypertension. *Hypertension research : official journal of the Japanese Society of Hypertension* 28: 229-236, 2005.

113. **Kocabas F, Mahmoud AI, Sosic D, Porrello ER, Chen R, Garcia JA, DeBerardinis RJ, and Sadek HA**. The hypoxic epicardial and subepicardial microenvironment. *Journal of cardiovascular translational research* 5: 654-665, 2012.

114. **Krege JH, Hodgin JB, Hagaman JR, and Smithies O**. A noninvasive computerized tail-cuff system for measuring blood pressure in mice. *Hypertension* 25: 1111-1115, 1995.

115. **Kreidberg JA, Sariola H, Loring JM, Maeda M, Pelletier J, Housman D, and Jaenisch R**. WT-1 is required for early kidney development. *Cell* 74: 679-691, 1993.

116. **Kubo A, Minamino N, Isumi Y, Katafuchi T, Kangawa K, Dohi K, and Matsuo H**. Production of adrenomedullin in macrophage cell line and peritoneal macrophage. *J Biol Chem* 273: 16730-16738, 1998.

117. **Kwee L, Baldwin HS, Shen HM, Stewart CL, Buck C, Buck CA, and Labow MA**. Defective development of the embryonic and extraembryonic circulatory systems in vascular cell adhesion molecule (VCAM-1) deficient mice. *Development* 121: 489-503, 1995.

118. **Lanner F, Lee KL, Ortega GC, Sohl M, Li X, Jin S, Hansson EM, Claesson-Welsh L, Poellinger L, Lendahl U, and Farnebo F**. Hypoxia-induced arterial differentiation requires adrenomedullin and notch signaling. *Stem cells and development* 22: 1360-1369, 2013.

119. **Lavine KJ, White AC, Park C, Smith CS, Choi K, Long F, Hui CC, and Ornitz DM**. Fibroblast growth factor signals regulate a wave of Hedgehog activation that is essential for coronary vascular development. *Genes Dev* 20: 1651-1666, 2006.

120. **Lavine KJ, Yu K, White AC, Zhang X, Smith C, Partanen J, and Ornitz DM**. Endocardial and epicardial derived FGF signals regulate myocardial proliferation and differentiation in vivo. *Developmental cell* 8: 85-95, 2005.

121. **Le TY, Ashton AW, Mardini M, Stanton PG, Funder JW, Handelsman DJ, and Mihailidou AS**. Role of androgens in sex differences in cardiac damage during myocardial infarction. *Endocrinology* 155: 568-575, 2014.

122. **Lea R, Papalopulu N, Amaya E, and Dorey K**. Temporal and spatial expression of FGF ligands and receptors during Xenopus development. *Developmental dynamics : an official publication of the American Association of Anatomists* 238: 1467-1479, 2009.

123. **Lee KF, Simon H, Chen H, Bates B, Hung MC, and Hauser C**. Requirement for neuregulin receptor erbB2 in neural and cardiac development. *Nature* 378: 394-398, 1995.

124. **Lepilina A, Coon AN, Kikuchi K, Holdway JE, Roberts RW, Burns CG, and Poss KD**. A dynamic epicardial injury response supports progenitor cell activity during zebrafish heart regeneration. *Cell* 127: 607-619, 2006.

125. **Leskinen H, Rauma-Pinola T, Szokodi I, Kerkela R, Pikkarainen S, Uusimaa P, Hautala T, Vuolteenaho O, and Ruskoaho H**. Adaptive or maladaptive response to adenoviral adrenomedullin gene transfer is context-dependent in the heart. *The journal of gene medicine* 10: 867-877, 2008.

126. **Li M, Schwerbrock NM, Lenhart PM, Fritz-Six KL, Kadmiel M, Christine KS, Kraus DM, Espenschied ST, Willcockson HH, Mack CP, and Caron KM**. Fetal-derived adrenomedullin mediates the innate immune milieu of the placenta. *J Clin Invest* 123: 2408-2420, 2013.

127. **Li M, Wetzel-Strong SE, Hua X, Tilley SL, Oswald E, Krummel MF, and Caron KM**. Deficiency of RAMP1 Attenuates Antigen-Induced Airway Hyperresponsiveness in Mice. *PLoS One* 9: e102356, 2014.

128. **Li P, Cavallero S, Gu Y, Chen TH, Hughes J, Hassan AB, Bruning JC, Pashmforoush M, and Sucov HM**. IGF signaling directs ventricular cardiomyocyte proliferation during embryonic heart development. *Development* 138: 1795-1805, 2011.

129. **Li Y, Staessen JA, Li LH, Gao PJ, Thijs L, Brand E, Brand-Herrmann SM, Zhu DL, and Wang JG**. Blood pressure and urinary sodium excretion in relation to the A-1984G adrenomedullin polymorphism in a Chinese population. *Kidney Int* 69: 1153-1158, 2006.

130. **Limana F, Bertolami C, Mangoni A, Di Carlo A, Avitabile D, Mocini D, Iannelli P, De Mori R, Marchetti C, Pozzoli O, Gentili C, Zacheo A, Germani A, and Capogrossi MC**. Myocardial infarction induces embryonic reprogramming of epicardial c-kit(+) cells: role of the pericardial fluid. *Journal of molecular and cellular cardiology* 48: 609-618, 2010.

131. **Limana F, Zacheo A, Mocini D, Mangoni A, Borsellino G, Diamantini A, De Mori R, Battistini L, Vigna E, Santini M, Loiaconi V, Pompilio G, Germani A, and Capogrossi MC**. Identification of myocardial and vascular precursor cells in human and mouse epicardium. *Circ Res* 101: 1255-1265, 2007.

132. **Lippton H, Chang JK, Hao Q, Summer W, and Hyman AL**. Adrenomedullin dilates the pulmonary vascular bed in vivo. *J Appl Physiol* 76: 2154-2156, 1994.

133. **Liu H, Yanamandala M, Lee TC, and Kim JK**. Mitochondrial p38beta and manganese superoxide dismutase interaction mediated by estrogen in cardiomyocytes. *PLoS One* 9: e85272, 2014.

134. **Lobov IB, Cheung E, Wudali R, Cao J, Halasz G, Wei Y, Economides A, Lin HC, Papadopoulos N, Yancopoulos GD, and Wiegand SJ**. The Dll4/Notch pathway controls postangiogenic blood vessel remodeling and regression by modulating vasoconstriction and blood flow. *Blood* 117: 6728-6737, 2011.

135. **Locati EH, Zareba W, Moss AJ, Schwartz PJ, Vincent GM, Lehmann MH, Towbin JA, Priori SG, Napolitano C, Robinson JL, Andrews M, Timothy K, and Hall WJ**. Age- and sex-related differences in clinical manifestations in patients with congenital long-QT syndrome: findings from the International LQTS Registry. *Circulation* 97: 2237-2244, 1998.

136. **Lu J, Landerholm TE, Wei JS, Dong XR, Wu SP, Liu X, Nagata K, Inagaki M, and Majesky MW**. Coronary smooth muscle differentiation from proepicardial cells requires rhoA-mediated actin reorganization and p160 rho-kinase activity. *Dev Biol* 240: 404-418, 2001.

137. **Lu JT, Son YJ, Lee J, Jetton TL, Shiota M, Moscoso L, Niswender KD, Loewy AD, Magnuson MA, Sanes JR, and Emeson RB**. Mice lacking alpha-calcitonin gene-related peptide exhibit normal cardiovascular regulation and neuromuscular development. *Mol Cell Neurosci* 14: 99-120, 1999.

138. **Lu SY, Sheikh F, Sheppard PC, Fresnoza A, Duckworth ML, Detillieux KA, and Cattini PA**. FGF-16 is required for embryonic heart development. *Biochem Biophys Res Commun* 373: 270-274, 2008.

139. **Luczak ED, and Leinwand LA**. Sex-based cardiac physiology. *Annu Rev Physiol* 71: 1-18, 2009.

140. **Luodonpaa M, Leskinen H, Ilves M, Vuolteenaho O, and Ruskoaho H**. Adrenomedullin modulates hemodynamic and cardiac effects of angiotensin II in conscious rats. *Am J Physiol Regul Integr Comp Physiol* 286: R1085-1092, 2004.

141. **Maisel A, Mueller C, Nowak R, Peacock WF, Landsberg JW, Ponikowski P, Mockel M, Hogan C, Wu AH, Richards M, Clopton P, Filippatos GS, Di Somma S, Anand I, Ng L, Daniels LB, Neath SX, Christenson R, Potocki M, McCord J, Terracciano G, Kremastinos D, Hartmann O, von Haehling S, Bergmann A, Morgenthaler NG, and Anker SD**. Mid-region pro-hormone markers for diagnosis and prognosis in acute dyspnea: results from the BACH (Biomarkers in Acute Heart Failure) trial. *J Am Coll Cardiol* 55: 2062-2076, 2010.

142. **Maisel A, Mueller C, Nowak RM, Peacock WF, Ponikowski P, Mockel M, Hogan C, Wu AH, Richards M, Clopton P, Filippatos GS, Di Somma S, Anand I, Ng LL, Daniels LB, Neath SX, Christenson R, Potocki M, McCord J, Hartmann O, Morgenthaler NG, and Anker SD**. Midregion prohormone adrenomedullin and prognosis in patients presenting with acute dyspnea: results from the BACH (Biomarkers in Acute Heart Failure) trial. *J Am Coll Cardiol* 58: 1057-1067, 2011.

143. **Martinez-Herrero S, and Martinez A**. Cancer protection elicited by a single nucleotide polymorphism close to the adrenomedullin gene. *J Clin Endocrinol Metab* 98: E807-810, 2013.

144. **Maudsley S, Pierce KL, Zamah AM, Miller WE, Ahn S, Daaka Y, Lefkowitz RJ, and Luttrell LM**. The beta(2)-adrenergic receptor mediates extracellular signal-regulated kinase activation via assembly of a multi-receptor complex with the epidermal growth factor receptor. *J Biol Chem* 275: 9572-9580, 2000.

145. **McLatchie LM, Fraser NJ, Main MJ, Wise A, Brown J, Thompson N, Solari R, Lee MG, and Foord SM**. RAMPs regulate the transport and ligand specificity of the calcitonin-receptor-like receptor. *Nature* 393: 333-339, 1998.

146. **Meeran K, O'Shea D, Upton PD, Small CJ, Ghatei MA, Byfield PH, and Bloom SR**. Circulating adrenomedullin does not regulate systemic blood pressure but increases plasma prolactin after intravenous infusion in humans: a pharmacokinetic study. *J Clin Endocrinol Metab* 82: 95-100, 1997.

147. **Mellgren AM, Smith CL, Olsen GS, Eskiocak B, Zhou B, Kazi MN, Ruiz FR, Pu WT, and Tallquist MD**. Platelet-derived growth factor receptor beta signaling is required for efficient epicardial cell migration and development of two distinct coronary vascular smooth muscle cell populations. *Circ Res* 103: 1393-1401, 2008.

148. **Mendell JT, and Olson EN**. MicroRNAs in stress signaling and human disease. *Cell* 148: 1172-1187, 2012.

149. **Merki E, Zamora M, Raya A, Kawakami Y, Wang J, Zhang X, Burch J, Kubalak SW, Kaliman P, Izpisua Belmonte JC, Chien KR, and Ruiz-Lozano P**. Epicardial retinoid X receptor alpha is required for myocardial growth and coronary artery formation. *Proc Natl Acad Sci U S A* 102: 18455-18460, 2005.

150. **Meyer D, and Birchmeier C**. Multiple essential functions of neuregulin in development. *Nature* 378: 386-390, 1995.

151. **Minamino N, Shoji H, Sugo S, Kangawa K, and Matsuo H**. Adrenocortical steroids, thyroid hormones and retinoic acid augment the production of adrenomedullin in vascular smooth muscle cells. *Biochem Biophys Res Commun* 211: 686-693, 1995.

152. **Montuenga LM, Mariano JM, Prentice MA, Cuttitta F, and Jakowlew SB**. Coordinate expression of transforming growth factor-beta1 and adrenomedullin in rodent embryogenesis. *Endocrinology* 139: 3946-3957, 1998.

153. **Montuenga LM, Martinez A, Miller MJ, Unsworth EJ, and Cuttitta F**. Expression of adrenomedullin and its receptor during embryogenesis suggests autocrine or paracrine modes of action. *Endocrinology* 138: 440-451, 1997.

154. **Moore AW, McInnes L, Kreidberg J, Hastie ND, and Schedl A**. YAC complementation shows a requirement for Wt1 in the development of epicardium, adrenal gland and throughout nephrogenesis. *Development* 126: 1845-1857, 1999.

155. **Morgenthaler NG, Struck J, Alonso C, and Bergmann A**. Measurement of midregional proadrenomedullin in plasma with an immunoluminometric assay. *Clin Chem* 51: 1823-1829, 2005.

156. **Moses KA, DeMayo F, Braun RM, Reecy JL, and Schwartz RJ**. Embryonic expression of an Nkx2-5/Cre gene using ROSA26 reporter mice. *Genesis* 31: 176-180, 2001.

157. **Nagaya N, Goto Y, Satoh T, Sumida H, Kojima S, Miyatake K, and Kangawa K**. Intravenous adrenomedullin in myocardial function and energy metabolism in patients after myocardial infarction. *Journal of cardiovascular pharmacology* 39: 754-760, 2002.

158. **Nagaya N, Nishikimi T, Uematsu M, Satoh T, Oya H, Kyotani S, Sakamaki F, Ueno K, Nakanishi N, Miyatake K, and Kangawa K**. Haemodynamic and hormonal effects of adrenomedullin in patients with pulmonary hypertension. *Heart* 84: 653-658, 2000.

159. **Nagaya N, Satoh T, Nishikimi T, Uematsu M, Furuichi S, Sakamaki F, Oya H, Kyotani S, Nakanishi N, Goto Y, Masuda Y, Miyatake K, and Kangawa K**. Hemodynamic, renal, and hormonal effects of adrenomedullin infusion in patients with congestive heart failure. *Circulation* 101: 498-503, 2000.

160. **Navar LG, Zou L, Von Thun A, Tarng Wang C, Imig JD, and Mitchell KD**. Unraveling the Mystery of Goldblatt Hypertension. *News in physiological sciences : an international journal of physiology produced jointly by the International Union of Physiological Sciences and the American Physiological Society* 13: 170-176, 1998.

161. **Nesbitt TL, Roberts A, Tan H, Junor L, Yost MJ, Potts JD, Dettman RW, and Goodwin RL**. Coronary endothelial proliferation and morphogenesis are regulated by a VEGF-mediated pathway. *Developmental dynamics : an official publication of the American Association of Anatomists* 238: 423-430, 2009.

162. **Nicoli S, Tobia C, Gualandi L, De Sena G, and Presta M**. Calcitonin receptor-like receptor guides arterial differentiation in zebrafish. *Blood* 111: 4965-4972, 2008.

163. **Nikitenko LL, Fox SB, Kehoe S, Rees MC, and Bicknell R**. Adrenomedullin and tumour angiogenesis. *Br J Cancer* 94: 1-7, 2006.

164. **Nilsson S, Makela S, Treuter E, Tujague M, Thomsen J, Andersson G, Enmark E, Pettersson K, Warner M, and Gustafsson JA**. Mechanisms of estrogen action. *Physiological reviews* 81: 1535-1565, 2001.

165. **Nishida H, Sato T, Miyazaki M, and Nakaya H**. Infarct size limitation by adrenomedullin: protein kinase A but not PI3-kinase is linked to mitochondrial KCa channels. *Cardiovasc Res* 77: 398-405, 2008.

166. **Nishikimi T, Karasawa T, Inaba C, Ishimura K, Tadokoro K, Koshikawa S, Yoshihara F, Nagaya N, Sakio H, Kangawa K, and Matsuoka H**. Effects of long-term intravenous administration of adrenomedullin (AM) plus hANP therapy in acute decompensated heart failure: a pilot study. *Circ J* 73: 892-898, 2009.

167. **Nishikimi T, Mori Y, Kobayashi N, Tadokoro K, Wang X, Akimoto K, Yoshihara F, Kangawa K, and Matsuoka H**. Renoprotective effect of chronic adrenomedullin infusion in Dahl salt-sensitive rats. *Hypertension* 39: 1077-1082, 2002.

168. **Nishikimi T, Tadokoro K, Akimoto K, Mori Y, Ishikawa Y, Ishimura K, Horio T, Kangawa K, and Matsuoka H**. Response of adrenomedullin system to cytokine in cardiac fibroblasts-role of adrenomedullin as an antifibrotic factor. *Cardiovasc Res* 66: 104-113, 2005.

169. **Nishikimi T, Tadokoro K, Mori Y, Wang X, Akimoto K, Yoshihara F, Minamino N, Kangawa K, and Matsuoka H**. Ventricular adrenomedullin system in the transition from LVH to heart failure in rats. *Hypertension* 41: 512-518, 2003.

170. **Nishikimi T, Yoshihara F, Horinaka S, Kobayashi N, Mori Y, Tadokoro K, Akimoto K, Minamino N, Kangawa K, and Matsuoka H**. Chronic administration of adrenomedullin attenuates transition from left ventricular hypertrophy to heart failure in rats. *Hypertension* 42: 1034-1041, 2003.

171. **Niu P, Shindo T, Iwata H, Iimuro S, Takeda N, Zhang Y, Ebihara A, Suematsu Y, Kangawa K, Hirata Y, and Nagai R**. Protective effects of endogenous adrenomedullin on cardiac hypertrophy, fibrosis, and renal damage. *Circulation* 109: 1789-1794, 2004.

172. **Nothnick WB, and Healy C**. Estrogen induces distinct patterns of microRNA expression within the mouse uterus. *Reprod Sci* 17: 987-994, 2010.

173. **Okumura H, Nagaya N, Itoh T, Okano I, Hino J, Mori K, Tsukamoto Y, Ishibashi-Ueda H, Miwa S, Tambara K, Toyokuni S, Yutani C, and Kangawa K**. Adrenomedullin infusion attenuates myocardial ischemia/reperfusion injury through the phosphatidylinositol 3-kinase/Akt-dependent pathway. *Circulation* 109: 242-248, 2004.

174. **Ong KL, Tso AW, Leung RY, Cherny SS, Sham PC, Lam TH, Cheung BM, and Lam KS**. A genetic variant in the gene encoding adrenomedullin predicts the development of dysglycemia over 6.4 years in Chinese. *Clin Chim Acta* 412: 353-357, 2011.

175. **Onitsuka H, Imamura T, Yamaga J, Kuwasako K, Kitamura K, and Eto T**. Angiotensin II stimulates cardiac adrenomedullin production and causes accumulation of mature adrenomedullin independently of hemodynamic stress in vivo. *Horm Metab Res* 37: 281-285, 2005.

176. **Pace P, Taylor J, Suntharalingam S, Coombes RC, and Ali S**. Human estrogen receptor beta binds DNA in a manner similar to and dimerizes with estrogen receptor alpha. *J Biol Chem* 272: 25832-25838, 1997.

177. **Pan Q, Luo X, Toloubeydokhti T, and Chegini N**. The expression profile of micro-RNA in endometrium and endometriosis and the influence of ovarian steroids on their expression. *Mol Hum Reprod* 13: 797-806, 2007.

178. **Peace RA, Adams PC, and Lloyd JJ**. Effect of sex, age, and weight on ejection fraction and end-systolic volume reference limits in gated myocardial perfusion SPECT. *Journal of nuclear cardiology : official publication of the American Society of Nuclear Cardiology* 15: 86-93, 2008.

179. **Pedram A, Razandi M, O'Mahony F, Harvey H, Harvey BJ, and Levin ER**. Estrogen reduces lipid content in the liver exclusively from membrane receptor signaling. *Science signaling* 6: ra36, 2013.

180. **Pennisi DJ, Ballard VL, and Mikawa T**. Epicardium is required for the full rate of myocyte proliferation and levels of expression of myocyte mitogenic factors FGF2 and its receptor, FGFR-1, but not for transmural myocardial patterning in the embryonic chick heart. *Developmental dynamics : an official publication of the American Association of Anatomists* 228: 161-172, 2003.

181. **Perez-Castells J, Martin-Santamaria S, Nieto L, Ramos A, Martinez A, Pascual-Teresa B, and Jimenez-Barbero J**. Structure of micelle-bound adrenomedullin: a first step toward the analysis of its interactions with receptors and small molecules. *Biopolymers* 97: 45-53, 2012.

182. **Perez-Pomares JM, and de la Pompa JL**. Signaling during epicardium and coronary vessel development. *Circ Res* 109: 1429-1442, 2011.

183. **Phillips MD, Mukhopadhyay M, Poscablo C, and Westphal H**. Dkk1 and Dkk2 regulate epicardial specification during mouse heart development. *International journal of cardiology* 150: 186-192, 2011.

184. **Pio R, Martinez A, Unsworth EJ, Kowalak JA, Bengoechea JA, Zipfel PF, Elsasser TH, and Cuttitta F**. Complement factor H is a serum-binding protein for adrenomedullin, and

the resulting complex modulates the bioactivities of both partners. *J Biol Chem* 276: 12292-12300, 2001.

185. **Plavicki JS, Hofsteen P, Yue MS, Lanham KA, Peterson RE, and Heideman W**. Multiple modes of proepicardial cell migration require heartbeat. *BMC developmental biology* 14: 18, 2014.

186. **Poss KD, Wilson LG, and Keating MT**. Heart regeneration in zebrafish. *Science* 298: 2188-2190, 2002.

187. **Prenzel N, Zwick E, Daub H, Leserer M, Abraham R, Wallasch C, and Ullrich A**. EGF receptor transactivation by G-protein-coupled receptors requires metalloproteinase cleavage of proHB-EGF. *Nature* 402: 884-888, 1999.

188. **Qiu Z, Cang Y, and Goff SP**. c-Abl tyrosine kinase regulates cardiac growth and development. *Proc Natl Acad Sci U S A* 107: 1136-1141, 2010.

189. **Raab-Graham KF, Radeke CM, and Vandenberg CA**. Molecular cloning and expression of a human heart inward rectifier potassium channel. *Neuroreport* 5: 2501-2505, 1994.

190. **Rademaker MT, Charles CJ, Lewis LK, Yandle TG, Cooper GJ, Coy DH, Richards AM, and Nicholls MG**. Beneficial hemodynamic and renal effects of adrenomedullin in an ovine model of heart failure. *Circulation* 96: 1983-1990, 1997.

191. **Rajabi M, Kassiotis C, Razeghi P, and Taegtmeyer H**. Return to the fetal gene program protects the stressed heart: a strong hypothesis. *Heart failure reviews* 12: 331-343, 2007.

192. **Register TC, and Adams MR**. Coronary artery and cultured aortic smooth muscle cells express mRNA for both the classical estrogen receptor and the newly described estrogen receptor beta. *The Journal of steroid biochemistry and molecular biology* 64: 187-191, 1998.

193. **Rudat C, and Kispert A**. Wt1 and epicardial fate mapping. *Circ Res* 111: 165-169, 2012.

194. **Russell JL, Goetsch SC, Gaiano NR, Hill JA, Olson EN, and Schneider JW**. A dynamic notch injury response activates epicardium and contributes to fibrosis repair. *Circ Res* 108: 51-59, 2011.

195. **Sabatine MS, Morrow DA, de Lemos JA, Omland T, Sloan S, Jarolim P, Solomon SD, Pfeffer MA, and Braunwald E**. Evaluation of multiple biomarkers of cardiovascular stress for risk prediction and guiding medical therapy in patients with stable coronary disease. *Circulation* 125: 233-240, 2012.

196. **Saito T, Ciobotaru A, Bopassa JC, Toro L, Stefani E, and Eghbali M**. Estrogen contributes to gender differences in mouse ventricular repolarization. *Circ Res* 105: 343-352, 2009.

197. **Salloum FN, Chau VQ, Hoke NN, Abbate A, Varma A, Ockaili RA, Toldo S, and Kukreja RC**. Phosphodiesterase-5 inhibitor, tadalafil, protects against myocardial ischemia/reperfusion through protein-kinase g-dependent generation of hydrogen sulfide. *Circulation* 120: S31-36, 2009.

198. **Salvatore CA, Moore EL, Calamari A, Cook JJ, Michener MS, O'Malley S, Miller PJ, Sur C, Williams DL, Jr., Zeng Z, Danziger A, Lynch JJ, Regan CP, Fay JF, Tang YS, Li CC, Pudvah NT, White RB, Bell IM, Gallicchio SN, Graham SL, Selnick HG, Vacca JP, and Kane SA**. Pharmacological properties of MK-3207, a potent and orally active calcitonin gene-related peptide receptor antagonist. *J Pharmacol Exp Ther* 333: 152-160, 2010.

199. **Sano M, Kuroi N, Nakayama T, Sato N, Izumi Y, Soma M, and Kokubun S**. Association study of calcitonin-receptor-like receptor gene in essential hypertension. *Am J Hypertens* 18: 403-408, 2005.

200. **Sasaki H, Nagayama T, Blanton RM, Seo K, Zhang M, Zhu G, Lee DI, Bedja D, Hsu S, Tsukamoto O, Takashima S, Kitakaze M, Mendelsohn ME, Karas RH, Kass DA, and Takimoto E**. PDE5 inhibitor efficacy is estrogen dependent in female heart disease. *J Clin Invest* 124: 2464-2471, 2014.

201. **Schwenk F, Baron U, and Rajewsky K**. A cre-transgenic mouse strain for the ubiquitous deletion of loxP-flanked gene segments including deletion in germ cells. *Nucleic acids research* 23: 5080-5081, 1995.

202. **Seissler J, Feghelm N, Then C, Meisinger C, Herder C, Koenig W, Peters A, Roden M, Lechner A, Kowall B, and Rathmann W**. Vasoregulatory peptides pro-endothelin-1 and pro-adrenomedullin are associated with metabolic syndrome in the population-based KORA F4 study. *Eur J Endocrinol* 167: 847-853, 2012.

203. **Shimosawa T, Shibagaki Y, Ishibashi K, Kitamura K, Kangawa K, Kato S, Ando K, and Fujita T**. Adrenomedullin, an endogenous peptide, counteracts cardiovascular damage. *Circulation* 105: 106-111, 2002.

204. **Shindo T, Kurihara Y, Nishimatsu H, Moriyama N, Kakoki M, Wang Y, Imai Y, Ebihara A, Kuwaki T, Ju KH, Minamino N, Kangawa K, Ishikawa T, Fukuda M, Akimoto Y, Kawakami H, Imai T, Morita H, Yazaki Y, Nagai R, Hirata Y, and Kurihara H**. Vascular abnormalities and elevated blood pressure in mice lacking adrenomedullin gene. *Circulation* 104: 1964-1971, 2001.

205. **Small EM, and Olson EN**. Pervasive roles of microRNAs in cardiovascular biology. *Nature* 469: 336-342, 2011.

206. **Smart N, Bollini S, Dube KN, Vieira JM, Zhou B, Davidson S, Yellon D, Riegler J, Price AN, Lythgoe MF, Pu WT, and Riley PR**. De novo cardiomyocytes from within the activated adult heart after injury. *Nature* 474: 640-644, 2011.

207. **Smart N, Dube KN, and Riley PR**. Epicardial progenitor cells in cardiac regeneration and neovascularisation. *Vascular pharmacology* 58: 164-173, 2013.

208. **Smith CL, Baek ST, Sung CY, and Tallquist MD**. Epicardial-derived cell epithelial-to-mesenchymal transition and fate specification require PDGF receptor signaling. *Circ Res* 108: e15-26, 2011.

209. **Smith JG, Newton-Cheh C, Almgren P, Struck J, Morgenthaler NG, Bergmann A, Platonov PG, Hedblad B, Engstrom G, Wang TJ, and Melander O**. Assessment of conventional cardiovascular risk factors and multiple biomarkers for the prediction of incident heart failure and atrial fibrillation. *J Am Coll Cardiol* 56: 1712-1719, 2010.

210. **Stainier DY, Weinstein BM, Detrich HW, 3rd, Zon LI, and Fishman MC**. Cloche, an early acting zebrafish gene, is required by both the endothelial and hematopoietic lineages. *Development* 121: 3141-3150, 1995.

211. **Stangl V, Dschietzig T, Bramlage P, Boye P, Kinkel HT, Staudt A, Baumann G, Felix SB, and Stangl K**. Adrenomedullin and myocardial contractility in the rat. *Eur J Pharmacol* 408: 83-89, 2000.

212. **Struck J, Tao C, Morgenthaler NG, and Bergmann A**. Identification of an Adrenomedullin precursor fragment in plasma of sepsis patients. *Peptides* 25: 1369-1372, 2004.

213. **Stuckmann I, Evans S, and Lassar AB**. Erythropoietin and retinoic acid, secreted from the epicardium, are required for cardiac myocyte proliferation. *Dev Biol* 255: 334-349, 2003.

214. **Sucov HM, Gu Y, Thomas S, Li P, and Pashmforoush M**. Epicardial control of myocardial proliferation and morphogenesis. *Pediatric cardiology* 30: 617-625, 2009.

215. **Sugo S, Minamino N, Shoji H, Kangawa K, and Matsuo H**. Effects of vasoactive substances and cAMP related compounds on adrenomedullin production in cultured vascular smooth muscle cells. *FEBS Lett* 369: 311-314, 1995.

216. **Szokodi I, Kinnunen P, and Ruskoaho H**. Inotropic effect of adrenomedullin in the isolated perfused rat heart. *Acta Physiol Scand* 156: 151-152, 1996.

217. **Szokodi I, Kinnunen P, Tavi P, Weckstrom M, Toth M, and Ruskoaho H**. Evidence for cAMP-independent mechanisms mediating the effects of adrenomedullin, a new inotropic peptide. *Circulation* 97: 1062-1070, 1998.

218. **Takimoto E, Champion HC, Li M, Belardi D, Ren S, Rodriguez ER, Bedja D, Gabrielson KL, Wang Y, and Kass DA**. Chronic inhibition of cyclic GMP phosphodiesterase 5A prevents and reverses cardiac hypertrophy. *Nat Med* 11: 214-222, 2005.

219. **Tandon P, Miteva YV, Kuchenbrod LM, Cristea IM, and Conlon FL**. Tcf21 regulates the specification and maturation of proepicardial cells. *Development* 140: 2409-2421, 2013.

220. **Tao J, Doughman Y, Yang K, Ramirez-Bergeron D, and Watanabe M**. Epicardial HIF signaling regulates vascular precursor cell invasion into the myocardium. *Dev Biol* 376: 136-149, 2013.

221. **Tomanek RJ, Ishii Y, Holifield JS, Sjogren CL, Hansen HK, and Mikawa T**. VEGF family members regulate myocardial tubulogenesis and coronary artery formation in the embryo. *Circ Res* 98: 947-953, 2006.

222. **Tomoda Y, Kikumoto K, Isumi Y, Katafuchi T, Tanaka A, Kangawa K, Dohi K, and Minamino N**. Cardiac fibroblasts are major production and target cells of adrenomedullin in the heart in vitro. *Cardiovasc Res* 49: 721-730, 2001.

223. **Torigoe Y, Takahashi N, Hara M, Yoshimatsu H, and Saikawa T**. Adrenomedullin improves cardiac expression of heat-shock protein 72 and tolerance against ischemia/reperfusion injury in insulin-resistant rats. *Endocrinology* 150: 1450-1455, 2009.

224. **Townsend RR**. Attending rounds: a patient with drug-resistant hypertension. *Clinical journal of the American Society of Nephrology : CJASN* 6: 2301-2306, 2011.

225. **Tremblay A, Tremblay GB, Labrie F, and Giguere V**. Ligand-independent recruitment of SRC-1 to estrogen receptor beta through phosphorylation of activation function AF-1. *Molecular cell* 3: 513-519, 1999.

226. **Tristani-Firouzi M, Jensen JL, Donaldson MR, Sansone V, Meola G, Hahn A, Bendahhou S, Kwiecinski H, Fidzianska A, Plaster N, Fu YH, Ptacek LJ, and Tawil R**. Functional and clinical characterization of KCNJ2 mutations associated with LQT7 (Andersen syndrome). *J Clin Invest* 110: 381-388, 2002.

227. **Trivedi CM, Lu MM, Wang Q, and Epstein JA**. Transgenic overexpression of Hdac3 in the heart produces increased postnatal cardiac myocyte proliferation but does not induce hypertrophy. *J Biol Chem* 283: 26484-26489, 2008.

228. **Troughton RW, Lewis LK, Yandle TG, Richards AM, and Nicholls MG**. Hemodynamic, hormone, and urinary effects of adrenomedullin infusion in essential hypertension. *Hypertension* 36: 588-593, 2000.

229. **Truong QA, Siegel E, Karakas M, Januzzi JL, Jr., Bamberg F, Mahabadi AA, Dasdemir S, Brady TJ, Bergmann A, Kunde J, Nagurney JT, Hoffmann U, and Koenig W**. Relation of natriuretic peptides and midregional proadrenomedullin to cardiac chamber volumes by computed tomography in patients without heart failure: from the ROMICAT Trial. *Clin Chem* 56: 651-660, 2010.

230. **Tsujikawa K, Yayama K, Hayashi T, Matsushita H, Yamaguchi T, Shigeno T, Ogitani Y, Hirayama M, Kato T, Fukada S, Takatori S, Kawasaki H, Okamoto H, Ikawa M, Okabe M, and Yamamoto H**. Hypertension and dysregulated proinflammatory cytokine production in receptor activity-modifying protein 1-deficient mice. *Proc Natl Acad Sci U S A* 104: 16702-16707, 2007.

231. **Tsuruda T, Kato J, Kitamura K, Kuwasako K, Imamura T, Koiwaya Y, Tsuji T, Kangawa K, and Eto T**. Adrenomedullin: a possible autocrine or paracrine inhibitor of hypertrophy of cardiomyocytes. *Hypertension* 31: 505-510, 1998.

232. **Uusimaa P, Risteli J, Niemela M, Lumme J, Ikaheimo M, Jounela A, and Peuhkurinen K**. Collagen scar formation after acute myocardial infarction: relationships to infarct size, left ventricular function, and coronary artery patency. *Circulation* 96: 2565-2572, 1997.

233. **van Wijk B, Gunst QD, Moorman AF, and van den Hoff MJ**. Cardiac regeneration from activated epicardium. *PLoS One* 7: e44692, 2012.

234. **Vega-Hernandez M, Kovacs A, De Langhe S, and Ornitz DM**. FGF10/FGFR2b signaling is essential for cardiac fibroblast development and growth of the myocardium. *Development* 138: 3331-3340, 2011.

235. **Viragh S, and Challice CE**. The origin of the epicardium and the embryonic myocardial circulation in the mouse. *The Anatomical record* 201: 157-168, 1981.

236. **Viragh S, Gittenberger-de Groot AC, Poelmann RE, and Kalman F**. Early development of quail heart epicardium and associated vascular and glandular structures. *Anatomy and embryology* 188: 381-393, 1993.

237. **Wang C, Dobrzynski E, Chao J, and Chao L**. Adrenomedullin gene delivery attenuates renal damage and cardiac hypertrophy in Goldblatt hypertensive rats. *Am J Physiol Renal Physiol* 280: F964-971, 2001.

238. **Wang J, Karra R, Dickson AL, and Poss KD**. Fibronectin is deposited by injury-activated epicardial cells and is necessary for zebrafish heart regeneration. *Dev Biol* 382: 427-435, 2013.

239. **Ward NL, Van Slyke P, Sturk C, Cruz M, and Dumont DJ**. Angiopoietin 1 expression levels in the myocardium direct coronary vessel development. *Developmental dynamics : an official publication of the American Association of Anatomists* 229: 500-509, 2004.

240. **Watanabe H, Takahashi E, Kobayashi M, Goto M, Krust A, Chambon P, and Iguchi T**. The estrogen-responsive adrenomedullin and receptor-modifying protein 3 gene identified by DNA microarray analysis are directly regulated by estrogen receptor. *J Mol Endocrinol* 36: 81-89, 2006.

241. **Watt AJ, Battle MA, Li J, and Duncan SA**. GATA4 is essential for formation of the proepicardium and regulates cardiogenesis. *Proc Natl Acad Sci U S A* 101: 12573-12578, 2004.

242. **Webb P, Nguyen P, Valentine C, Lopez GN, Kwok GR, McInerney E, Katzenellenbogen BS, Enmark E, Gustafsson JA, Nilsson S, and Kushner PJ**. The estrogen receptor enhances AP-1 activity by two distinct mechanisms with different requirements for receptor transactivation functions. *Mol Endocrinol* 13: 1672-1685, 1999.

243. **Wei X, Zhao C, Jiang J, Li J, Xiao X, and Wang DW**. Adrenomedullin gene delivery alleviates hypertension and its secondary injuries of cardiovascular system. *Human gene therapy* 16: 372-380, 2005.

244. **Wessels A, van den Hoff MJ, Adamo RF, Phelps AL, Lockhart MM, Sauls K, Briggs LE, Norris RA, van Wijk B, Perez-Pomares JM, Dettman RW, and Burch JB**. Epicardially derived fibroblasts preferentially contribute to the parietal leaflets of the atrioventricular valves in the murine heart. *Dev Biol* 366: 111-124, 2012.

245. **Wetzel-Strong SE, Li M, Klein KR, Nishikimi T, and Caron KM**. Epicardial-derived adrenomedullin drives cardiac hyperplasia during embryogenesis. *Developmental dynamics : an official publication of the American Association of Anatomists* 243: 243-256, 2014.

246. **Wetzker R, and Bohmer FD**. Transactivation joins multiple tracks to the ERK/MAPK cascade. *Nature reviews Molecular cell biology* 4: 651-657, 2003.

247. **Willerson JT, and Buja LM**. Cause and course of acute myocardial infarction. *Am J Med* 69: 903-914, 1980.

248. **Wu H, Lee SH, Gao J, Liu X, and Iruela-Arispe ML**. Inactivation of erythropoietin leads to defects in cardiac morphogenesis. *Development* 126: 3597-3605, 1999.

249. **Wu SY, Shin J, Sepich DS, and Solnica-Krezel L**. Chemokine GPCR signaling inhibits beta-catenin during zebrafish axis formation. *PLoS biology* 10: e1001403, 2012.

250. **Yurugi-Kobayashi T, Itoh H, Schroeder T, Nakano A, Narazaki G, Kita F, Yanagi K, Hiraoka-Kanie M, Inoue E, Ara T, Nagasawa T, Just U, Nakao K, Nishikawa S, and Yamashita JK**. Adrenomedullin/cyclic AMP pathway induces Notch activation and differentiation of arterial endothelial cells from vascular progenitors. *Arterioscler Thromb Vasc Biol* 26: 1977-1984, 2006.

251. **Zhao L, Borikova AL, Ben-Yair R, Guner-Ataman B, MacRae CA, Lee RT, Burns CG, and Burns CE**. Notch signaling regulates cardiomyocyte proliferation during zebrafish heart regeneration. *Proc Natl Acad Sci U S A* 111: 1403-1408, 2014.

252. **Zhou B, Honor LB, He H, Ma Q, Oh JH, Butterfield C, Lin RZ, Melero-Martin JM, Dolmatova E, Duffy HS, Gise A, Zhou P, Hu YW, Wang G, Zhang B, Wang L, Hall JL, Moses MA, McGowan FX, and Pu WT**. Adult mouse epicardium modulates myocardial injury by secreting paracrine factors. *J Clin Invest* 121: 1894-1904, 2011.

253. **Zhou B, Honor LB, Ma Q, Oh JH, Lin RZ, Melero-Martin JM, von Gise A, Zhou P, Hu T, He L, Wu KH, Zhang H, Zhang Y, and Pu WT**. Thymosin beta 4 treatment after myocardial infarction does not reprogram epicardial cells into cardiomyocytes. *Journal of molecular and cellular cardiology* 52: 43-47, 2012.

254. **Zhou B, Ma Q, Rajagopal S, Wu SM, Domian I, Rivera-Feliciano J, Jiang D, von Gise A, Ikeda S, Chien KR, and Pu WT**. Epicardial progenitors contribute to the cardiomyocyte lineage in the developing heart. *Nature* 454: 109-113, 2008.

255. **Zhou B, von Gise A, Ma Q, Hu YW, and Pu WT**. Genetic fate mapping demonstrates contribution of epicardium-derived cells to the annulus fibrosis of the mammalian heart. *Dev Biol* 338: 251-261, 2010.